論文 / 著書情報
Article / Book Information

題目(和文)	ナフサ接触分解反応におけるH-ZSM5ゼオライト触媒の長寿命化
Title(English)	Improvement in Durability of H-ZSM5 Zeolite Catalyst for the Catalytic Cracking of Naphtha
著者(和文)	秋山聰
Author(English)	Satoshi Akiyama
出典(和文)	学位:博士(工学), 学位授与機関:東京工業大学, 報告番号:甲第10511号, 授与年月日:2017年3月26日, 学位の種別:課程博士, 審査員:野村 淳子,松下 伸広,北村 房男,馬場 俊秀,鎌田 慶吾
Citation(English)	Degree:Doctor (Engineering), Conferring organization: Tokyo Institute of Technology, Report number:甲第10511号, Conferred date:2017/3/26, Degree Type:Course doctor, Examiner:,,,,
学位種別(和文)	博士論文
Type(English)	Doctoral Thesis

Doctor thesis

Improvement in Durability of H-ZSM5 Zeolite Catalyst for the Catalytic Cracking of Naphtha

（ナフサ接触分解反応における H-ZSM5 ゼオライト触媒の長寿命化）

Satoshi Akiyama

Department of Electronic Chemistry

Interdisciplinary Graduate School of Science and Engineering

Tokyo Institute of Technology

Contents

Chapter 1 General introduction

in Acid amount and metal loading amount

Chapter 1

General Introduction

1.1 Objective

1.1.1 Background

The chemical industry in Japan is in the position to produce many basic materials and to provide materials in the manufacture of products of other industries, providing materials of excellent quality, and supporting the development of other industries greatly. The chemical industry is an indispensable component supply source that is key to the production volume and quality of products of other industries.

In view of the recent rise in oil prices, concern about the depletion of oil, and the problem of suppressing CO_2 emissions associated with global warming, further energy saving of the chemical industry, reduction of the basic unit, and reduction of CO_2 emissions are required.

From the viewpoint of reducing CO_2 emissions, the emission ratio of naphtha cracking process is high, estimated at about 1/3 of the total petrochemical industry. Normally, in the thermal cracking process of naphtha, heating at 1073 K or higher is performed. In principle, catalytic cracking of naphtha can be carried out at a lower temperature compared with the pyrolysis process, and heating at about 923 K is enough to perform the catalytic cracking process using catalyst. It is expected not only to lower the temperature, but also to reduce the basic unit by improving the selectivity to useful products such as ethene, propene, butenes, BTX and energy saving of separation process by reducing by-products such as methane. Furthermore, the range of products by operating process factors is not so wide in the conventional thermal reaction,

whereas the catalytic cracking process has a potential to increase it.

In the catalytic cracking process of naphtha, there is a possibility that the selectivity of the product can be controlled by improving the performance of the catalyst, and it can be a process that makes it possible to make products matching it based on market trends as described above. That is, it is a process that can respond more flexibly than thermal cracking process to demand from demand trend such as variable propylene / ethylene ratio, C_4 component, increased production of BTX [1].

As mentioned above, from the viewpoints of energy saving, reduction of CO_2 emissions, and advanced use of petroleum, at the present time, it is important to develop catalytic cracking technology to replace naphtha thermal cracking technology and it has high priority.

1.1.2 Environment surrounding the petrochemical industry

Demand for petrochemical products such as polyethylene and polypropylene is expected to continue growing mainly in emerging countries such as China. Petrochemical foundation products such as ethene and propene, which are raw materials of these raw materials, are expected to grow in the medium to long term in the whole world. In order to cope with this situation, the many newly construction plans are planed. Many ethane crackers in the Middle East have been in operation since around 2008, new large naphtha crackers in China and all over Asia, and coal to olefins (CTO) plant in China are planned (Table 1) [2]. If these newly established plans proceed smoothly, it is expected that the overcapacity of about 40 million tons will continue worldwide (Fig. 1) [2]. In the US, from around the year 2011, the competitiveness of ethane cracking derived from Shale gas has increased, and it is planned to drastically increase the ethylene production capacity (Table 2) [2]. Whether all plans will be realized is uncertain, but it is no doubt that ethene and ethene derivative products

produced in the United States will be exported to areas mainly made of naphtha such as Europe and Asia.

Propene, butens, and aromatics are hardly produced from ethane crackers, so construction of plants that produce them and development of technology are progressing. Propene is produced by propane dehydrogenation (PDH) utilizing propane derived from Shale gas, methanol to propene (MTP) using natural gas or methanol derived from coal, deep catalytic cracking (DCC) in petroleum refining fluid catalytic cracking process.

Meanwhile, domestic ethylene demand in Japan has been around 5 million tons / year and domestic demand cannot be expected to grow in the future as compared with the production capacity of 7.21 million tons at the end of 2012. Although domestic plants have been operating by exporting to China etc., it will be exposed to severe competition with the Middle East, the US, and the newly established naphtha crackers for maintaining the export amount of ethylene. Amid such a business environment, domestic petrochemical companies have promoted the restructuring of business and announced a series of ethene plant outage plans one after another, but further reduction in ethene surplus capacity, corporate collaboration beyond industries, integration of complexes in neighboring areas, and other bold structural reforms are required. Olefin manufacturing companies from naphtha cracker including Japan need technologies to dramatically improve the competitiveness of naphtha crackers and strategies that are not confined to the conventional framework amidst the relative competitiveness of naphtha as a petrochemical raw material has declined.

Table 1　New ethene production plants in China (METI 2016)

Company	Process type	Capacity (1000 tons)	from
中国石化海南煉化有限公司	naphtha cracker	1,000	2015
中国石化上海石油化工股份公司		1,000	2020
広州石化・KPC 総合		1,000	2017
中海石油煉化公司恵州煉化分公司		1,000	2019
古雷石化		1,200	2019
内蒙古中煤蒙大新能源公司	CTO	300	2016
蒲城清潔能源化工有限責任公司		300	2015
神華集団/DOW		450	2016
蘭花煤化工有限公司		300	2016
神華寧夏煤化集団		300	2016
安徽中安聯合煤業化工有限公司		300	2017
中天合創鄂尔多斯		650	2017
中国石化中原石油化工有限責任公司	MTO	300	2016
久泰能源集団		300	2017

Table 2　New ethene production plants in US (METI 2016)

Company	Process type	Capacity (1000 tons)	from
Chevron Phillips	ethane cracker	1,500	2017
Dow Chemical		1,500	2017
ExxonMolib		1500	2017
Formosa		1,150	2018
Indorama		363	2018
LACC		1,000	2020
Oxy/Mexichem JV		550	2017
Sasol		1,550	2018
Shinetsu		500	2018

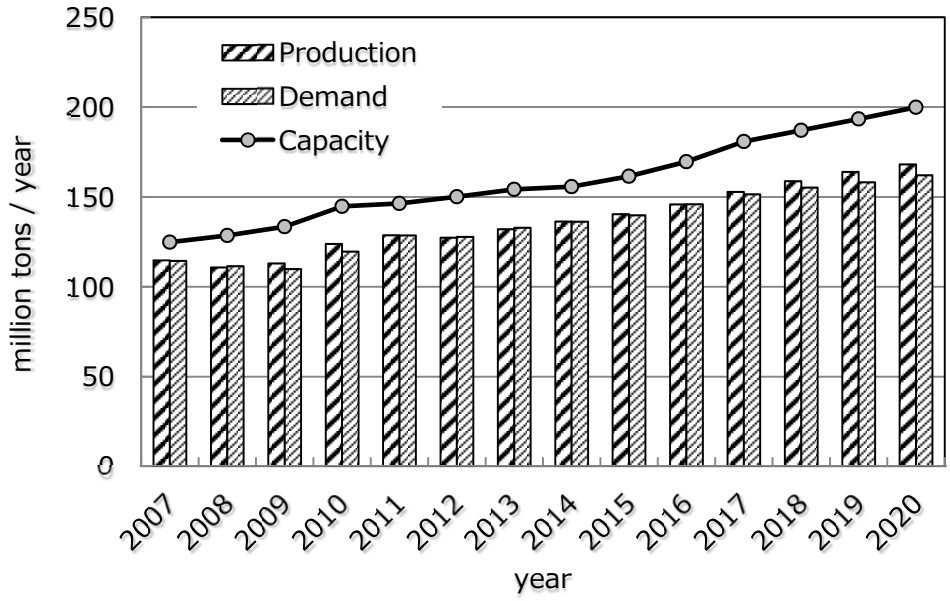

Fig. 1 Supply and demand results and future prospects of ethene in the world (METI 2016)

1.1.3 Research premise

(1) Process

There are three types of naphtha catalytic cracking reactors as follows.

・Fluidized bed type (FCC type)

・Fixed bed type (reformer type)

・Platformer type (combination of radial flow type reactor and reheater)

However, a platformer type system is considered to be difficult to supply a very large endothermic energy with a short contact time, so it is excluded from options.

In addition, for fluidized bed type (FCC type) naphtha catalytic cracker, demonstration plant (40,000 MTA / (ethylene + propylene) production of ACO (Advanced Catalytic Olefins) process of US KBR and South Korea SK Innovation (formerly SK Energy) as capability) has started demonstration operation at the Ulsan plant in Korea since the end of October 2010.

The fixed bed type reactor has merits as follow:

・ a lower construction cost and cost competitiveness than the FCC type reactor

・ easy to operate for the ethylene production company because of similarity to the thermal cracking furnace of the ethene plant

・ capability of replacement of existing processes and concurrent use

so, the fixed bed reformer type was selected.

Since the yield of ethane and propane in the cracked product gas from the naphtha catalytic cracker is about 5 times larger than that of the pyrolysis process, a process flow combining a catalytic cracking reactor and a thermal cracking furnace is advantageous so that ethane and propane recovered from the purification system are further decomposed in a thermal cracking furnace and recovered as products (mainly ethene and propene). It is also considered that the purification system can apply the flow of the conventional ethene plant.

This indicates that integration with existing ethylene plants is effective by scrap & build replacing the naphtha catalytic cracking reactor with an older pyrolysis furnace whose lifetime is getting close.

(2) Raw feedstock

n-Hexane was used as a raw material as a typical light naphtha model compound currently used in the petrochemical industry in Japan. It is expected that this type of naphtha will be used as a raw material in the future.

1.1.4 Task

There are many reports of hydrocarbon cracking reactions using zeolite catalysts, and at the present time, examples of research by Yoshimura and Mizukami et al. can be mentioned as the catalysts with the highest performance [1]. Yoshimura and colleagues reported that catalytic decomposition of hydrocarbons with a catalyst modified with

lanthanum oxide and phosphorus to ZSM5, La_2O_3/P/ZSM5, significantly reduced the deposition of coke [47, 48]. As a result, La_2O_3/P/ZSM5 presented high olefin yield and long catalyst life. However, in previous research examples such as those mentioned above, there are many examples in which raw materials were diluted with nitrogen as well as water, which is a condition that is unlikely to cause a decrease in activity. Furthermore, they were short-term tests and didn't describe the long-term change in activity considering the plant operability such as 24 hours and 48 hours. Therefore, it can be said that they were not necessarily evaluated under practical conditions [1]. In the case of applying the catalyst developed up to now on the investigation of patents, literatures etc., it is presumed that the continuous reaction time (catalyst life) is insufficient for use as a fixed bed although the initial activity is high when applied to a fixed bed. Therefore, in this research, research and development was conducted considering lengthening this durability (catalyst lifetime) as the most important issue.

1.2. Cracking of naphtha

1.2.1 Cracking reaction

Cracking reaction is one of the most important reactions in petrochemical industry. Cracking is the process of braking of hydrocarbons into smaller and more useful paraffins and olefins. There are two types of cracking reaction.

・non-catalytic cracking: by free radical

・catalytic cracking: by acid catalyst

1.2.2 Non-catalytic cracking: Steam cracking

Non-catalytic cracking need high temperature to generate fee radical species. The source of heat is mainly high temperature steam. Steam cracking precess is a major industrial method for producing light alkenes including ethene and propene. Steam cracker unit is a facility for thermally cracking raw materials such as naphtha, LPG, ethane, propane or butane by using steam of pyrolysis furnace to produce light hydrocarbons. The products distribution depends on the composition on the feedstock, the hydrocarbon to steam ratio, the cracking temperature and the furnace residence time. In steam cracking, a gaseous or liquid hydrocarbon feedstock such as naphtha, LPG or ethane is diluted with steam and briefly heated in the furnace. The reaction temperature is as high as about 1123 K or higher, but the reaction is carried out in a very short time.

At high cracking temperature, it is advantageous for the production of ethene and benzene, whereas at low temperature it is advantageous for the production of propene, butenes and liquid products. This process also slows the deposition of coke, which is in the form of carbon on the reactor wall. Reaction conditions are designed to minimize coke formation as coke reduces reactor efficiency, but steam cracking furnaces usually need to be decoking once every few months.

1.2.3 Mechanism of steam cracking reaction

The cracking reaction by free radical proceeds in the following form [3].

(1) Initiation

A hydrocarbon molecule breaks into two free radicals. Only a little of the feedstock undergo initiation, but this reaction is necessary to generate free radicals driving the remaining reaction (Scheme 1). In steam cracking, initiation usually involves breaking chemical bonds between two carbon atoms rather than carbon and hydrogen atoms.

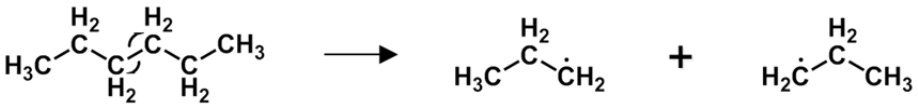

(Scheme 1)

(2) Radical decomposition

A free radical breaks apart into two molecules, one an alkene, the other a free radical by β-scission reaction. This is the process that results in alkene products (Scheme 2).

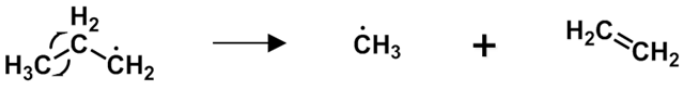

(Scheme 2)

(3) Hydrogen abstraction

A free radical removes a hydrogen atom from another molecule, turning the second molecule into a free radical (Scheme 3).

(Scheme 3)

(4) Radical addition

Reverse reaction of radical decomposition reaction. A radical reacts with an alkene to form a single, larger free radical (Scheme 4). This process is involved in forming aromatic products.

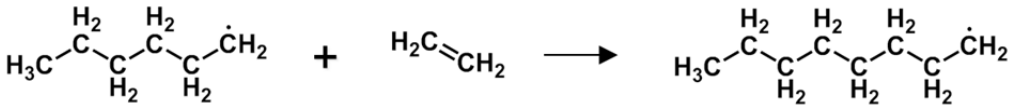

(Scheme 4)

(5) Termination

Two radicals react with each other to produce non radical products (Scheme 5).

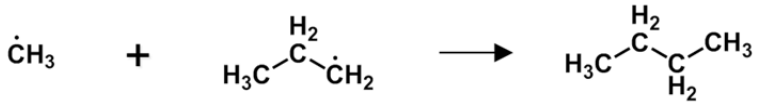

(Scheme 5)

1.2.4 Catalytic cracking

Catalytic cracking reaction proceeds with acid catalysts such as silica-alumina and zeolites. This reaction is applied to the conversion reaction of heavy oil to gasoline and the conversion reaction of petrochemical raw materials to lower olefins. This process is adopted mainly in FCC (fluid catalytic cracking) process [4]. Demand for gasoline in the US increased in the 1950s, and production of gasoline was increased by catalytic cracking to respond to it. At that time, amorphous silica-alumina was used as a solid catalyst, but development of a catalyst with higher activity and high thermal stability was desired. On the other hand, in the 1950's Socony vacuum oil Co. (present Exxon Mobil) found that zeolite exhibited high activity and shape selectivity not seen in conventional catalysts for hydrocarbon reactions, and application researches of zeolite

catalysts have started [5].

1.2.5 Mechanism of catalytic cracking reaction

Cracking of paraffins proceed through the carbenium ion mechanism and/or penta-coordinated carbonium ion mechanism [6-15].

(1) Carbenium ion mechanism

In this mechanism, formation of carbenium ion from alkane by hydride transfer and β-scission of carbon-carbon bond of carbenium ion are elementary reactions. A small olefin and a smaller carbenium ion are produced through the latter reaction [9]. However, in the case of "*n*"-alkanes, this type of β-scission practically does not occur. This is because primary carbenium ions with low stability are generated. Sie advocated cracking mechanism of "*n*"-alkanes via β-scission with 1,3-hydride shift and 1,2-hydride shift from reaction intermediates in the form of protons added to the cyclopropane ring (Scheme 6) [13].

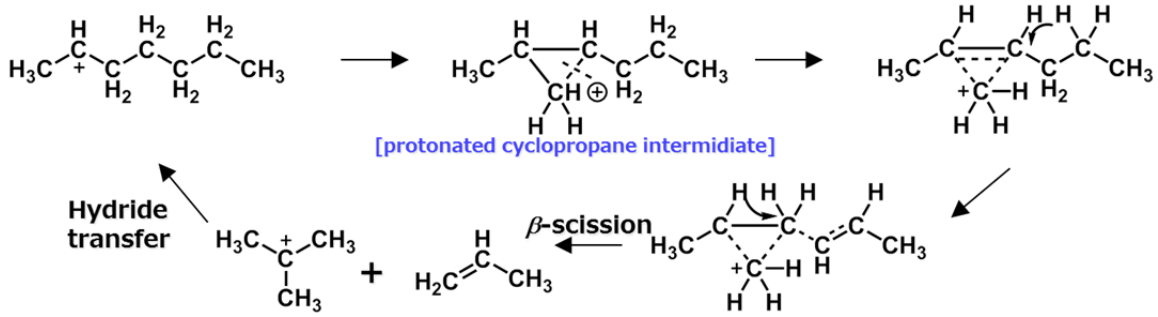

(Scheme 6)

In this mechanism, the hydrocarbons smaller than C2 are rarely formed because of formation of primary carbenium ions. Therefore, production of propene and butens are easier than that of ethene [6-8]. There are several possibilities or the initiation step leading

to formation of carbenium ions. An example is protonation to olefins by catalyst. Olefins come from impurities in the feed, products of free-radical cracking, products of hydride abstraction from paraffins by Lewis acid sites on the catalysts, or products of cracking via carbonium ion mechanism described blow.

(2) Carbonium ion mechanism

In the carbenium ion mechanism, the formation of hydrogen, methane and ethane can not occur. The cracking of long chain alkanes produces little of these products, but these are produced by relatively short alkane cracking. To explain the formation of hydrogen, methane, and ethane, Haag and Dessau proposed a mechanism by which a proton directly reacts with an alkane via a pentacoordinate carbonium ion [10, 15]. Carbonium ion is a pentacoordinate carbocation and was proposed by Olah to explain the reaction of hydrocarbon in superstrong acid. In this mechanism, protons attack not only carbon-hydrogen bonds but also carbon-carbon bonds. This way of thinking can explain the formation of methane and ethane in cracking (Scheme 7) [14].

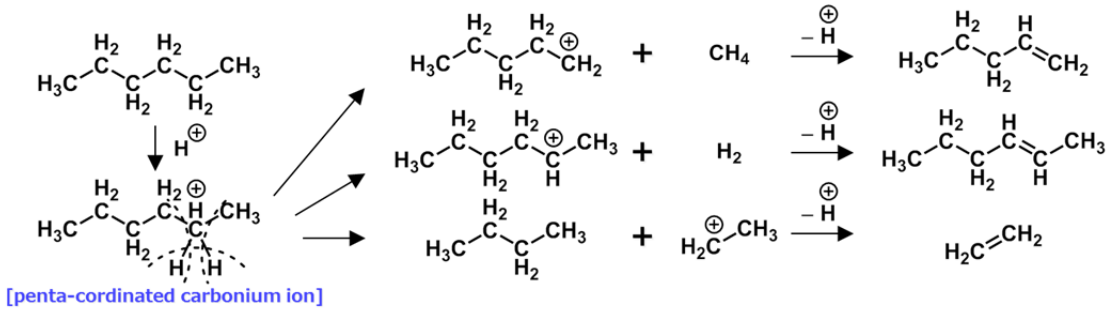

(Scheme 7)

1.3 Zeolite

As mentioned above, catalytic cracking of paraffin is catalyzed by acid. Preferred conditions as a catalyst for catalytic cracking are as follows.

・Since a very large throughput is assumed, it is a heterogeneous catalyst which facilitates separation of catalyst and product.

・High energy is necessary for decomposition of paraffin, and it is necessary to perform reaction at high temperature, so it must have a structure that can withstand high temperatures.

・It must have a pore structure that can improve the shape selectivity of the product.

Zeolite is the first candidate as a catalyst satisfying all these conditions (Fig. 2).

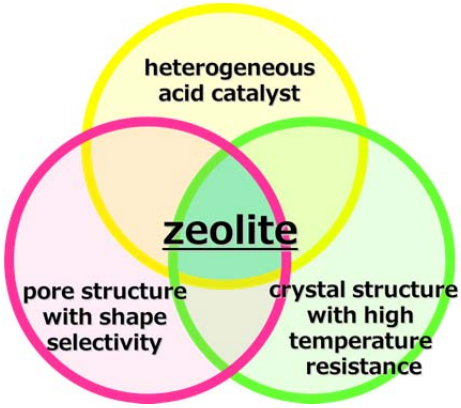

Fig. 2 Zeolite as a catalyst satisfying the conditions for performing paraffin catalytic cracking.

1.3.1 Zeolite

Zeolite is a natural mineral discovered in 1756. Currently it is used as a generic term for crystalline porous aluminosilicate, metallosilicate, or aluminophosphate. The basic unit of the structure is $(SiO_4)^{4-}$ and $(AlO_4)^{5-}$ unit (described as TO_4) with a tetrahedral structure (Fig. 3). One TO_4 unit shares four vertex oxygen molecules with

each of the four TO_4 units next to each other, so that it sequentially and three-dimensionally connects to form crystals. Since this crystal is porous and the size of the pore is about 0.4 - 0.8 nm (micro pore), molecules smaller than the pore size can penetrate into the pores, but molecules larger than the pore size cannot enter the molecule. Zeolite has a molecular sieving effect[16-19]. When zeolite is classified by the geometry (topology) of the skeleton, 232 types of zeolite are currently found or synthesized [20].

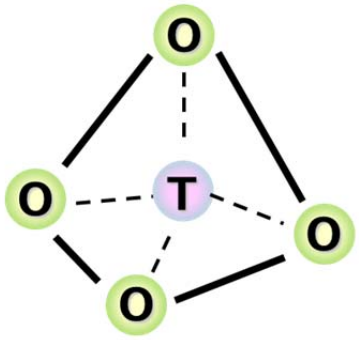

Fig. 3 TO_4 unit. ($T = Si^{4+}$ or Al^{3+})

The nature of the zeolite depends greatly on its pore structure and is classified by the pore size. The number of member rings is determined by the number of oxygen atoms (the same as the number of T atoms) contained in the ring structure of the pore cross section. In the case of zeolites with multiple pores, the pore system with the largest diameter among them is defined as the pores of the zeolite (Table 3).

Table 3 Classification of zeolite by number of T atoms at pore entry

number of Member Ring	Zeolite (structure code)
8 MR: small pore	SAPO56 (AFX), SAPO34 (CHA) , SAPO17 (ERI), RUB50 (LEV), ITQ29 (LTA), UTM1 (MTF), UZM5 (UFI)…
10 MR: medium pore	SAPO11 (AEL), Ferrierite (FER), IM5 (IMF), ZSM11 (MEL), ZSM5 (MFI), MCM22 (MWW), RUB41 (RRO), SUZ4 (SZR), ZSM522 (TON)…
12 MR: large pore	SAPO5 (AFI), Linde type L (LTL), CIT1 (CON), Y (FAU), SSZ55 (ATS), SSZ42 (IFR), ZSM12 (MTW), Mordenite (MOR), MCM68 (MSE), beta (BEA)…
>14 MR: extra-large pore	VPI5 (VMF), $AlPO_4$8 (AET), CIT5 (CFI), UTD1 (DON)…

Molecular diffusion in the pores is greatly affected by the pore dimensions. Therefore, the pore system is also classified by dimension number (Table 4).

Table 4 Classification of zeolite by pore dimensions

number of dimensions	Zeolite (structure code)
3 dimensions	SAPO56 (AFX), Beta (BEA), SAPO34 (CHA), CIT1 (CON), SAPO17 (ERI), Y (FAU), IM5 (IMF), ITQ29 (LTA), ZSM11 (MEL), ZSM5 (MFI), MCM68 (MSE), SUZ4 (SZR)…
2 dimensions	Ferrierite (FER), MCM22 (MWW), RUB50 (LEV), RUB41 (RRO), UZM5 (UFI)…
1 dimension	SAPO11 (AEL), SAPO5 (AFI), SSZ55 (ATS), SSZ42 (IFR), Linde type L (LTL), Mordenite (MOR), ZSM12 (MTW), UTM1 (MTF), ZSM22 (TON)…

Many of the reactions using zeolites as catalysts take advantage of their properties

as acids. An acidic hydroxyl group having a Bronsted acidity catalyzes various reactions. The hydroxyl group showing solid acidity is due to the partial structure of the zeolite framework. That is, an acidic hydroxyl group is generated when the proton necessary for compensating the charge is bonded to the oxygen ion bridged to the ions of Al and Si when the Si ion of the silicate isomorphously substituted with the Al ion (Fig. 4). When infrared absorption spectrum was measured, stretching vibration of this hydroxyl group was observed [21]. This absorption disappeared when pyridine which was a basic molecule was adsorbed, and instead absorption of pyridinium ion appeared. Thus, it was shown that hydroxyl groups brideged with Al ions and Si ions had a function as acid. The amount of acid is determined by the ratio of Si and Al, and when the Si / Al ratio is small, that is, when the number of Al is large, the acid amount is large.

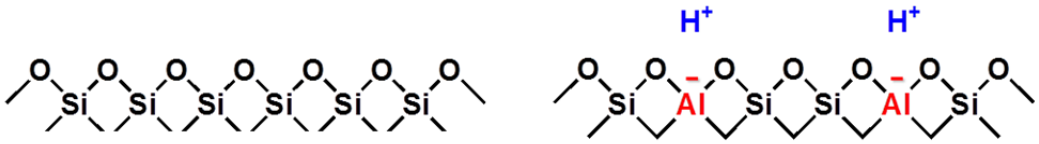

Fig. 4 Mechanism of exhibition of zeolite acidity

Characteristics of zeolite as a catalyst are summarized as Maxwell's description below [22].

1. Structural stability is high and the structure is not destroyed even under high temperature reaction conditions. It is difficult to destroy the structure even in a high temperature steam atmosphere.
2. Because of the restricted pores, the partial pressure of the reactants inside the pores becomes high, which is advantageous in terms of chemical equilibrium compared with other solid catalysts.
3. Because it has the pore with uniform molecular size, shape selectivity called

molecular sieve exhibits.

4. Zeolite has many kinds of crystals with different skeleton structure. These are rich in diversity, such as the pore size being different, the pore structure also existing in one-dimensional, two-dimensional, three-dimensional, and the channel format being different.

5. Even with the same crystal structure, reactivity can be controlled by changing the Si / Al ratio of the skeleton or by replacing skeletal cations.

6. Exchangable cations are present, and acid properties can be controlled by species, exchange rate, etc.

7. Catalytic reaction using zeolite is a reaction in the micropore, so the collision frequency is higher than other active surfaces.

1.3.2 MFI zeolite

ZSM5 zeolite having the MFI topology has been widely applied in many important catalytic reactions because of its special porous structures. The MFI structure has twelve distinct T-sites and consists of parallel and straight 10-membered ring (MR) channels intersected by sinusoidal 10-MR channels. The ZSM5 zeolite has 10-MR channels (0.56 x 0.53 nm) with linear pores in the b-axis direction, and also has a 10-membered ring (0.55 x 0.51 nm) and zigzag pores in the a-axis direction. These pores cross each other and form three dimensional pores (Fig. 5) [20]. The intersection is a rather large space, and it becomes a reaction field when used as a catalyst. The pore diameter is slightly larger than the benzene ring and shows selectivity specific to the catalytic reaction of aromatic hydrocarbons. ZSM11 has a composition similar to that of ZSM 5 and has linear 10-membered ring pores also in the a-axis direction.

ZSM5 was first synthesized in 1965 by Mobil [23]. Thereafter, a lot of hydrocarbon conversion reaction processes utilizing the shape selectivity of ZSM5 were

developed. For example, oligomerization [24, 25], hydrocracking [26], cracking of olefin [27-33] and paraffin [1, 34-36], methanol to olefin [37], aromatization [38, 39], isomerization, disproportionation and alkylation of aromatic compounds processes [40-42]. The superior catalytic performance of ZSM5 for various reactions are caused by several excellent features as following,

1. ZSM5 synthesis with a wide range of Si / Al ratio up to infinity is easily possible and the structure is stable.
2. Al content of the skeleton and hydrocarbon decomposition activity linearly change, correlation between basic physical properties and catalytic activity is high.
3. Compared to FAU and MOR, activity is high even with a small amount of Al.
4. Easy skeleton substitution of T atoms, easy control of solid acidity and selectivity.
5. Since there are no large vacancies as present in the FAU crystals, coke formation is suppressed.
6. Shape selectivity is more pronounced than other zeolites.

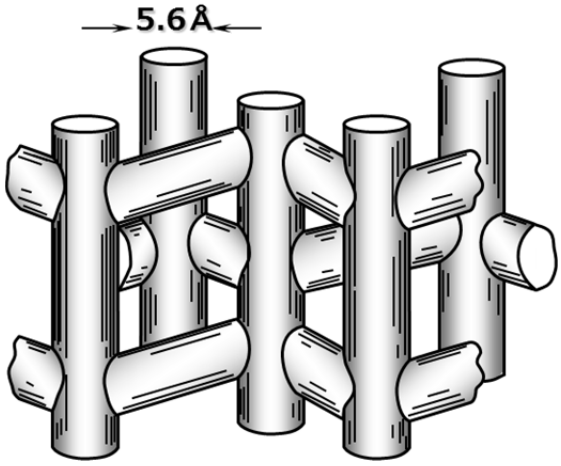

Fig.5 Schematic diagram of ZSM 5 zeolite structure.

1.4 Deactivation of zeolite catalyst

Improvement of catalyst life is an important issue for practical application of naphtha catalytic cracking process. Deactivation factors include deterioration due to coke and deterioration due to dealumination. In order to carry out naphtha cracking reaction for a long time, it is necessary to focus on these two causes and to take measures.

1.4.1 Coke

The zeolite catalyst is deactivated with coke material which is a by-product of the reaction. That is, the catalytic reaction is a fight with coke. The formation of coke cannot be avoided during naphtha cracking at high temperature. Coke is a high molecular weight hydrocarbon, and is produced by randomly repeating oligomerization, cyclization, and aromatization of raw materials, intermediates, or products (Scheme 8) [43]. This reaction is accelerated by acid and heat.

The deactivation of the catalyst occurs when the acidic hydroxyl group which is the catalytic activity point is covered with coke or the pores are covered with coke. Since the formation of coke is remarkable in the reaction under high temperature, how to reduce the inactivation by coke and advance the desired reaction is the key.

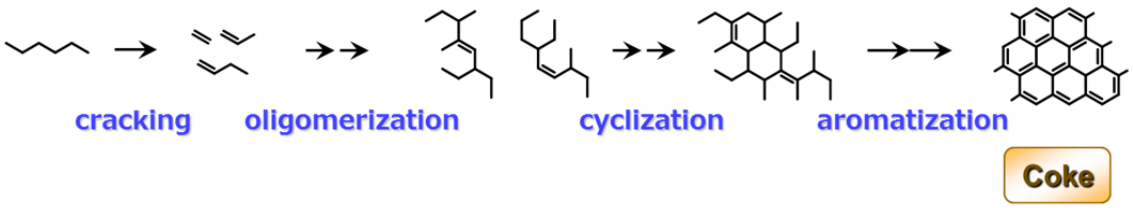

(Scheme 8)

1.4.2 Dealmination

The zeolite crystals are metastable. Therefore, in a high-temperature steam atmosphere, a phenomenon occurs in which aluminum in the zeolite skeleton exhibiting the acid property is detached to the outside of the skeleton in an effort to return to the stable state SiO_2. This phenomenon is called dealumination (Scheme 9) [44]. Sano et al. reported the dealumination of H-ZSM5 in the presence of high temperature steam and measurement its Al concentration [49]. As a result, they found that the dealumination rate was proportional to the Al concentration by the third order and the water vapor partial pressure by 1.5.

Aluminum ion out of the skeleton shows no Bronsted acidity and loses its performance as a catalyst. In catalytic cracking reaction of naphtha, high temperature steam is generated when burning coke with oxygen at catalyst regeneration and when steam is introduced for diluting reaction raw materials. Since both operations are indispensable, raising the hydrothermal resistance of the catalyst is also a key technology for practical application of naphtha catalytic cracking. On the other hand, there are also reports that dealumination increases the activity of ZSM5 in catalytic cracking of *n*-hexane. Lago reported that the activity of H-ZSM5 in catalytic cracking of hexane increases by subjecting to gentle steam treatment [50]. They explained that this increase in activity was due to the generation of new active sites. Sendoda also reported that the mild steam treatment of H-ZSM5 increased the activity in the catalytic decomposition of various hydrocarbons [51]. They explained that the increase in activity was due to the formation of strong acid sites due to the interaction between dealuminated species and acidic OH groups. At present, this hypothesis is most likely to be the increase in acid strength. Even so, under high temperature and long-time steam atmosphere, the progress of dealumination cannot be stopped, eventually losing catalytic activity.

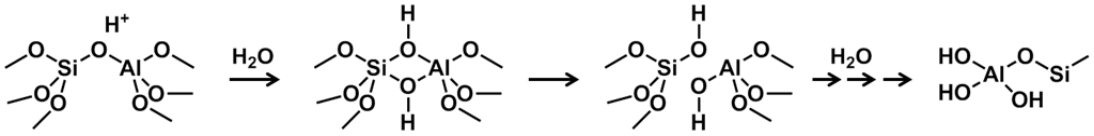

(Scheme 9)

In order to increase the hydrothermal resistance of the zeolite, it is generally known to support phosphorus in the zeolite (scheme 10) [45, 46]. ZSM5 zeolite is used as an additive for FCC catalyst, and phosphorus is added with most of the catalyst in order to prevent deactivation under coexistence with high temperature steam. It has been reported that when the amount of phosphorus supported is 0.6 equivalent to Al of the zeolite framework, the hydrothermal stability and catalytic activity are high [52]. If it is loaded in an amount larger than that, the acid property of the zeolite is suppressed by phosphorus and the catalytic activity is lowered. Phosphorus is supported on zeolite as a phosphoric acid species, but phosphoric acid species is not necessarily high boiling point, and it may volatilize at high temperature like naphtha decomposition reaction.

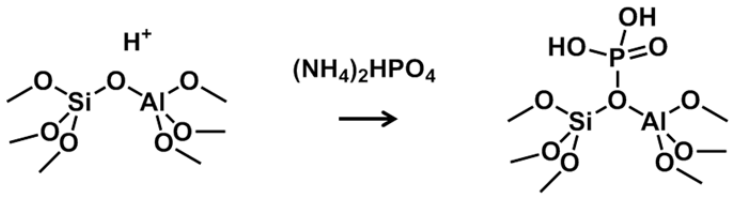

(Scheme 10)

1.5. Outline of this thesis

This thesis consists of six chapters. The main purpose of this research is to prolong the catalyst life and enable long operation time by finding a variety of countermeasures against the cause of deactivation of the ZSM5 zeolite catalyst for the naphtha catalytic cracking reaction.

In Chapter 2, the result of the screening of zeolite topologies for naphtha catalytic cracking was reported. A few of 20 zeolites that seemed promising and had a topology that could be obtained and synthesized were evaluated. As a result, ZSM5 (MFI) zeolite showed the highest activity and the conversion rate was slightly reduced. Therefore, in this research, the performance improvements of ZSM 5 zeolite were examined.

In Chapter 3, in order to inactivation of the acid sites which cause formation of coke materials, the result of the silylation of the acid sites on the external surface of H-ZSM5 with various silylation compounds was reported. Since the acid sites on the external surface of zeolite have no shape selectivity, the formation of coke which causes deactivation of catalyst occurs on them. Among the various silylatin reagents, cyclic siloxanes were effective compound for the deactivation of acid sites on the external surface. The effect of silylation was confirmed not only by the reaction but also by infra-red analysis.

In Chapter 4, in order to estimate the influence of the zeolite acid amount and the promoter component loading on the catalyst life, the result of the control of the acid amount of zeolite and the amount of loading metal having dehydrogenation activity was reported. It revealed that loading of metal controlled the amount to low Aluminum

content H-ZSM5 was effective for the durability and lower olefins selectivity. The kinetic study and the reaction regeneration repeated test of real naphtha cracking also were carried out.

In Chapter 5, for the purpose of prolonging the catalyst life by oxidizing and removing coke produced as the reaction progresses during the reaction, the result of using oxidizing gas for cracking reaction was reported. By utilizing CO_2, catalyst life dramatically increased. Using H_2O was also carried out as the oxidizing gas. It was confirmed that Pd/ZSM5 and Pd/CeO_2 catalyzed gasified coke or coke precursor during reaction. When H_2O is introduced into the reaction system, Aluminum ion in zeolite skeleton is desorbed from the zeolite framework and loses its catalytic function. Improvement of hydrothermal stability by modification of zeolite was also examined to suppress deactivation of zeolite caused by high temperature steam.

Finally, in Chapter 6, this research was summarized.

References

[1] N. Rahimi, R. Karimzadeh, Appl. Catal. A: Gen. 398 (2011) 1.

[2] METI "Supply and demand trend of petrochemical products worldwide" (2016).

[3] P. Wiseman, J. Chem. Edu. 54 (1977) 154.

[4] W.C. Cheng, G. Kim, A.W. Peters, X. Zhao, K. Rajagopalan, Catal. Rev. Sci. Eng. 40 (1998) 39.

[5] P.B. Weisz, ACS Symposium Series 738 (2000) 28.

[6] A. Corma, A.V. Orchilles, Micropor. Mesopor. Mater. 35 (2000) 21.

[7] S. Kotrel, H. Knozinger, B.C. Gates, Micropor. Mesopor. Mater. 35 (2000) 11.

[8] A.F.H. Wielers, M. Waarkamp, M.F.M. Post, J. Catal. 127 (1991) 51.

[9] B.S. Greensfelder, H.H. Voge, G.M. Good, Ind. Eng. Chem. 41 (1949)2573.

[10] W.O. Haag, R.M.Dessau, Proc. 8th Int. Congr. Catalysis. Berlin, 2 (1984) 305.

[11] W.O. Haag, R.M.Dessau, R.M. Lago, Stud. Surf. Sci. Catal. 60 (1991) 255.

[12] H. Krannila, W.O. Haag, B.C. Gates, J. Catal. 135 (1992) 115.

[13] S.T. Sie, Ind. Eng. Chem. Res. 31 (1992) 1881.

[14] G.A. Olah, J. Am. Chem. Soc. 94 (1972) 808.

[15] C. Stefandis, B. Gates, W.O. Haag, J. Mol. Catal. 67 (1991) 303.

[16] A.F. Cronstedt, K. Vetenskaps, Academiens Handlingar Stockholm, 17 (1756) 120.

[17] D.W. Breck, Zeolite Molecular Sieves; Wiley: New York, 1974.

[18] R.M. Barrer, Hydrothermal Chemistry of Zeolites; Academic Press: London, 1982.

[19] R. Szostak, Molecular Sieves - Principles of Synthesis and Identification, 1st ed.; Van Nostrand Reinhold: New York, 1989; 2nd ed.; Blackie: London, 1998.

[20] www.iza-structure.org (1.1.2017)

[21] J. Ward, J. Catal. 9 (1967) 225.

[22] I.E. Maxwell, H.J. Strok, Stud. Surf. Sci. Catal. 137 (2001) 775.

[23] R.J. Argauer, G. R. Landolt, U.S. Patent (1972) 3,702,886.

[24] C. Knottenbelt, Catal. Today 71 (2002) 437.

[25] W. Lieber, M. Wagner, Erdoel Erdgas Kohle 120 (2004) 323.

[26] C. Ringelhan, G. Burgfels, J. G. Neumayr, W. Seuffert, J. Klose, V. Kurth, Catal. Today 97 (2004) 277.

[27] S. Zinger, Petroleum Technology Quarterly 10(4) (2005) 125.

[28] W. Vermeiren, D. H. Wei, R. B. James, J. M. Andersen, Hydrocarbon Eng. 8(10) (2003) 79.

[29] U. Koss, Hydrocarbon Eng. (1999) 66.

[30] P.A. Ruziska, T.R. Steffens, AIChE Spring meeting, Houston, 2001.

[31] T.Tsunoda, M. Sekiguchi, Catal. Surv. Asia. 12 (2008) 1.

[32] M. Tallman, S. Borsos, EPTC, Prague. 2000.

[33] J. Teng, Z. Xie, ERTC petrochemical conference, Brussels, 2007.

[34] P.B. Venuto, E.T. Habib, Fluid catalytic cracking with zeolite catalysts. Marcel Dekker, Inc., New York, 1979.

[35] Y. Yoshimura, N. Kijima, T. Hayakawa, K. Murata, K. Suzuki, F. Mizukami, K. Matano, T. Konishi, T. Oikawa, M. Saito, T. Shiojirna, K. Shiozawa, K. Wakui, G. Sawada, K. Sato, S. Matsuo, N. Yamaoka, Catal. Surv. Jpn. 4 (2000) 157.

[36] C. Eng, AIChE Spring national neeting, Houston, 2007.

[37] H. Koempel, W. Liebner, Stud. Surf. Sci. Catal. 167 (2007) 261.

[38] L. Wang, L. Tao, M. Xie, G. Xu, J. Huang, Y. Xu, Catal. Lett. 21 (1993) 35.

[39] K. Honda, X. Chen, Z-G. Zhang, Appl. Catal. A: General, 351 (2008) 122.

[40] T.F. Degnan Jr., C.M. Smith, C.R. Venkat, Appl. Catal. A: Gen. 221 (2001) 283.

[41] C. Perego, P. Ingallina, Catal. Today 73 (2002) 3.

[42] J.P. Breen, R. Burch, M. Kulkarni, D. McLaughlin, P.J. Collier, S.E. Golunski, Appl. Catal. A: Gen. 316 (2007) 53.

[43] M. Guisnet, P. Magnoux, Appl. Catal. A: Gen. 212 (2001) 83.

[44] S. Malola, S. Svelle, F.L. Benken, O. Swang, Angew. Int. Ed. 51 (2012) 652.

[45] G. Caeiro, P. Magnoux, J.M. Lopes, F.R. Ribeiro, S.M.C. Menezes, A.F. Costa, H.S. Cerqueira, Appl. Catal. A 312 (2006) 160.

[46] H.E. Bij, B.M. Weckhuysen, Chem. Soc, Rev. 44 (2015) 7406.

[47] Y. Yoshimura, N. Kijima, T. Hayakawa, K. Murataa, K. Suzuki, F. Mizukami, K. Matano, T. Konishi, T. Oikawa, M. Saito, T. Shiojima, K. Shiozawa, K. Wakui, G. Sawada, K. Sato, S. Matsuo, N. Yamaoka, Catal. Surv. Jpn. 4 (2000) 157.

[48] Y. Yoshimura, K. Matano, F. Mizukami, Catalysts 43 (2001) 218.

[49] T. Sano, H. Ikeya, T. Kasuno, Z. B. Wang, Y. Kawakami, K. Soga, Zeolites 19 (1997) 80.

[50] R. M. Lago, W. O. Haag, R. J. Mikovsky, D. H. Olson, S. D. Hellring, K. D. Schmitt, G. T. Kerr, Stud. Surf. Sci. Catal. 28 (1986) 677.

[51] Y. Sendoda, Y. Ono, Zeolites 8 (1988) 101.

[52] T. Blasco, A. Corma, J. Martínez-Triguero, J. Catal. 237 (2006) 267.

Chapter 2

Screening of Zeolite Topologies for the Catalytic Cracking of Naphtha

Abstract

As a research start, screening tests of zeolite topology were carried out with the aim of investigating which topology zeolite was effective for naphtha cracking. Since it was practically impossible to test all the 232 kinds of topologies, 26 kinds of zeolites that seemed promising and had a topology that could be obtained and synthesized were evaluated. As a result, ZSM5 (MFI) zeolite showed the highest activity and the conversion rate was slightly reduced. In addition, MCM22 (MWW), Beta (BEA), MCM68 (MSE) also showed relatively high activity, but the activity decreased comparatively faster.

2.1 Introduction

For production of lower olefins by catalytic cracking from saturated hydrocarbons such as naphtha as raw materials, materials having a stable crystal structure even at high temperature, pores with shape selectivity of product, high surface area and acidic property are selected as a good catalyst. Zeolite can be mentioned as materials satisfying such conditions. Depending on the type of zeolite, the arrangement of the skeleton forming pores is different. There are 232 kinds of topology, the difference of this skeleton, presently. Screening was carried out with the aim of investigating which topology zeolite was effective for this reaction. Since it was practically impossible to test all topologies, a few of 20 zeolites that seemed promising and had a topology that could be obtained and synthesized were evaluated.

2.2 Experimental

2.2.1 Catalytic cracking of n-hexane

The catalytic performance of various zeolite were tested by the catalytic cracking of *n*-hexane (Wako, 96%). *n*-Hexane was selected as a model alkane compound because of the similar molecular weight as the mean one of light naphtha. The cracking of *n*-hexane was carried out in a 7 mm hastelloy C276 tubular flow reactor loaded with 0.36 g of 250–500 μm zeolite pellets without a binder, which was the catalyst was centered at the reactor in a furnace. The reactor was heated to the reaction temperature (873 K) with N_2 flow into the temperature of catalyst bed at 823K. N_2 flow rate was changed to 52 Ncc/min and *n*-hexane was introduced. The weight hourly space velocity of *n*-hexane (WHSV) was set to 10 h^{-1}. The reaction products were analyzed with on-line gas chromatographs (Shimadzu GC-2014) with two FID detectors and a TCD detector. The selectivity to the products and the *n*-hexane conversion were calculated based on the carbon numbers.

2.2.2 Measurement of coke amount deposited on catalyst

The amount of coke deposited on the catalyst was analyzed by raising the temperature to 1173 K at 10 K per a minute under air flow using a thermogravimetric

analyzer (Thermoplus EVO Ⅱ TG-8120 manufactured by Rigaku). The weight of the burned coke with respect to the catalyst weight excluding coke was taken as the coke amount (wt%).

2.3 Results and discussion

2.3.1 Screening of zeolite topology by cracking test

26 kinds of zeolites that seemed promising and had a topology that could be obtained and synthesized were evaluated. Table 1 lists tested zeolites, its number of ring of pore and dimension of the pore. The catalytic cracking reaction of *n*-hexane was carried out by diluting to about 5 times with nitrogen for 10 h at 923 K, WHSV = 10 h^{-1}. Results of catalytic cracking of *n*-hexane are shown in Fig. 1. The product distribution for each zeolite topology 3 hours after the start of the reaction is shown in this figure. As a result, ZSM5 (MFI) [1] zeolite showed the highest activity and the conversion rate was slightly reduced. Since ZSM11 has the same skeleton as ZSM5, it was identified [2]. In addition, MCM22 (MWW) [3], Beta (BEA) [4], MCM68 (MSE) [5] also showed relatively high activity and high selectivity of propene. Furthermore, the time course of the hexane conversion and the total yield of ethene and propene for ZSM5, MCM22, Beta and MCM68 are shown in Fig. 2. ZSM5 zeolite was retained at a high conversion rate through 19 h, but other zeolites showed a decrease in activity from the start of the reaction despite the fact that nitrogen was circulated for the purpose of preventing decrease in activity. The amount of coke deposited to each zeolite catalyst after the reaction was measured and found to be 21 wt% for ZSM5, 15 wt% for MCM22, 2 wt% for Beta and 27 wt% for MCM68. Since Beta zeolite was found deactivated at only 2 wt%, it could be said that coke resistance was low. In addition, Beta zeolite has low thermal stability from the viewpoint of structure. Therefore, it was considered that the decrease in activity occurred due to progression of dealumination. The amount of coke in MCM68 was as high as 27 wt%. This was presumed to be the result of the accumulation of coke in the large space existing in the intersection of this topology. Comparing ZSM5 and MCM22, ZSM5 showed less activity decline despite the higher coke content. Therefore, it can be said that ZSM5 has higher coke resistance. In order to

carry out operation for a long period of time under the condition that coke is likely to be generated, zeolite with less deactivation is preferable, and among these zeolites, ZSM5 can be said to be the zeolite most suitable for naphtha decomposition. Even so, these other three zeolites (MCM22, Beta and MCM68) had high propene selectivity, so there is room for further investigation [6-8]. Also interestingly, the zeolites of top 10 topologies with high activity all had 10 or more membered ring. Conversely, the 8-membered ring zeolite showed low activity. SAPO zeolite which is silica-aluminophosphate also showed little activity.

2.4 Conclusions

As a research start, 26 kinds of zeolites that seemed promising and had a topology that could be obtained and synthesized were evaluated. As a result, ZSM5 (MFI) zeolite showed the highest activity and the conversion rate was slightly reduced. In addition, MCM22 (MWW), Beta (BEA), MCM68 (MSE) also showed relatively high activity, but the activity decreased comparatively faster. Therefore, in this research, the performance improvements of ZSM 5 zeolite were examined.

References

[1] G.T. Kokotailo, S.L. Lawton, D.H. Olson, W.M. Meier, Nature, 272 (1978) 437.-438 (1978).

[2] C.A. Fyfe, H. Gies, G.T. Kokotailo, C. Pasztor, H. Strobl, D.E. Cox, J. Am. Chem. Soc. 111 (1989) 2470.

[3] M.E. Leonowicz, J.A. Lawton, S.L. Lawton, M.K. Rubin, Science, 264 (1994) 1910.

[4] J.B. Higgins, R.B. LaPierre, J.L. Schlenker,A.C. Rohrman, J.D. Wood, G.T. Kerr, W.J. Rohrbaugh, Zeolites 8 (1988) 446.

[5] D.L. Dorset, S.C. Weston, S.S. Dhingra, J. Phys. Chem. B 110 (2006) 2045.

[6] Y. Wang, T. Yokoi, S, Namba, J.N. Kondo, T. Tatsumi, J. Catal. 333 (2016) 17.

[7] Y. Wang, R. Otomo, T. Tatsumi, T. Yokoi, Micropor. Mesopor. Mater. 220 (2016) 275.

[8] Y. Kubota, S. Inagaki, K. Takechi, *Catal. Today* 226 (2014) 109.

Table 1 List of investigation into zeolite topology for catalytic cracking of *n*-hexane

Zeolite	**Framework type code**	**Ring size**	**Dimension**
H-ZSM11	MEL	10	3
H-ZSM5	MFI	10	3
H-MCM22	MWW	10	2
H-BETA	BEA	12	3
H-MCM68	MSE	12 10	3
H-Mordenite	MOR	12 8	1
H-ZSM22	TON	10	1
H-ZSM12	MTW	12	1
H-CIT1	CON	12 10	3
H-SSZ42	IFR	12	1
H-SSZ55	ATS	12	1
H-IM5	IMF	10	3
H-Y	FAU	12	3
H-UZM5	UFI	8	2
H-CIT1	CON	12 10	3
H-RUB41	RRO	10 8	2
H-UTM1	MTF	8	1
H-RUB50	LEV	8	2
SAPO34	CHA	8	3
SAPO11	AEL	10	1
Linde type L	LTL	12	1
H-SUZ4	SZR	10 8	3
H-Ferrierite	FER	10 8	2
SAPO17	ERI	8	3
SAPO5	AFI	12	1
SAPO56	AFX	8	3
H-ITQ29	LTA	8	3

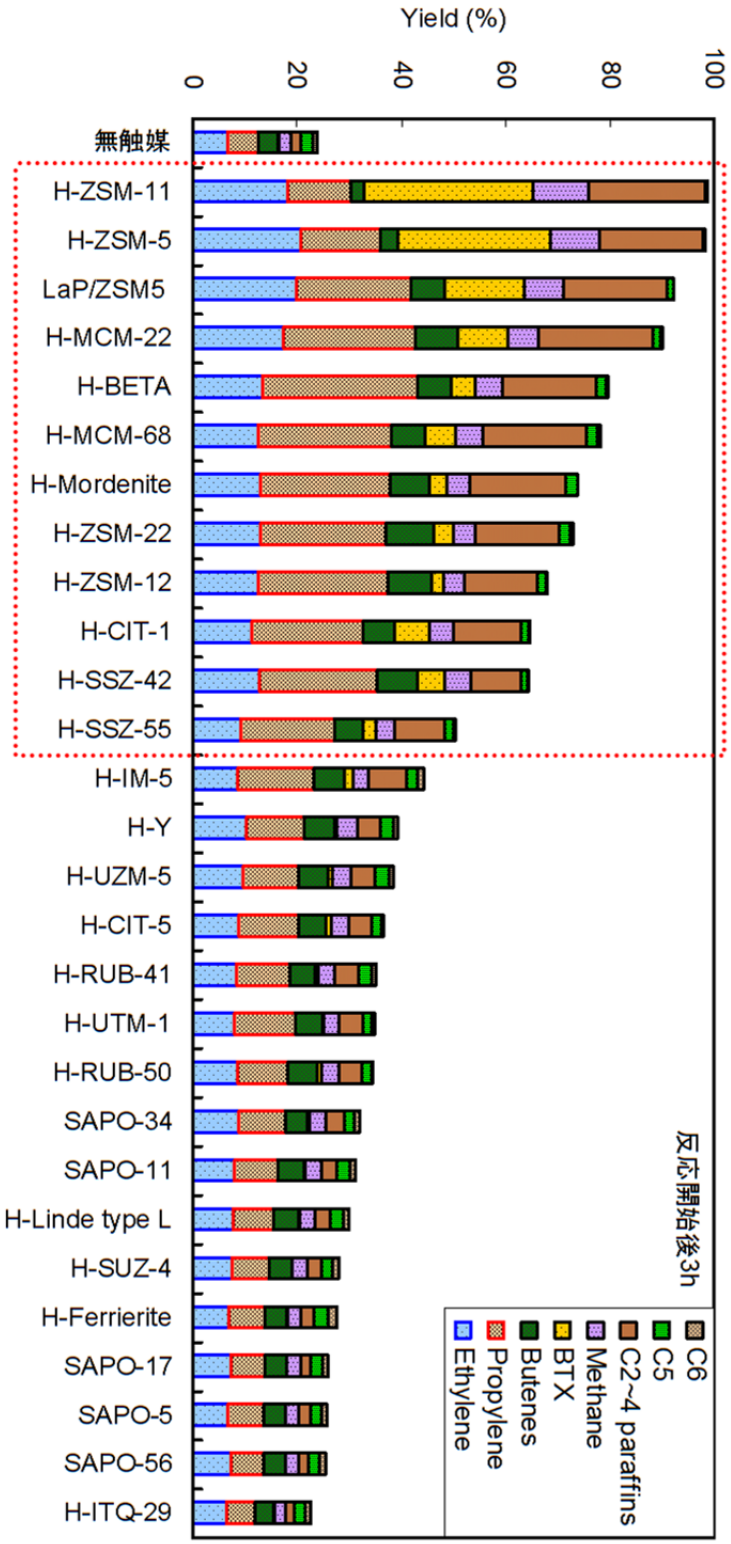

Fig. 1 The product distribution of *n*-hexane cracking over the various zeolite for the screening tests of zeolite topology.

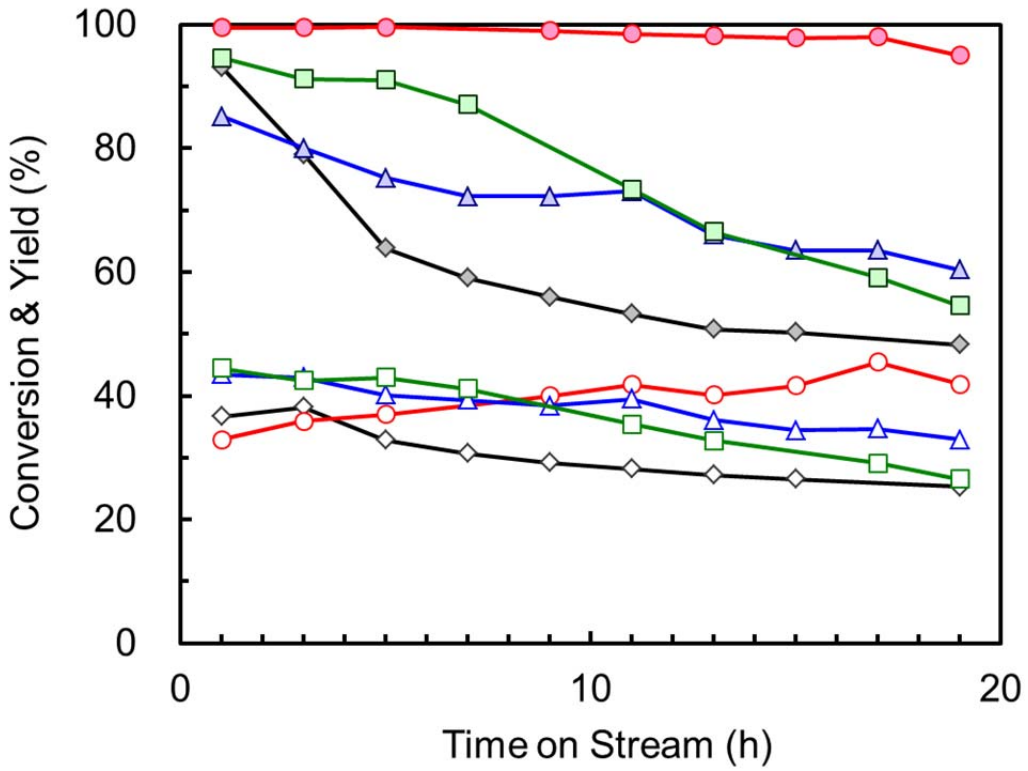

Fig. 2 The time course of the conversion of *n*-hexane cracking reaction and total yield of ethene and propene over ZSM5, MCM22, Beta, and MCM68. Fill plots are conversion of *n*-hexane; ●: ZSM5, ■: MCM22, ◆: MCM68, ▲: Beta. Blank plots are total yield of propene and ethene; ○: ZSM5, □: MCM22, ◇: MCM68, △: Beta.

Chapter 3

The Effective Silylation of External Surface on H-ZSM5 with Cyclic Siloxane for the Catalytic Cracking of Naphtha

Abstract

Acid sites existing on the external surface of zeolites are the main cause of the formation of coke materials, resulting in decreasing the catalytic activity. For the durability of the reaction, silylation of external acid sites was adopted. Among various silylation reagents, cyclic siloxanes were effective silylation compounds for the deactivation of the acid sites on external surface on zeolite without prohibiting the objective reaction, cracking of naphtha. The effect of silylation was confirmed not only by the reaction but also by infra-red analysis.

3.1 Introduction

Light olefins (ethene, propene, butenes and butadiene) and aromatic compounds represented by benzene, toluene and xylene are indispensable elemental chemicals for the production of such principal chemicals as plastics, synthetic fibers, synthetic rubbers, paints, synthetic detergents, medicines, and so on. These source chemicals are mainly produced by thermal cracking of naphtha at 1073 K and above because of the low reactivity of these components. Practically, the temperature range, where profitable product yield is gained, is very much limited. Since the product distribution of naphtha cracking solely depends on the cracking temperature, it is very difficult to selectively produce desirable chemicals for the demand. Nowadays, around middle-east, less expensive ethane is the most competitive feed stock of ethene than naphtha, and ethene and its derivatives flow in enormous Asian market. On the other hand, this process, starting with ethene, does not produce so much propene that it cannot supply the propene demand sufficiently. The demand for propene and its derivatives increases rapidly and exceeds that for ethene and its derivatives. This tendency is regarded accelerated from now on. Under such circumstances, any naphtha cracking processes that can control the product distribution so as to meet the demand has been desired. In particular, the catalytic cracking of naphtha has been expected as one of the valuable technologies. In comparison to conventional “energy-consuming” naphtha cracker, this technique suppresses the generation of carbon dioxide remarkably and limits the consumption of fossil resource efficiently [1].

The use of acidic zeolites have been proposed as precedent technology for naphtha cracking catalysts, and the temperature of cracking by using zeolites are decreased to 873–973 K [2–7]. In addition, the ratio of propene to ethene in total products can be increased due to the lower reaction temperature range. Not only the yield of ethene and

propene but also the yield of other valuable chemicals was controllable by this catalytic process. However, opened techniques of catalytic cracking of naphtha are not mature enough to substitute the conventional thermal cracking process. In fact, because the temperature of cracking has not been controlled well, primary products react sequentially and carbon material, so-called coke, is produced. Coke materials deposited on the surface of zeolite catalysts block pores or acidic sites, resulting in decreasing the catalytic activity. In order to idealize the process at the industrial level, durability of catalysts must be improved by suppressing the coke formation. The durability of catalyst also decreases both the fluctuation in product distribution and the cost of purification.

Coke is considered being produced by sequential side reactions of objective light olefin products, such as oligomerization, cyclization, dehydration, and so on. The coke formation becomes remarkable at temperatures above 873 K, where the catalytic cracking of naphtha is operated. In general, when zeolites are used as heterogeneous catalysts, objective products are generated by structurally selective reactions at acid sites in the zeolite pores. Nevertheless, acid sites also exist on the external surface of zeolite, and the non-selective reactions without restriction by porous structure are promoted, resulting in coke formation. It is reported that the selective deactivation of acid sites on the external surface leads to the suppression of coke formation and increases the selectivity of objective products, because coke formation proceeds mainly on the surface of zeolite [8–10]. As one of the deactivation methods of acid sites on the external surface of zeolite, silylation covering method of those sites is often adopted using silyl compounds [11–18]. Silylation compounds, which have steric hindrance represented by alkoxysilanes, alkylsilanes, halosilanes, polysiloxanes and so on, are generally often used. After silylation, simple calcination in air leads to the formation of silica species covering acid sites on external surface. Acid sites of zeolite exist

uniformly on internal and external surfaces. In order to encourage shape selective reactions over active sites on the internal surface, it is necessary to selectively deactivate acid sites on the external surface by silylation using silyl compounds, whose molecular sizes are larger than zeolite pores. If the molecular size of silyl compounds is similar to that of zeolite pores or if silyl compounds possess any side chains, which are inserted in pores, the compounds cover the inlet of zeolite pores to narrow the apparent pore size, resulting in the disturbance of diffusion of reactants. Therefore, silyl compounds whose molecular size are sufficiently larger than zeolite pores are desirable. On the other hand, if the size of silyl compounds is too large, the steric hindrance leads the decrease in efficiency of silylation [13]. In addition, large silicon oxide phase formed on the external surface of zeolite during calcination after silylation blocks zeolite pores. To evade those problems the selection of appropriate silylation compounds, which adapt to the number of member ring, pore size and pore shape of zeolites are required.

Based on the above considerations, typical sylilation compounds include polysiloxanes, orthosilicates and chlorosilanes. For example, Mobil reported that bulky polysiloxanes. Mobil reported that bulky polysiloxanes as silylation compounds were effective for toluene disproportionation with a high selectivity to *p*-xylene on MFI type zeolite [15–17]. They proposed that the silylation compounds were fed with toluene to compensate for low silylation efficiency because of steric hindrance. Zeolite catalysts were silylated continuously contacting silylation compounds. This process cannot evade not only low silylation efficiency of bulky silylation compounds but also continuously feed of silylation compound. If the silylated catalysts were calcined, covering of acid sites on the external surface of zeolite efficiently proceeded. For more efficiency of silylation, (1) before reaction, preliminary silylation of catalysts, and in reaction, silylation compounds are fed continuously or (2) silylation compounds are fed

continuously for more than 50 h during reacting at low selectivity and a certain degree of high selectivity reaction proceed. In this process, selectivity of p-xylene which was produced on acid sites in zeolite pore increased, although adding of silylation compounds resulted in decrease of conversion.

Can Li et. al. reported polydimethylsiloxanes were good silylation compounds for deactivation of the acid sites on the external surface of HZSM5 zeolite [13]. However, polydimethylsiloxanes don't have reactive functional group such as Si-H bond or Si-Cl bond, so they don't make chemical bonds with surface of zeolite. That's why in this case, after calcination under air for covering the acid sites on the external surface of zeolite, dimethylsilanes which were produced by decomposition of polydimethylsiloxane in the calcination condition entered the zeolite pore. It indicated bulky silylation reagents also partially deactivate internal acid sites of zeolite which have catalytic activity.

Kikkawa et al. reported silylation of surface of porous SiO_2 with cyclic polyhydrosiloxanes which have highly reactive Si-H bond [22]. Covering ratio of SiO_2 surface by chemical vaporization deposition method was controlable by using silylation reagents such as 1,3,5,7-tetramethylcyclotetrasiloxane which had ideal size and reactive functional group. Efficient silylation was resulted from fixation of cyclic polydhydrosiloxanes on surface of SiO_2 via Si-O-Si bond by multipoints. Fukui proposed that 1,3,5,7-tetramethylcyclotetrasiloxane formed network polymer by crosslinking with the surface of SiO_2, and inactivation of the surface was proceeded. These methods clarified that cyclic siloxanes which had many reactive functional groups and mild polymerization degree were ideal silylation compounds for inactivation for SiO2. However, the applications of the cyclic polyhydrosiloxanes were only for electronic circuit cards or cosmetics and not for catalyst application [25-27].

In summary, cyclic polyhydrosiloxanes which have highly reactive functional

group such as Si-H bond were used for silylation compounds for inorganic materials whose main component were SiO2, but materials silylated by cyclic hydrosiloxanes were not used as catalysts [28].

On the other hand, evaluation of acid amount on the external surface of zeolites is indispensable to perform silylation. The conventional evaluation methods were indirect: it was estimated by the change of the objective reaction or cracking reaction of 1, 3, 5-triisopropylbenzene before and after silylation [19]. Recently, Kubota, et. al. reported the direct evaluation of the amount of acid sites on the external surface not by reactions but using infrared (IR) spectroscopy [20]. In this paper, various new types of silylation compounds were employed to efficiently suppress coke formation without decreasing the catalytic performance of naphtha cracking over H-ZSM5. In addition, the location of acid sites on H-ZSM5 before and after silylation was confirmed by IR spectroscopy using adsorption of probe molecules with various sizes [28].

3.2 Experimental

3.2.1 Synthesis of H-ZSM5 zeolite

Tetraorthosilicate (TEOS, Wako Pure Chemical Industries, Ltd., > 95%) was added to tetrapropylammonium hydroxide (TPAOH, 25% aqueous solution, Tokyo Kasei). The resulting mixture was stirred at 353 K for 24 h. Thereafter, the solution containing water, $Al(NO_3)_3 \cdot 9H_2O$ (Wako, 99.9 %) and NaOH (Wako, 97%) was added to the mixture and stirred at 298 K for 1 h. Thus, prepared mother gel was crystallized at 443 K for 24 h. The molar composition of the final gel was 1 SiO_2: 0.0067 Al_2O_3: 0.25 TPAOH: 0.033 Na_2O: 8.3 H_2O. Then, the solid product was collected by filtration. The Na-ZSM5 sample was obtained by calcination of the as-synthesized sample in an oven at 823 K to remove TPA^+ species. The NH_4-ZSM5 sample was obtained by the treatment of

Na-ZSM5 samples with 1 M NH_4NO_3 (Wako, 99%) aq. at 353 K for 12 h twice. The H-ZSM5 samples were obtained by calcination of the NH_4-ZSM5 samples at 823 K for 10 h.

3.2.2 Silylation

For the silylation, a liquid phase method was adopted in order to perform the silylation by a simple operation with general versatility. Silylation of the H-ZSM5 was performed with each silylation compound in xylene. To 120 ml of xylene was added 6.0 g of H-ZSM5. After 4.0 mmol of 1, 3, 5, 7-Tetramethylchyclotetrasiloxane (TMCTS) was added dropwise under a nitrogen atmosphere at 298 K, the mixture was stirred at 343 K for 17 h, filtered, washed by *n*-hexane and dried. The dried sample was calcined at 823 K for 10 h to obtain silylated H-ZSM5 (TMSCT). In the same way, silylations of H-ZSM5 were perfomed with other silylation compounds (shown in table 1); 1, 3, 5, 7, 9-pentamethylcyclopentasiloxane (PMCPS), Tris (trimethylsiloxy) silane (TTMSS), Tetraethoxysilane (TEOS), Dichlorotetramethylsiloxane (DCTMSLX), Diphenyldichlorosilane (DPDCS), and Dichlorotetramethylsilane (DCTMS), to obtain silylated H-ZSM5 (PMCPS), H-ZSM5 (TTMSS), H-ZSM5 (TEOS), H-ZSM5 (DCTMSLX), H-ZSM5 (DPDCS), and H-ZSM5 (DCTMS), respectively.

3.2.3 N_2 adsorption

Nitrogen adsorption-desorption isotherms were measured to obtain information on the micro- and meso-porosities at 77 K on a Belsorp-max (Microtrac-Bel). The BET specific surface area (S_{BET}) was calculated from the adsorption data in the relative pressure ranging from 0.04 to 0.2. External surface area (S_{EXT}) was estimated by the *t*-plot method.

3.2.4 NH_3 TPD

Temperature-programmed desorption of ammonia (NH_3-TPD) spectra were recorded on Belcat-A (Microtrac-Bel). Typically, 25 mg catalyst was pretreated at 773 K in He for 1 h and then was cooled to adsorption temperature at 373 K. Prior to the adsorption of NH_3, the sample was evacuated. Approximately 5 vol% of NH_3 was allowed to contact with the sample for 30 min. Subsequently, the sample was evacuated to remove weakly adsorbed NH_3 for 15 min. Finally, the sample was heated from 373 to 973 K at a ramping rate of 10 K min^{-1} with the He flow passed through the reactor. A mass spectrometer (mass number 17) was used to monitor desorbed NH_3. The amount of acid sites was determined by using the area of the so-called *h*-peak in the profiles.

3.2.5 Si NMR and Al NMR

Solid state ^{27}Al magic-angle spinning (MAS) NMR spectra were obtained with $\pi/2$ pulse width of 6 μs and pulse delay of 5 s on a JEOL ECA-400 spectrometer. Al resonance frequency employed was at 104 MHz and the sample spinning rate speed was 5.3 KHz. ^{27}Al chemicals shifts were referenced to a saturated $Al(NO_3)_3$ solution.

3.2.6 Catalytic cracking of n-hexane

The catalytic performance of H-ZSM5 silylated by various silylation compounds were tested by catalysts the catalytic cracking of *n*-hexane (Wako, 96%). n-hexane was selected as a model alkane compound because of the similar molecular weight as the mean one of light naphtha. The cracking of *n*-hexane was carried out in a 7 mm hastelloy C276 tubular flow reactor loaded with 0.36 g of 250–500 μm zeolite pellets without a binder, which was the catalyst was centered at the reactor in a furnace. The reactor was heated to the reaction temperature (873 K) with N_2 flow into the temperature of catalyst bed at 823K, N_2 flow was stopped and *n*-hexane was introduced

without carrier gas. The weight hourly space velocity of *n*-hexane (WHSV) was set to 10 h^{-1}. The reaction products were analyzed with on-line gas chromatographs (Shimadzu GC-2014) with two FID detectors and a TCD detector. The selectivity to the products and the *n*-hexane conversion were calculated based on the carbon numbers.

3.2.7 Evaluation of acid sites on the external surface of zeolite

(1) Catalytic cracking of *n*-hexane

The H-ZSM5 silylated by various silylation compounds were used for the catalytic cracking of *n*-hexane (Wako, 96%). The reaction was carried out in a 6 mm quartz tubular flow microreactor loaded with 20 mg of 250–500 μm zeolite pellets without a binder. The catalyst was centered at the reactor in a furnace, and was heated to the reaction temperature (923 K) with He flow. The initial pressure of *n*-hexane was set at 4.8 kPa with He carrier gas. The weight hourly space velocity of *n*-hexane was set to 11 h^{-1}. The reaction products were analyzed with on-line gas chromatographs (Shimadzu GC-2014) with an FID detector.

(2) Catalytic cracking of 1, 3, 5-TIPB

The cracking of 1, 3, 5-triisopropylbenzene (TIPB, Tokyo Kasei, 95%) was carried out in a 6-mm quartz tubular flow microreactor loaded with 10 mg of 250–500 μm zeolite pellets without a binder. The catalyst was centered at the reactor in a furnace. The catalyst was calcined at 773 K for 1 h prior to the reaction. Then the reactor was cooled to the reaction temperature (573 K). The initial partial pressure of TIPB was set at 0.5 kPa. Helium was used as a carrier gas. The weight hourly space velocity of 1, 3, 5-TIPB (WHSV) was 2.6 h^{-1}. The reaction products were analyzed with an on-line gas chromatograph (Shimadzu GC-2014) with an FID detector.

3.2.8 IR analysis for calcination procedure of zeolite with silylation compound

H-ZSM5 was stirred wih 1, 3, 5, 7-tetramethylcyclotetrasiloxane in xylene at 343 K for 17 h under nitrogen atmosphere. After the reaction, the mixture was filtered, washed with *n*-hexane and dried. Then, the H-ZSM5-TMCTS sample, which was reacted with TMCTS, was obtained. H-ZSM5-TMCTS was pressed into a self-supporting disk (20 mm in diameter, 80 mg) and placed in the center of an IR cell attached to a conventional closed gas circulation system. The sample was pretreated by evacuation at 523 K for 1h. IR spectra were obtained at a resolution of 4 cm^{-1} using a Jasco 4100 FT-IR spectrometer equipped with a mercury cadmium telluride (MCT) detector. A total of 64 scans were averaged for each spectrum. The IR spectrum of the clean disk was recorded under evacuation at 523 K after 3.0 kPa of O_2 was introduced in order to observe the change of TMCTS species during combustion. The sample was heated from 523 to 773 K and the IR spectra were recorded at various temperatures.

3.2.9 IR analysis for HMI adsorption

Hexamethyleneimine (HMI) was used as a probe molecule to observed acid sites or to block on the external surface. CO was used to monitor the acid sites in the internal surface for the HMI-adsorbed samples. The various silylated H-ZSM5 samples was pressed into a self-supporting disk (20 mm in diameter, 50 mg) and placed in an IR cell attached to a conventional closed gas circulation system. After the sample was pretreated by evacuation at 773 K for 2 h, the IR spectrum of the clean disk was recorded under evacuation at 153 K. The sample was heated to 298 K and 0.3 kPa of HMI was introduced and evacuated at 298 K to remove the extra HMI. And then the sample was cooled to 153 K again, the IR spectrum was recorded. Finally CO was introduced at 153 K and the IR spectrum was recorded.

3.2.10 IR analysis for n-hexane adsorption for D_2 exchanged zeolite

The various silylated H-ZSM5 samples was pressed into a self-supporting disk (20 mm in diameter, 50 mg) and placed in an IR cell attached to a conventional closed gas circulation system. After the sample was pretreated by evacuation at 773 K for 1 h, the sample was cooled to 673 K, and then treated with 50 kPa of D_2 for 1.5 h. The sample was cooled to 90 K under evacuation and the IR spectrum of the clean disk was recorded under evacuation to 298 K as background spectra. Nextly, the sample was cooled to 90 K and 1 kPa of *n*-hexane was introduced. The IR spectra of the C_6-adsorbed disk were recorded under evacuation from 90 to 298 K.

3.3 Results and discussion

3.3.1 Catalysts characterization

Table 1 lists the BET surface area estimated by N_2 adsorption and the acid amounts estimated by NH_3-TPD analyses of H-ZSM5 catalysts. The surface area of all catalysts stayed almost unchanged except the catalyst silylated by TEOS due to the inclusion of a part of TEOS into zeolite pores or blocking of pore mouths on the external surface. The acid amounts of each silylated zeolite catalysts were lower than that of the parent H-ZSM5 as a result of silylation. No clear differences were found among all samples either by ^{29}Si or ^{27}Al MAS NMR analyses. In the ^{29}Si NMR spectra all signals appeared as a broad band above -108 ppm, indicating that catalysts consisted of mainly Q4 Si species. Because the Si/Al_2 ratio of all the catalysts was 150, i. e., the number of Al was low, Q3 Si species were not detected clearly. In ^{27}Al NMR spectra two signals existed; main signal centered around 53 ppm, and the other at -1 ppm in much smaller in intensity. This means that the Al atoms are mainly in tetrahedrally coordinated

atmosphere[21].

3.3.2 Catalytic tests

The time course of the conversion and yield of ethene and propene from *n*-hexane cracking over a series of silylated catalysts are shown in Fig. 1 (A) and (B), respecively. *n*-Hexane was used as a model compound of naphtha because of the similarity in molecular weight. While the deactivation over the original H-ZSM5 was noticed by the gradual decrease in conversion at the early stage of the time course, and the serious coking caused the pressure difference, resulting in the termination of the reaction in 17 h. On the other hand, evident improvement in durability was observed by silylation, especially for H-ZSM5 silylated by cyclic siloxanes (PMCPS and TMCTS). Consequently, the total yield of ethene and propene (Fig. 1(B)) was still higher than 35% for the two samples even at 25 h after the reaction started.

The acid amount on the external surface of zeolites was evaluated by catalytic cracking of 1, 3, 5-triisopropylbenzene (TIPB). Because of the sufficient large molecular size, TIPB cannot be incorporated inside the pores of H-ZSM-5, resulting in its cracking only at acid sites on the external surface. Thus, the conversion of TIPB cracking is proportional to the acid amounts on external surface of H-ZSM5 zeolite [19]. The comparison of *n*-hexane cracking and TIPB cracking reactions over each silylated H-ZSM5 catalyst are compared in Fig. 2. Slightly higher conversion was observed for TIPB cracking than *n*-hexane over the original H-ZSM5. While the conversion of *n*-hexane cracking reaction over silylated H-ZSM5 catalysts had similar to that of the original one, the conversion of cracking reaction of TIPB, a bulky reactant, decreased in the order H-ZSM5 (37%) > H-ZSM5 (DPDCS) (25%) > H-ZSM5 (TTMSS) (18%) > H-ZSM5 (TMCTS) (8%). Among the silylated H-ZSM5 samples, H-ZSM5 (TMCTS) had the least reactivity for TIPB cracking. So it reveals that cyclic siloxane covered acid

sites on the external surface of H-ZSM5 most efficiently and non-selective reaction on the external surface on H-ZSM5 (TMCTS) was suppressed.

3.3.3 IR analysis

In order to observe changes of the Brønsted acid and the silanol groups before and after silylation, IR spectra were measured during heating of the H-ZSM5 treated with cyclic siloxane (TMCTS) in the presence of oxygen (Fig. 3). Samples to be analyzed was H-ZSM5 zeolite which was stirred with TMCTS in xylene solvent, then filtered, washed and dried, and not calcined.While PMCPS was superior to TMCTS in Fig. 1, TMCTS is more often used in other researches as a cyclic silylation compound [22]. In addition, considering the generality and the lower cost, the characterization on the use of TMCTS seemed more informative. Thus, we carried out the characterization of TMCTS-silylated catalyst. Bands of Brønsted acid sites (BAS) and silanol groups (Si-OH) were observed at 3614 and 3750 cm^{-1}, respectively in the spectrum (Fig. 3A(a)) of H-ZSM5 before contact with TMCTS. At room temperature (298 K) under evacuation after contact with TMCTS, the signals derived from cyclic siloxane (2980 cm^{-1}: Si-CH_3, 2190 cm^{-1}: Si-H) and water adsorbed to sample (3500 cm^{-1}: H-O-H) were observed with decreasing the OH bands in intensity (b) in Fig. 3A [22]. After that, when the temperature was raised to 523 K under vacuum, the signal derived from Si-CH_3 decreased greatly (c) in Fig. 3A. This is because most of the methyl group of TMCTS was decomposed by heat. Since multiple peaks were observed around 2980 cm^{-1}, there was a possibility that species condensed with other methyl groups were generated during decomposition of methyl groups. Bands appearing below 2100 cm^{-1} are attributed to combination and overtone absorption bands of silica. The increase in temperature caused the combustion of Si-CH_3 and dehydrogenation of Si-H groups with the recovery of the silanol band in intensity. The protons of silanol were derived from

H_2O produced by burning methyl group or hydrogen group of TMCTS. Plots of the relationship between the integrated intensity of Si*OH* band and that of Si*CH_3* band on the IR spectra of the temperature raising process and the relationship between that of Si*OH* band and that of *SiH* band were shown in Fig. 3B. Since both plots showed linearity, it shows that the SiH and $SiCH_3$ species decreased with increasing silanol. Comparing spectra (a) and (l) in Fig. 3A, which were measured at the same temperature before and after a set of silylation treatment, the intensity of the band of Brønsted acid sites was weakened. Comparing the integrated intensity of the Brønsted acid sites to that of the SiOH bond before and after silylation, it decreased from 0.54 before silylation to 0.46 after silylation. Assuming that the amount of silanol was constant before and after silylation, the Brønsted acid amount has decreased by 13%. The 1,3,5-TIPB cracking activity decreased by about 75% before and after TMCTS treatment. The external surface area of the catalyst was calculated to be 69 m^2/g by t-plot. Of the total specific surface area of 415 m^2/g, the amount of the acid sites of external surface was reduced by 75 %, so 12 % of the total acid amount decreased. This value is in good agreement with the decrease value of the Brønsted acid amount measured by IR. With combination of results of cracking of TIPB (Fig. 2), this is most probably due to the selective silylation of Brønsted acid sites on the external surface by cyclic siloxane.

Next, IR characterization of catalysts silylated by cyclic siloxanes was performed for the examination of the site of silylation using adsorption of basic probe molecules. Hexamethyleneimine (HMI), which can hardly enter inside H-ZSM5 zeolite pores like collidine (2,4,6-trimethylpyridine), was adsorbed as the basic probe molecule to each silylated H-ZSM5 catalyst for the observation of acid sites on the external surface (Fig. 4) [23]. The intensity of spectra for different samples was normalized by the intensity of combination and overtone absorption bands of silica appearing at 2200–1400 cm^{-1}. IR spectra of background and HMI-adsorbed catalysts are shown in Fig. 4(A) and (B),

respectively. Subtracted spectra of (A) from (B) are also calculated to see changes clearly (spectra in (C)). The ratio of integrated intensity of acidic OH and silanol groups in background and subtracted spectra are also shown. The negative bands of the isolated OH groups in spectra (C) indicate the occurrence of adsorption of HMI. By comparing the change of the ratio of integrated intensity, (BAS)/(Si-OH), it is found that the acidic OH groups were more accessible by HMI than silanol groups in bottom 6 samples in Fig. 4, whereas they were less consumed as adsorption sites in case cyclic siloxanes were used (top 2 samples). Therefore, cyclic siloxanes preferentially occupy the external acid sites.

CO adsorption was observed for HMI-adsorbed parent and silylated H-ZSM5 in order to observe acid sites inside pores. Background spectra of HMI-adsorbed samples were subtracted from spectra measured after CO adsorption at 153 K (Fig. 5A). The isolated acidic OH band at 3617 cm^{-1} was converted to a broad hydrogen-bonded one at lower frequency, which is related to the band of adsorbed CO at 2174 cm^{-1}. In the IR spectra when the introduction amount of CO was increased, the relationship between the integrated intensity of acidic hydroxyl group band and that of adsorbed CO band or that of hydrogen-bonded hydroxyl group band are showed in Fig. 5B. Both plots show linearity, and the decrease in the amount of Brønsted acid sites are correlated with the increase of hydrogen bonding hydroxyl group and adsorbed CO. Since the adsorption of CO was observed for all samples, it is concluded that acidic sites inside pores are still active after silylation by TMCTS and DPDCS.

For obtaining the information on the behavior of hydrocarbons, adsorption of *n*-hexane was observed by IR [24]. Zeolite samples were deuterated to convert OH to OD groups by D_2 treatment before adsorption in order to distinguish them from hydrogen in adsorbate. *n*-Hexane was introduced into the cell at 123 K followed by evacuation. FT-IR spectra were recorded during the gradual warming procedure up to

293 K under evacuation (spectra (A) and (B) in Fig. 6). Subtracted spectra of background measured before *n*-hexane adsorption are shown. At 123 K introduced *n*-hexane was trapped onto the inner wall of cell, then the *n*-hexane was released in gas phase and adsorption commenced on the surface of the zeolite as the temperature was raised. Then, intensity of bands derived from the adsorbed species (CH bands of *n*-hexane at 3000–2800 cm^{-1}) increased. While inverse band of acidic OD groups 2667 cm^{-1} was observed from 208 K on the parent H-ZSM5, it was absent at temperatures below 215 K on the silylated sample. At the same time, band of hydrogen-bonding OD groups interacting with hexane was observed as a broad peak at 2540 cm^{-1}. Since the diffusion of *n*-hexane was prohibited at low temperature, adsorption occurred only at the external surface. Thus the effective silylation by TMCTS on the outer surface was convinced. Then, by increasing temperature, gradual adsorption on the acidic OD groups was observed also on the silylated sample due to the excitation of breathing mode of zeolite pores, which allowed the diffusion of *n*-hexane inside the pores. These results indicate that the temperature of *n*-hexane adsorption accompanied by diffusion can be a measure of the extent of blocking of external acid sites.

3.4 Conclusions

On the external surface of the zeolite, there are acid sites which do not have shape selectivity. Since this acid sites are not subjected to steric constraints, oligomerization of cracking products proceeds and the growth of coke materials are promoted. Since the catalyst is deactivated by coke formation, investigation was made to cover the acid sites on the external surface of the zeolite with a silylating reagent for the purpose of prolonging the lifetime of the ZSM5 zeolite catalyst in the hexane cracking reaction. H-ZSM5 silylated by cyclic siloxanes such as TMCTS, PMCPS and so on have more

durability for the catalytic cracking of *n*-hexane than H-ZSM5 silylated by other silylation compounds. IR analysis in addition to reaction results revealed that silylation by cyclic siloxanes covered the acid sites on the external surface of zeolite more efficiently. Thus, the suppression of coke formation was attained, and increases of the selectivity of objective products were achieved.

References

[1] T. Ren, M. Patel, K. Blok, Enegy, 31 (2006) 425.

[2] N. Rahimin, R. Karimzadeh, Appl. Catal. A: Gen. 1 (2011) 398.

[3] S.M. Alipour, Chenese J. Catal. 37 (2016) 67.

[4] A. Corma, A.V. Orchilles, Micropor. Mesopor. Mater. 35–36 (2000) 21.

[5] Y, Nakasaka, T. Tago, T. Masuda, Chem. Eng. J. 278 (2015) 159.

[6] S.M. Sadrameli, Fuel 140 (2015) 102.

[7] S.M. Sadrameli, Fuel 173 (2016) 285.

[8] D.M. Bibby, N.B. Milestone, J.E. Patterson, L.P. Aldridge, J. Catal. 97 (1986) 493.

[9] K. Urata, S. Furukawa, T. Komatsu, Appl. Catal. A: Gen. 475 (2014) 335.

[10] H. Konno, T. Tago, Y. Nakasaka, R. Ohnaka, J. Nishimura, T. Masuda, Micropor. Mesopor. Mater. 175 (2013) 25.

[11] M. Niwa, S. Kato, T. Hattori, Y. Murakami, J. Chem. Soc., Faraday Trans. 1. 80 (1984) 3135.

[12] K. Tominaga, S. Muraoka, M. Gotoh, N. Katada, M. Niwa, M. Micropor. Mesopor. Mater. 117 (2009) 523.

[13] Z. Zhu, Z. Xie, Q. Chen, D. Kong, W. Li, W. Yang, C. Li, Micropor. Mesopor. Mater. 101 (2007) 169.

[14] T. Tago, M. Sakamoto, K. Iwakai, H. Nishihara, S. Mukai, T. Tanaka, T.; Masuda, J. Chem. Eng. Jpn. 42 (2009) 162.

[15] P.G. Rodewald, US Patent (1983) 4477583.

[16] C.D. Chang, P.G. Rodewald, US Patent (1997) 5607888.

[17] J.S. Beck, T.F. Kinn, S.B. McCullen, D.H. Olson, D.L. Sterm, US Patent (1997) 5659098.

[18] R. Ryoo, J.H. Kwak, L.-C. Menorval, J. Phys. Chem. 98 (1994) 7101.

[19] C.S.H. Chen, S.E. Schramm, Micropor. Mesopor. Mater. 7 (1996) 125.

[20] S. Inagaki, S. Shinoda, Y. Kaneko, K. Takechi, R. Komatsu, Y. Tsuboi, H. Yamazaki, J.N. Kondo, Y. Kubota, ACS Catal. 3 (2013) 74.

[21] J.V. Prasad, K.V. Rao, Y.S. Bhat, A.B. Hargeri, Catal. Lett. 14 (1992) 349.

[22] Y. Kayaba, K. Kohmura, H. Tanaka, Y. Seino, T. Ohdaira, S. Chikaki, T. Kikkawa, Thin Solid Films 519 (2010) 674.

[23] M.S. Holm, S. Svelle, F. Joensen, P. Beato, C. Christensen, S. Bordiga, M. Brørgen, Appl. Catal., A 356 (2009) 23.

[24] J.N. Kondo, F. Wakabayashi, K. Domen, J. Phys. Chem. B 102 (1998) 2259.

[25] H. Fukui, Hyomen (1994) 131.

[26] K. Komura, S. Oike, T. Kubota, M. Murakami, Y. Kurano Jp Patent (2009) 4261297.

[27] T. Kanamaru, H. Fukui, M. Yamaguchi, Jp Patent (1996) 92484.

[28] J.S. Yoo, Catal. Today 41 (1998) 409.

Table 1 The BET surface area estimated by N_2 adsorption and the acid amounts estimated by NH_3-TPD analyses of H-ZSM5 catalysts.

Catalyst	**Silylating reagent**	**S_{BET} / $m^2 \cdot g^{-1}$**	**Acid amount / $mmol \cdot g^{-1}$**
H-ZSM5	-	415	0.19
H-ZSM5 (TMCTS)	TMCTS	403	0.10
H-ZSM5 (PMCPS)	PMCPS	394	0.07
H-ZSM5 (TTMSS)	TTMSS	411	0.12
H-ZSM5 (TEOS)	TEOS	360	0.10
H-ZSM5 (DCTMSLX)	DCTMSLX	398	0.12
H-ZSM5 (DPDCS)	DPDCS	401	0.15
H-ZSM5 (DCTMS)	DCTMS	406	0.14

List of silylating compounds

TMCTS:

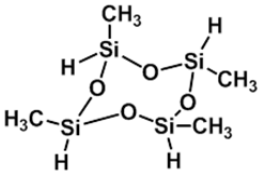

PMCPS:

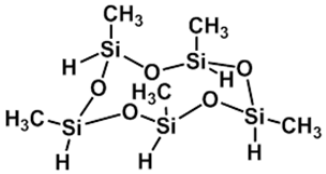

TTMSS:

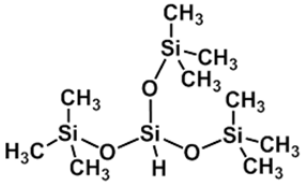

TEOS:

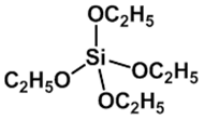

DCTMSLX:

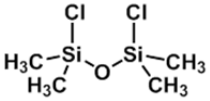

DPDCS:

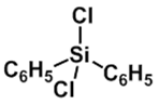

DCTMS:

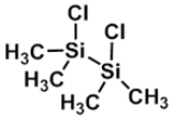

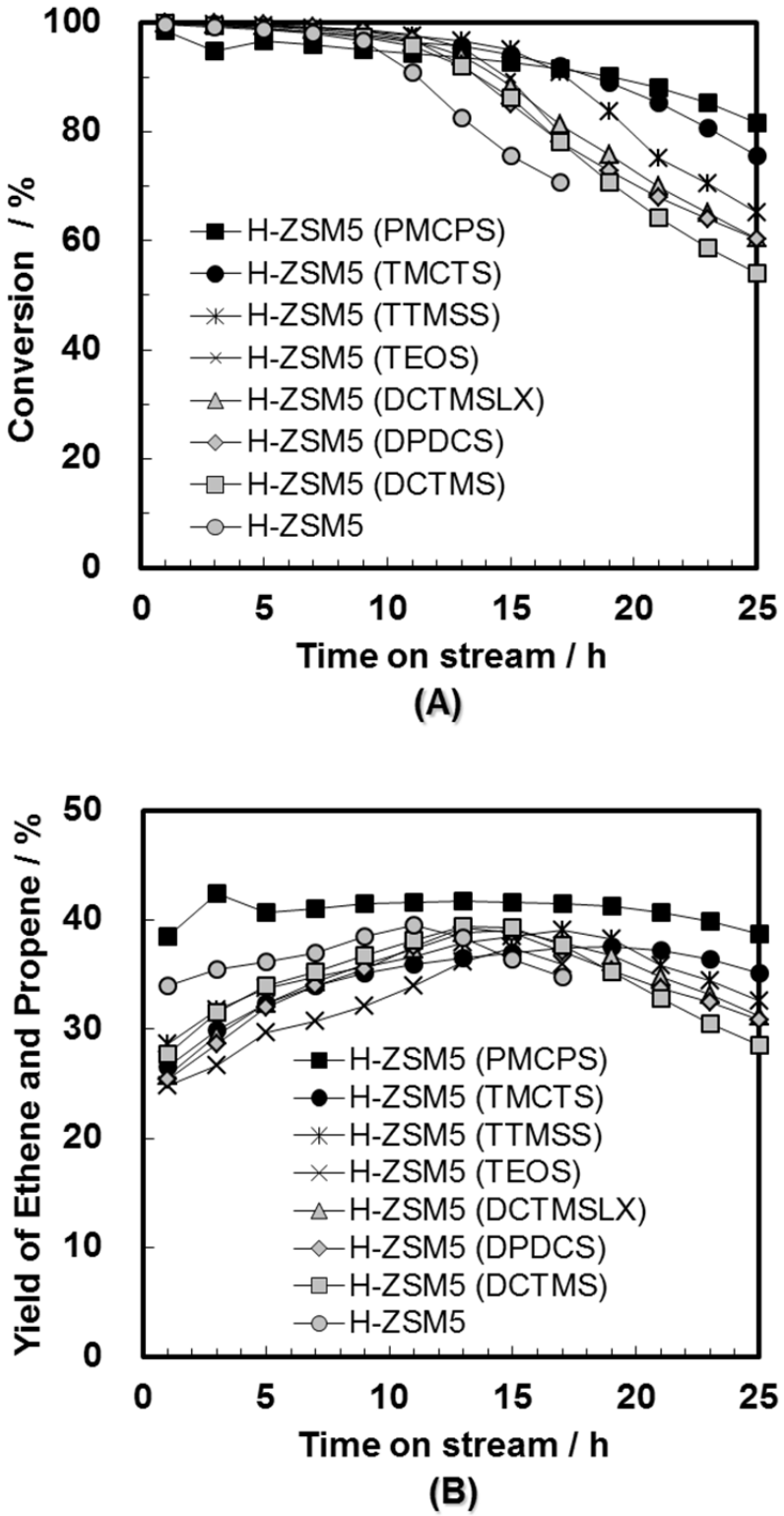

Fig. 1 The time course of the conversion (A) and yield of ethene and propene (B) from *n*-hexane cracking over a series of silylated catalysts.

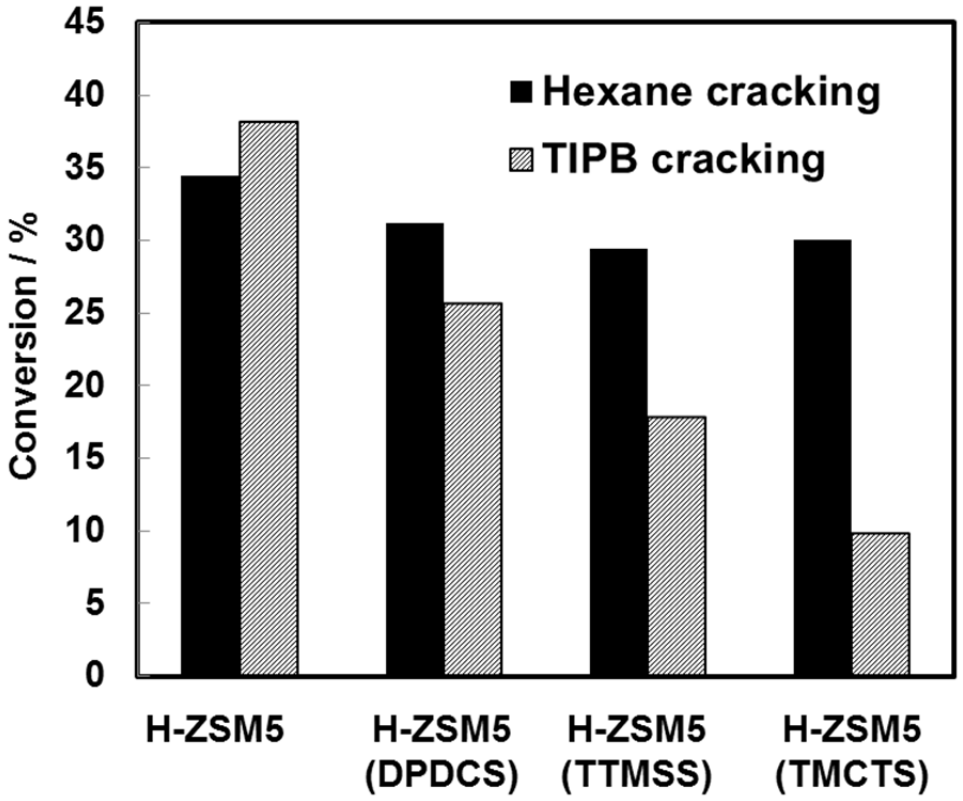

Fig. 2 The comparison of *n*-hexane cracking and TIPB cracking reactions over each silylated H-ZSM5 catalyst.

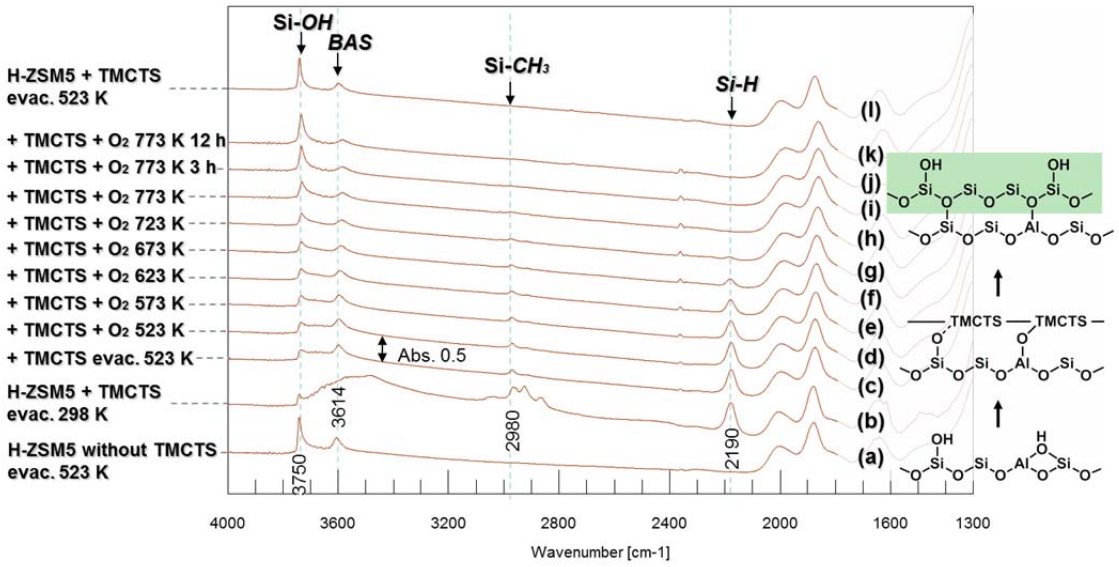

(A)

Fig. 3A IR spectra during heating of the H-ZSM5 treated with cyclic siloxane (TMCTS) in the presence of oxygen. Spectrum (a) was measured at 523 K before treating with TMCTS. Spectrum (b) was measured at 298 K after treating with TMCTS. Spectrum (c) was measured before introduction of oxygen at 523 K, and after introduction of oxygen at (d) 523 K, (e) 573 K, (f) 623 K, (g) 673 K, (h) 723 K, (i) 773 K, (j) after 3 h, and (k) after 12 h, then, (l) after evacuation and cooling to 523 K.

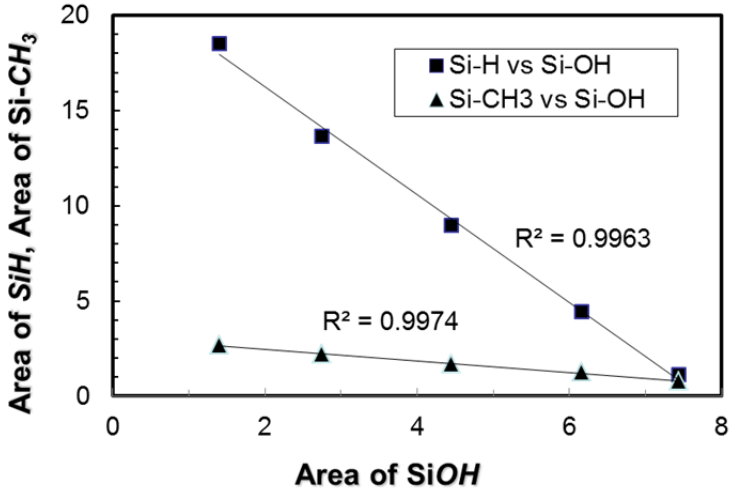

Fig. 3B Plots of relationship between the area of SiCH_3 band and the area of Si*OH* band and relationship between that of *SiH* band and thato of Si*OH* band in temperature raising process in the presence of oxygen from 523 K to 723 K.

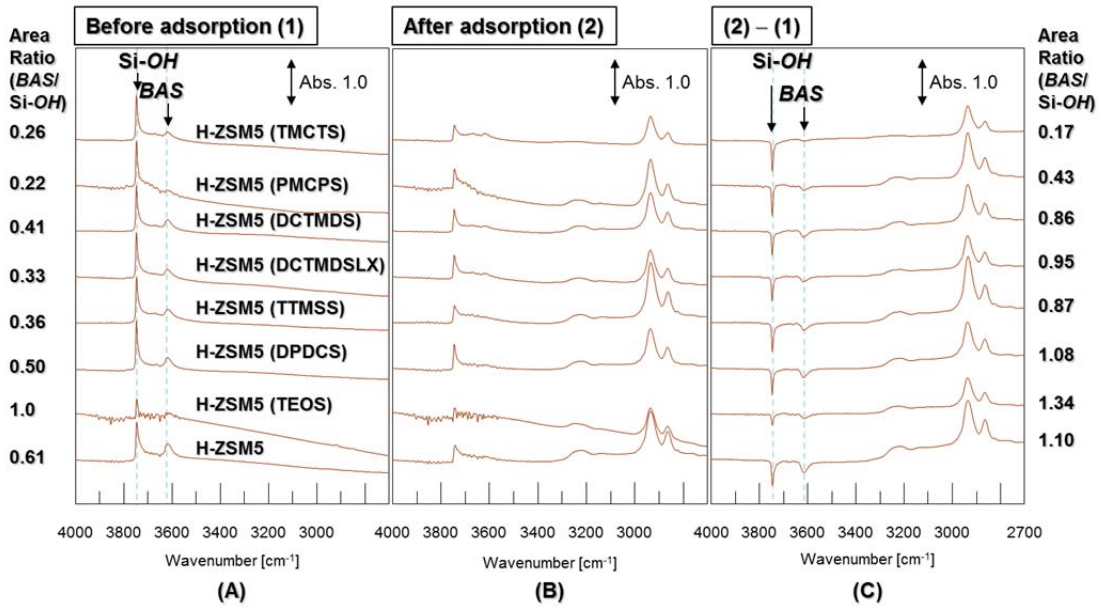

Fig. 4A IR spectra (A) before and (B) after adsorption of hexamethyleneimine to parent and silylated H-ZSM5 and (C) subtracted spectra of (A) from (B)

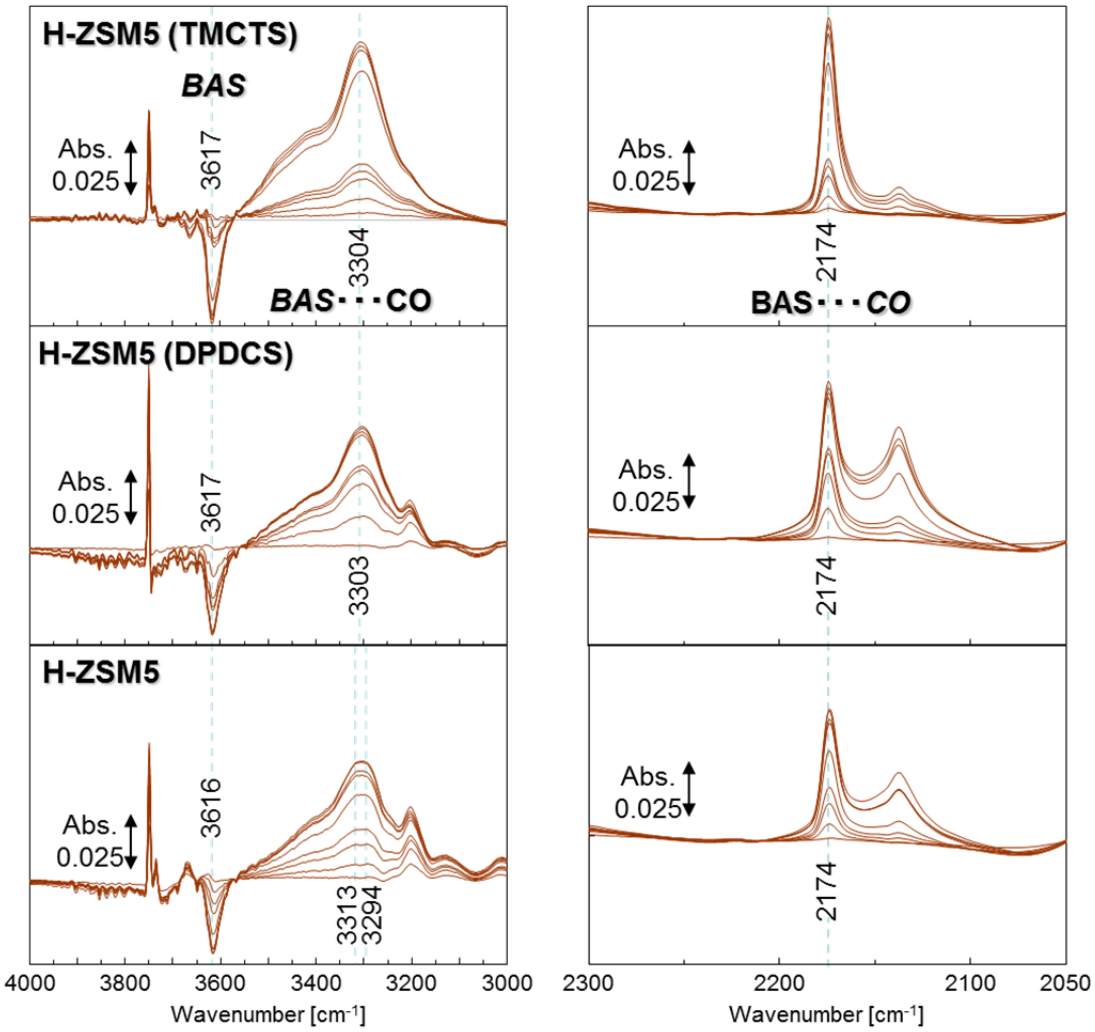

Fig. 5 IR spectra of CO adsorption after pre-adsorption of HMI on parent and silylated H-ZSM5

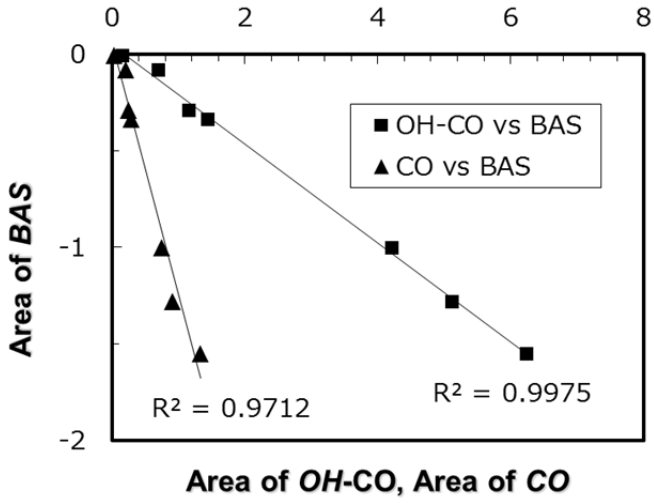

Fig. 5B Plots of relationship between the area of *OH*-CO band and the area of *BAS* band and relationship between that of *CO* band and that of *BAS* band in introduction of CO at 153 K.

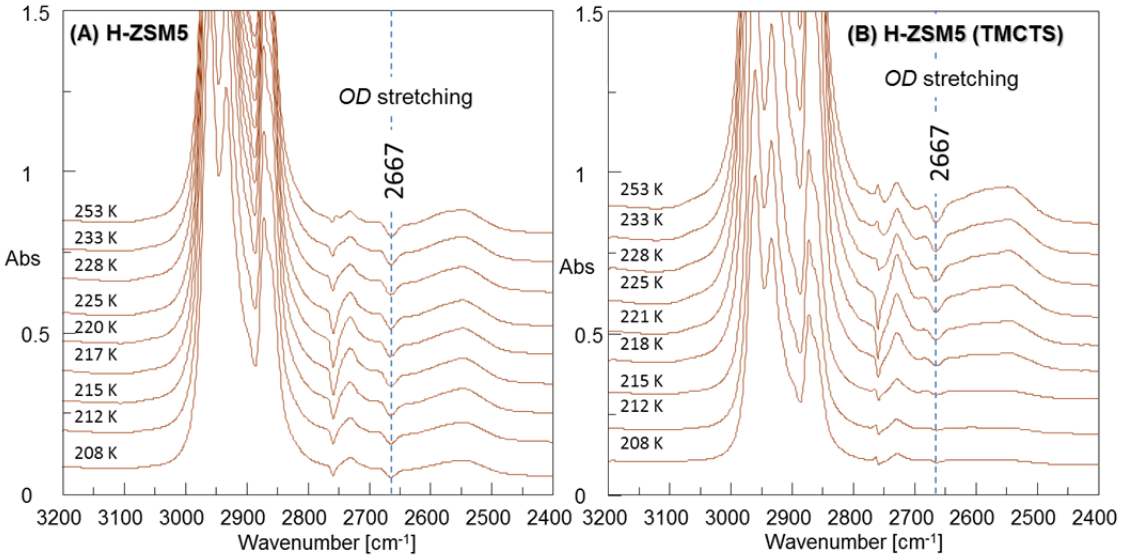

Fig. 6 IR spectrum of *n*-hexane adsorption on (A) parent and (B) silylated (TMCTS) H-ZSM5. Temperature was increased from 208 to 253 K.

Chapter 4

Catalytic Cracking of Naphtha over H-ZSM5 Catalyst Controlled in Acid amount and metal loading amount

Abstract

In order to promote the cracking of naphtha, metal having dehydrogenation performance was supported to H-ZSM5 catalysts. Effects of the Al content (Si/Al_2 ratio = 30 – 500) in the H-ZSM5, that is the amount of acid sites of H-ZSM5, the amount of loaded metal, and the kind of loaded metal having dehydrogenation performance were evaluated by cracking reaction of *n*-hexane and naphtha. It revealed that loading of metal controlled the amount to low Aluminum content H-ZSM5 (Si/Al2 ratio: 260 or more) was effective for the durability and lower olefins selectivity. By conducting reaction rate analysis, it was found that the *n*-hexane cracking over Pd-loaded H-ZSM5 and non-Pd-loaded HZSM5 obeyed the first-order kinetics regardless of different Si/Al2 ratio. Pd loading to low Al content H-ZSM5 led low activation energy of the conversion of *n*-hexane and the formation of propene and hydrogen. That is because the acid property of zeolite and the dehydrogenation property were well balanced in low Al content H-ZSM5. Investigation of the product immediately after starting the cracking reaction of *n*-hexane at the initial stage also revealed that metal loaded cracking reaction and dehydrogenation reaction proceeded concertedly. To evaluate the effect of sulfur as a catalyst poison, catalytic cracking of real naphtha was tested. Even when sulfur containing naphtha was used as the raw feedstock, the improvement of durability and selectivity of lower olefin was observed. The reaction regeneration repeated test was conducted and no noticeable catalyst degradation was observed.

4.1 Introduction

Light olefin and aromatics are important feedstock forming the basis of petrochemical industry. These basic chemical materials are mainly produced from naphtha, which is made by straight light distillate of crude oil as a raw material. Among these basic petrochemical feedstock, lower olefins (ethene, propene, butane, butadiene, and so on) are produced by thermal decomposition of light naphtha with steam at over 1073 K.

As the same time, aromatics (benzene, toluene, ethylbenzene, xylenes and so on) are also co-produced by thermal cracking of light naphtha. In generally, these aromatics are produced from a fraction corresponding to heavy naphtha with many high boiling point components than light naphtha in a more efficient process comparing to production from light naphtha. From this viewpoint, it is desirable that the ratio of light olefins is increased in the cracking of light naphtha as much as possible and that of aromatics is decreased.

Focusing on the recent demand trends of lower olefins, the demand of propylene derivatives (polypropylene, cumene, propyleneoxide and so on) is getting larger. The extension of propene demand is larger than that of ethene demand and this difference will spread considerably in the future.

On the other hand, light saturated hydrocarbons have less reactivity, so it is needed high temperature over 1073 K for the decomposition of these components and to obtain a yield with economical merit the temperature range of cracking of naphtha is limited. In generally, the ratio of propene/ethene is 0.6～0.7 in this temperature range. It is extremely difficult to change the ratio and to make only propene selectively.

Thus, since the distribution of products depends on the cracking temperature, it is difficult for existing naphtha cracker to respond flexibly to the change of balance of

supply and demand of each product. In addition, feedstock exchange proceed rapidly in mainly natural gas producing countries such as the Middle East, so ethene which have highly cost competitiveness produced from very cheaper ethane than naphtha enter the market. That's why adjustment of production has been done in many Asian naphtha crackers. Under the tight situation, naphtha cracking processes that can control the product distribution to suit demand has been hoped, and the methods of catalytic cracking of naphtha over acid type zeolite catalyst as the prospective technology have been disclosed [1]. This technology leads energy reducing as comparison to the current naphtha crackers which are type of energy consumption, and intended to enable the reduction of CO2 in large scale [2].

In the published catalytic cracking technology of naphtha or light saturated hydrocarbons, medium pore zeolites, in particular MFI type zeolites typified by ZSM5, have superior performance upon the generation of light olefins and aromatic compounds. It is possible to decrease the reaction temperature to 973 K below, and it is possible to greatly improve the ratio of the propene selectivity and propene/ ethene. Also by lowering the reaction temperature, the amount of low value methane as a chemical feedstock is also suppressed. However, these disclosures technologies have not reached to be mature technologies enough to replace the existing thermal decomposition process.

In order to make catalytic cracking technology of lower saturated hydrocarbons with zeolite catalysts practically possible levels, it is necessary to extend the catalyst life significantly. Further, the catalyst life is a major challenge that is common to a reaction process using a zeolite catalyst, the more particularly harsh reaction conditions cause a significant loss of catalyst performance. Deterioration of catalyst performance causes depression of yield of the desired product or the increase of purification process load due to the change of product distribution. Degradation of the performance of

zeolite catalyst is caused mainly by the pore blockage by carbonaceous deposition called coke, and the disappearance of the acid properties by aluminum components elimination from the zeolite framework caused by contact with high-temperature steam.

Generation of coke in the harsh reaction conditions is caused by setting sequentially of side reactions such as multimerization, cyclization, aromatization of lower olefins. Meanwhile, since the zeolite catalyst has a definite pore size derived from the crystal structure, shape selective reactions progress in the acid sites within the pores. Therefore, particularly by using the zeolite catalyst which does not have a large pore of the above 12-membered ring, in the pores sequential side reactions leading to coke formation is limited by the spatial limitations. However, acid sites on surface of zeolite exist at a constant rate, coke formation occurs by progress of non-selective reaction [3]. Because the catalytic cracking of lower hydrocarbons such as naphtha is a reaction at a high temperature, degradation of performance of the zeolite catalyst by such coking is a serious problem, and techniques for suppressing coking is the key for the practical use.

It is generally known that decrease of acid amount of zeolite by decrease of Al content of zeolite or replacement the protons of zeolite with alkali metal ions can suppress sequential side reaction in the reaction using a zeolite catalyst. However, since the catalytic activity of the zeolite decreases as the amount of acid decreases, it can be an effective technique for a reaction which does not require high activity, for example, catalytic decomposition of a raw material mainly composed of highly reactive olefin [4].. On the other hand, in order to apply zeolite catalysts to the decomposition reaction of lower reactive light saturated hydrocarbons, a certain amount of acid is necessary [5]. For this reason, it is considered difficult to efficiently promote the decomposition reaction of lower saturated hydrocarbons and suppress sequential side reactions simply by lowering the acid amount of zeolite.

The conversion reaction of saturated hydrocarbons by the zeolite catalyst is

promoted by adding a metal having high dehydrogenation ability, to convert low active saturated hydrocarbons into olefins in the reaction system. For example, a method for producing aromatic hydrocarbons from saturated hydrocarbons using an MFI zeolite catalyst containing Gallium is disclosed [6]. However, in this prior report, the yield of lower olefins was low and it cannot be said to be a suitable catalyst for the production of lower olefins.

When lower olefins by catalytic decomposition of lower saturated hydrocarbons are produced, it is not necessarily preferable to add a metal having a high dehydrogenation ability to the zeolite catalyst to promote the aromatization reaction [7]. For example, in this report, MFI zeolite whose ratio of Silica / Alumina was 153 was impregnated mixed with one metal of Cr, Mo, W, Ru, Os, Rh, Ir, Ni, Fe, Pd or Pt. In comparison with the reaction result using the metal-free MFI zeolite catalyst, the yield of the aromatic compounds increased and the total lower olefins yield of ethylene and propylene decreased. This example showed that the metal-added MFI zeolite catalyst is still insufficient industrially for the problem of efficient production of lower olefins from light saturated hydrocarbons. Furthermore, all of the examples in this report were results at the initial stage of the reaction up to the start of the reaction up to 40 minutes, practical continuous operation has not been carried out from the practical point of view, and no mention is made of the catalyst life.

Asashi-Kasei also reported an example in which the reaction was controlled by adding a metal catalyst to a zeolite catalyst in which the amount of acid was reduced by addition of Na+ in the catalytic cracking reaction of lower saturated hydrocarbons [8]. In this report, Na+ type ZSM5 having substantially no acid amount was prepared by adding Na+ to the ZSM5 zeolite having a SiO2 / Al2O3 molar ratio of 126, AgNa type ZSM5 catalyst prepared by adding Ag+ was applied to the catalytic cracking of lower saturated hydrocarbons. Total yield of ethene and propene was improved as compared

with the results of Na+ type ZSM5 and Ag+ type ZSM5. However, this example was still insufficient industrially for the problem of efficient production of lower olefins from lower saturated hydrocarbons, and it was confirmed that the AgNa type ZSM5 catalyst at a practically usable level has not been reached. Furthermore, this example was the result at the initial stage of the reaction at 6 minutes after the start of the reaction, and realistic continuous operation has not been carried out practically from the practical point.

Asahi-Kasei also reported that the catalytic cracking reaction of lower hydrocarbons was controlled by metal loaded zeolite catalyst of which the acid amount was reduced by steaming at high temperature [9]. In this report, the catalyst loaded with Ag in an MFI zeolite having a SiO2 / Al2O3 molar ratio of 126 was applied to the catalytic cracking of lower saturated hydrocarbons. It is well known that mild steamed zeolite catalyst has high performance for cracking or isomerization of hydrocarbons by modifying the acid properties, although severe steaming leads reduction of activity because of elimination of Aluminum from zeolite framework [10-11]. However, focusing on the total yield of ethylene and propylene, It was lower than that of the reaction result using steam treated MFI zeolite that wasn't loaded Ag. That is, the prior art was still insufficient industrially for the problem of efficient production of lower olefins from lower saturated hydrocarbons, and it has not reached the practically usable level. Furthermore, all of the examples were results at the initial stage of the reaction at 6 minutes after the start of the reaction, and realistic continuous operation has not been carried out practically.

Thus, the metal-containing zeolite catalyst has not necessarily been studied in detail in terms of both the efficient production of lower olefins and the catalyst life in the catalytic cracking reaction of lower saturated hydrocarbons such as naphtha, and it can't be said that the technology has been reached practically level. In view of these

circumstances, metal-containing zeolite catalysts capable of suppressing sequential overreactions and efficiently producing lower olefins for a long time are expected in the catalytic cracking reaction of naphtha.

In this work, Palladium was mainly selected as metal having capability of dehydrogenation, and the durability and selectivity of lower olefins for catalytic cracking of naphtha catalyzed by Pd loaded ZSM5 were scoped.

4.2 Experimental

4.2.1 H-ZSM5 zeolites

Ammonium type ZSM5 sample, NH_4-ZSM5 zeolite (Si/Al_2 = 500), was supplied from Sud-Chemie, and NH_4-ZSM5 zeolites (Si/Al_2 = 30, 50, 80, 150, and 260) were supplied from Zeolyst International. The proton type ZSM5, H-ZSM5 (500), was obtained by calcination of the NH_4-ZSM5 (Si/Al_2 = 500) at 823 K for 10 h. In the same way, the other zeolite samples, NH_4-ZSM5 (Si/Al_2 = 30, 50, 80, 150), were calcined at 823 K for 10 h to obtained H-ZSM5 (30), H-ZSM5 (50), H-ZSM5 (80), H-ZSM5 (150), and H-ZSM5 (260).

4.2.2 Impregnation of Palladium to H-ZSM5

Palladium loaded H-ZSM5 (500) was prepared by impregnation of Tetraammine-palladium-dichloride monohydrate salt ($Pd(NH_3)_4Cl_2 \cdot H_2O$). 0.044 g of $Pd(NH_3)_4Cl_2 \cdot H_2O$ was dissolved in 100 ml of ion-exchanged water. 5.0 g of H-ZSM5 (500) was introduced to the Palladium solution and stirred at 353 K for 3 h, and the solution was evaporated to obtain powder sample. Finally, the powder sample was calcined at 823 K for 10 h to obtain Pd/ZSM5 (500) to which 0.35 wt% of Palladium (0.033 mmol of Palladium to 1.0 g of zeolite, [Pd]/[Al] = 0.5 in H-ZSM5 (500)) was

loaded. In the same way, the other zeolite samples, H-ZSM5 (30), H-ZSM5 (50), H-ZSM5 (80), H-ZSM5 (150), and H-ZSM5 (260), were impregnated and calcined to obtained Pd/ZSM5 (30), Pd/ZSM5 (50), Pd/ZSM5 (80), Pd/ZSM5 (150), and Pd/ZSM5 (260), respectively (0.033 mmol of Palladium to 1.0 g of each zeolite).

In the same manner except that the amount of Pd solt was changed to 0.17 g, Pd/ZSM5 (500)-2 loading of 1.4 wt% of Palladium (0.132 mmol of Palladium to 1.0 g of zeolite, [Pd]/[Al] = 2.0 in H-ZSM5 (500)) was obtained.

In the same manner except that the amount of Pd solt was changed to 0.009 g, Pd/ZSM5 (500)-3 loading of 0.07 wt% of Palladium (0.007 mmol of Palladium to 1.0 g of zeolite, [Pd]/[Al] = 0.1 in H-ZSM5 (500)) was obtained.

In the same manner except that 0.044 g of the Pd solt was changed to 0.051 g of hexaammine ruthenium trichloride ($Ru(NH_3)_6Cl_3$), Ru/ZSM5 (500) loading of 0.33 wt% of Ruthenium (0.033 mmol of Ruthenium to 1.0 g of zeolite, [Ru]/[Al] = 0.5 in H-ZSM5 (500)) was obtained.

In the same manner except that 0.044 g of the Pd solt was changed to 0.086 g of hexachloroplatinic acid hexahydrate salt ($H_2PtCl_6 \cdot 6H_2O$), Pt/ZSM5 (500) loading of 0.64 wt% of Platinum (0.033 mmol of Platinum to 1.0 g of zeolite, [Pt]/[Al] = 0.5 in H-ZSM5 (500)) was obtained.

4.2.3 N_2 adsorption

Nitrogen adsorption-desorption isotherms were measured to obtain information on the micro- and meso-porosities at 77 K on a Belsorp-max (Microtrac-Bel). The BET specific surface area (S_{BET}) was calculated from the adsorption data in the relative pressure ranging from 0.04 to 0.2. External surface area (S_{EXT}) was estimated by the *t*-plot method.

4.2.4 NH_3 TPD

Temperature-programmed desorption of ammonia (NH_3-TPD) spectra were recorded on Belcat-A (Microtrac-Bel). Typically, 25 mg catalyst was pretreated at 773 K in He for 1 h and then was cooled to adsorption temperature at 373 K. Prior to the adsorption of NH_3, the sample was evacuated. Approximately 5 vol% of NH_3 was allowed to contact with the sample for 30 min. Subsequently, the sample was evacuated to remove weakly adsorbed NH_3 for 15 min. Finally, the sample was heated from 373 to 973 K at a ramping rate of 10 K min^{-1} with the He flow passed through the reactor. A mass spectrometer (mass number 17) was used to monitor desorbed NH_3. The amount of acid sites was determined by using the area of the so-called *h*-peak in the profiles.

4.2.5 IR analysis for CO adsorption for D2 exchanged zeolite

Pd/ZSM5 (500), Pd/ZSM5(150), H-ZSM5 (500), and H-ZSM5 (150) sample was pressed into a self-supporting disk (20 mm in diameter, 50 mg) and placed in an IR cell attached to a conventional closed gas circulation system. After the sample was pretreated by evacuation at 773 K for 1 h, the sample was cooled to 673 K, and then treated with 50 kPa of D_2 for 1.5 h. The sample was cooled to 153 K under evacuation and the IR spectrum of the clean disk was recorded. Nextly, CO was introduced at 153 K and the IR spectra were recorded.

4.2.6 Catalytic cracking of n-hexane

The catalytic performance were tested by the catalytic cracking of *n*-hexane (Wako, 96%). *n*-Hexane was selected as a model alkane compound because of the similar molecular weight as the mean one of light naphtha. The cracking of *n*-hexane was carried out in a 7 mm hastelloy C276 tubular flow reactor loaded with 0.36 g of 250–

500 μm zeolite pellets without a binder, which was the catalyst was centered at the reactor in a furnace. The reactor was heated to the reaction temperature (873 K) with N_2 flow into the temperature of catalyst bed at 923K, N_2 flow was stopped and *n*-hexane was introduced without carrier gas. The weight hourly space velocity of *n*-hexane (WHSV) was set to 10 h^{-1}. The reaction products were analyzed with on-line gas chromatographs (Shimadzu GC-2014) with two FID detectors and a TCD detector. The selectivity to the products and the *n*-hexane conversion were calculated based on the carbon numbers.

4.2.7 Evaluation of rate constant and activation energy

The catalytic cracking of *n*-hexane was performed in a conventional fixed reactor under Helium at atmospheric pressure. Pd/ZSM5 (500), Pd/ZSM5(150), H-ZSM5 (500), and H-ZSM5 (150) sample was put into a 4 mm quartz reactor and activated in flowing He at 923 K, and then cooled to the reaction temperature ranging from 833 to 923 K. The W/F (W: amount of catalyst /g, F: total flow rate /$molh^{-1}$) was adjusted to obtain < 25% of the *n*-hexane conversion. The reaction products were analyzed with on-line gas chromatographs (Shimadzu, GC-2014) with an FID detector and a capillary column (PLOT Fused Silica 30 m x 0.53ｍｍ, 6 μm film thickness). Hydrogen was analyzed by a GC with a TCD detector and a packed column.

4.2.8 Detect of initial products for n-hexane cracking

Platinum loaded ZSM5 was obtained in the same manner of Pd/ZSM5. 0.294 g of $Pt(NH_3)_4Cl_2 \cdot H_2O$ was dissolved in 100 ml of ion-exchanged water. 5.0 g of H-ZSM5 (500) was introduced to the Platinum solution and stirred at 353 K for 3 h, and the solution was evaporated to obtain powder sample. Finally, the powder sample was calcined at 823 K for 10 h to obtain Pt/ZSM5 (500) to which 3.2 wt% of Platinum

(0.170 mmol of Platinum to 1.0 g of zeolite, [Pd]/[Al] = 2.5 in H-ZSM5 (500)) was loaded. And Pt/SiO2 which 3.2 wt% of Platinum was loaded to was prepared in the same way. Catalyst performance was tested by the manner described at section 2.6 and initial production detected by starting GC analyses at 5 min after starting the reaction.

4.2.9 Catalytic cracking of naphtha containing Sulfur

In the same manner described in paragraph 2.6 except for using naphtha containing sulfur as feedstock, catalyst performance was tested. Naphtha was obtained from a petrochemical company having steam cracker of naphtha. The reaction products were analyzed with on-line gas chromatographs (Shimadzu GC-2014) with two FID detectors and a TCD detector. The selectivity to the products and the naphtha conversion were calculated based on the carbon numbers. The conversion of naphtha was defined as the total yield of saturated and unsaturated hydrocarbons having 1 to 5 carbon atoms and aromatics.

4.2.10 Repeated reaction and regeneration test of naphtha catalytic cracking

After the naphtha catalytic cracking test over Pd/ZSM5 (500) for 25 h, supply of raw materials was stopped and the reactor was cooled to the regeneration temperature (773 K) with N_2 flow, and the temperature of catalyst bed reached at 773K, finally, N_2 flow was stopped and 200 Ncc/min of air was introduced for 8 h. After the end of regeneration, naphtha cracking was tested repeatedly 6 times in total.

2.11 TEM analysis of Pd/ZSM5 (500) before and after naphtha cracking test

Field-mission transmission electron microscopy (FE-TEM) images of the Pd/ZSM5 (500) sample before and after naphtha cracking were obtained on JEM-2200FS (JEOL). The sample was embedded in resin, trimmed, sliced, and

mounted on an organic supporting film before observation.

4.3 Results and discussion

4.3.1 Catalysts characterization

Table 1 lists the BET surface area estimated by N_2 adsorption and the acid amounts estimated by NH_3-TPD analyses of H-ZSM5 catalysts and Palladium loaded H-ZSM5 catalysts. In comparison Pd/ZSM5 with H-ZSM5 which had the same Si/Al_2 ratio, the surface area of each catalyst almost unchanged. Loaded Palladium didn't aggregate as blocking pore mouth of zeolite. The acid amount of each Pd/ZSM5 catalyst was slightly lower than that of the parent H-ZSM5 as a result of impregnation of Palladium. Ion-exchange occurred to Palladium ion from proton of parent H-ZSM5 zeolite samples at impregnation [12]. There were not clear differences among Pd-loaded or not Pd-loaded ZSM5 samples (Si/Al_2 ratio = 500 and 150) by CO adsorption FT-IR analyses at 153 K. No peak was observed around 2200, 2180, 2140, and 2120 cm^{-1} derived from Pd-CO species [13-14]. It indicated that loaded Palladium on ZSM5 samples was highly dispersed.

4.3.2 Catalytic tests

The time course of the conversion and yield of ethene and propene from *n*-hexane cracking over a series of Pd/ZSM5 catalysts and non Pd-loaded H-ZSM5 catalysts (Si/Al2 ratio: 30, 50, 80, 150, 260, and 500) are shown in Fig. 1 (A) ～ (F), respectively. *n*-Hexane was used as a model compound of naphtha because of the similarity in molecular weight. While H-ZSM5 catalysts having high Al content (Si/Al2 = 30, 50, 80, and 150) deactivated in early stage of reaction, H-ZSM5 catalysts having low Al content (Si/Al_2= 260 and 500) deactivated gradually. In the case of high Al

content ZSM5 catalysts, H-ZSM5 (30), H-ZSM5 (50), H-ZSM5 (80), and H-ZSM5 (150), loading of Pd to ZSM5 resulted in decrease of the durability for cracking of *n*-hexane. Pd has the character of dehydrogenation [15]. Since not only the cracking reaction catalyzed by acid sites of zeolite but also dehydrogenation reaction catalyzed by loaded Pd occurred, side reaction such as oligomerization, isomerization, aromatization proceeded to generate coke more than non Pd-loading H-ZSM5 catalyst and to decrease in selectivity of lower olefins and in activity. On the other hand, loading of Pd to the low Al content catalysts (Si/Al_2 ratio more than 260) led longer durability and higher propene selectivity (Fig. 1 (E) and (F)). Acid property of ZSM5 zeolite and dehydrogenation property of Pd were gotten good balance, so cracking reaction proceeded efficiently by concerted mechanism.

4.3.3 Effect of Pd loading to H-ZSM5 on activity for n-hexane cracking

To evaluate the effect of Pd loading in the H-ZSM5 zeolites on *n*-hexane cracking behavior having various Si/Al2 ratio, kinetics of *n*-hexane cracking over the H-ZSM5 catalysts at various reaction temperatures and W/F were examined. It is known that the catalytic cracking of *n*-hexane obeys the first-order kinetics regard1ess of reaction mechanisms [16-17]. Thus, the rate constant for cracking *(k_c)* can be expressed as follows:

$$k_c \text{ x } W / F = -\ln (1 - x) \quad (1)$$

W is the amount of catalyst, *F* is the total flow rate including raw feedstock and carrier gas and *x* is the *n*-hexane conversion. *n*-Hexane was converted also by thermal cracking at above 823 K in these reaction conditions. Both the catalytic cracking and the thermal cracking at high temperatures obey the first-order kinetics [18]. Therefore, the following equation can be applied in this reaction:

$$k_c \text{ x } W / F + k_t \text{ x } V / F = -1n(1-x) \quad (2)$$

$$k_c \text{ x } W / F = \text{-ln(l-x)- } k_t \text{ x } V / F \quad (3)$$

k_t is the rate constant for thermal cracking, V is the volume of high temperature region in the reactor. Figure 2 (A) and 2 (B) shows the effect of the W/F on the rate of *n*-hexane cracking over the Pd/ZSM5 (500) and H-ZSM5 (500) or Pd/ZSM5 (150) and H-ZSM5 (150) respectively at 833, 863, 893 and 923 K. It was apparent that *n*-hexane cracking over the H-ZSM5 zeolites obeyed the first-order kinetics regard1ess of the reaction temperature and Pd loading or not. From the equations (1) and (3), the slope of the plots in Figure 2 (A) and (B) exhibits the rate constant about *n*-hexane conversion for the *n*-hexane cracking (k_c). The Arrhenius plots for the cracking of *n*-hexane over Pd/ZSM5 and H-ZSM5 catalysts (Si/Al_2 ratio: 500 and 150) from 833 to 923 K are shown in Fig. 3. Each rate constant (k_c) of all the catalysts and activation energy (E_a) were listed in Table 2. The reaction rate constants for *n*-hexane conversion over Pd/ZSM5 were lower than H-ZSM5 in the same Si/Al_2 ratio. It was resulted from decrease of the acid amount of Pd/ZSM5 sample because of ion-exchange from proton to Pd ion. In comparison the activation energy of *n*-hexane conversion over Pd loaded ZSM5 samples with that of non-Pd loaded ZSM5 samples, loading of Pd led lower activation energy. And the activation energy of Pd/ZSM5 (500) (100 kJ/mol) was lower than that of Pd/ZSM5 (150) (110 kJ/mol). Generally, lower activation energy of naphtha cracking derived from bimolecular reaction [19]. However, in the case of this catalyst, the cracking reaction was promoted by dehydrogenation property resulted from Pd loading. And the cracking reaction and the dehydrogenation reaction were progressed concertedly resulted in efficiently propene production for long time when Pd was loaded to the zeolite with small amount of acid sites. In addition, as additional information, the activation energy of the formation of hydrogen and propene in this reaction over Pd/ZSM5 (500) were the lowest among all the samples although it was not clear whether a specific reaction or contributed to the reduction of activation energy or

the overall reaction contributed to that (Table 3 and 4).

4.3.4 Effect of the amount of Palladium loaded to H-ZSM5

In order to produce lower olefins efficiently and continuously over a long period of time from lower saturated hydrocarbons such as naphtha, the reaction promoted by the metal having dehydrogenation property such as Pd and the reaction promoted by the acidity of the intermediate pore zeolite were needed to be well balanced to progress in concert. Therefore, when amount of metal loading was too much, the dehydrogenation reaction accelerated by the metal proceeded excessively, for example Pd/ZSM5 (500)-2 shown in Fig 4, and when amount of metal loading was too less, side reaction such as oligomerization or polimerization due to acidity of the intermediate pore zeolite proceeded excessively, for example Pd/ZSM5 (500)-3 shown in Fig 4. And in any case, it inhibited efficient and long-term continuous conversion of raw feedstock and production of lower olefins.

4.3.5 Effect of other metals having dehydrogenation property

H-ZSM5 (500) catalysts loading of metals having dehydrogenation property other than Pd were also tested (Fig. 5). Improvement in durability and selectivity of propene was observed by H-ZSM5 (500) containing Pt or Ru in an Metal / Al molar ratio of 0.5, Pt/ZSM5 (500) and Ru/ZSM5 (500), compared to non-metal-loaded H-ZSM5 (500) [20-21]. Impregnation of metal having dehydrogenation property to lower Al content ZSM5 increased the catalyst performance and the propene selectivity proceeding dehydrogenation on metal and cracking on acid sites concertedly like Pd/ZSM5 (500).

4.3.6 Initial product of the cracking of n-hexane over metal supported catalyst

Platinum was selected as metal having dehydrogenation performance like Pd [20].

The initial product of *n*-hexane cracking reaction was compared between catalyzed by zeolite and silica which was loaded Pt (Pt/ZSM5 (500) and Pt/SiO_2). The series of product distribution at 5 min after starting the reaction and 1 to 10 h was shown in Fig. 6 (A) and (B), respectively. While not only benzene but also toluene, and xylenes were produced by using Pt/ZSM5 (500), only benzene among aromatics was produced by using Pt/SiO2. Since the acid sites of zeolite catalyzed oligomerization of hydrocarbons or isomerization (right arrow in Fig. 7) before aromatization, alkyl benzene such as toluene or xylenes were produced. On the other hand, Pt/SiO2 catalyzed mainly dehydrogenation of *n*-hexane (down arrow in Fig. 7), so benzene was produced mainly. In addition, the product distribution after 1 h passed was different from initial distribution in each catyalyst. Rapidly change of catalyst performance occurred. In the case of Pt/ZSM5 (500), high conversion of *n*-hexane kept for even 10 h and propene yield increased from 21 % to 25 %, although the yield of BTX decreased at the early stage of the reaction. Coke materials which resulted in inactivation of catalysts formed on the Pt/ZSM5 (500), but the acid sites of zeolite were still active. Thus, the amount of coke materials was small or coke materials deposited on metal rather than acid sites. As a result, acidity of zeolite and dehydrogenation property of metal was well balanced without further deposition of coke on metal because of proceeding decomposition of hydrocarbons before sequential reaction around metal. In the case of Pt/SiO2, the yield of benzene decreased rapidly and the conversion of *n*-hexane also decreased. The coke material deposited on metal and dehydrogenation activity of metal was disappeared.

4.3.7 Cracking of naphtha containing sulfur over zeolite

Light naphtha (density: 0.6848, Mw: 87.06) was obtained from a petrochemical company. Hydrocarbon composition of naphtha, the impurity and the aspect are listed in Table 5 and 6. The sulfur content was 265 ppm. Catalytic cracking reaction of naphtha

was carried out similarly to the cracking of *n*-hexane. It was found that when the Si/Al_2 ratio was 260 or more, the life of the palladium-supported ZSM5 was longer than that of the unsupported ZSM5 (Fig. 8 (B) and (C)). Conversely, Pd/ZSM5 (150) had a short catalyst lifetime than H-ZSM5 (150) (Fig. 8 (A)). Even during naphtha cracking, zeolite with a small acid content balanced the acid reaction and the dehydrogenation reaction by loading of palladium, thus prolonging the life and improving the propylene yield like *n*-hexane cracking. The improvement effect appeared by the loading of Pt or Ru to H-ZSM5 (500) (Fig. 8 (C)). However, when compared with *n*-hexane catalytic cracking, the ranking of durability changed from Pt/ZSM5 (500) > Pd/ZSM5 (500) > Ru/ZSM5 (500) to Pd/ZSM5 (500) > Ru/ZSM5 (500) > Pt/ZSM5 (500). That is, the effect of prolonging the lifetime of Pt decreased. Sulfur is known to adsorb to metals and to inactivate the catalyst. Furthermore, poisoning of sulfur is likely to occur in the order of Pt > Pd > Ru. Therefore, it is possible that Pt/ZSM 5 was poisoned with sulfur. Subsequently, in order to investigate whether sulfur contained in naphtha adversely affected Pd supported to zeolite, repeated tests of reaction and regeneration were conducted. Regeneration of the catalyst was carried out by passing air through the catalyst layer at 773 K. The results of a total 6 reactions are shown in Fig. 9. In the six repeated tests, there was no noticeable change in both activity and propylene yield. Since hydrogen was present during the reaction and catalyst was in a reduced state, even though sulfur was bonded to active metal, it was considered that the catalyst was immediately reduced and discharged as hydrogen sulfide in the case of Pd. Finally, TEM observation of Pd/ZSM5 (500) sample before the cracking reaction (Fig. 10 (A)) and the catalyst withdrawn after repeating the reaction regeneration test (Fig. 10 (B)) was carried out. Before conducting the reaction, Pd particles of about 1 to 10 nm were observed and found to be highly dispersed in the zeolite. After the reaction regeneration test, Pd particles of about 1 to 30 nm were observed but this degree of aggregation

didn’t deteriorate the reaction results. Suppressing aggregation will be a future issue.

4.4 Conclusions

Loading of metals having dehydrogenation property such as Palladium, Platinum, or Ruthenium by controlling the amount to H-ZSM5 which had low Al content led improvement in durability for the catalytic cracking of *n*-hexane and higher yield of propene. Kinetic analysis of Pd-loading and non-Pd-loading H-ZSM5 samples and high and low Al content H-ZSM5 samples indicated that cracking and dehydrogenation were concertedly proceeded by loading of Pd to low Al content H-ZSM5. The same effect was observed at the catalytic cracking of sulfur containing naphtha.

References

[1] S. Takahashi, F. Kanashima, JP Patent (1994) 192135.

[2] T. Ren, M. Patel, K. Blok, Enegy, 31 (2006) 425.

[3] T. Tago, M. Sakamoto, K. Iwakai, H. Nishihara, S. R. Mukai, T. Tanaka, T. MasudaJ. Chem. Eng. Jpn, 42 (2009) 162.

[4] JP Patent (1999) 246445.

[5] JP Patent (1994) 346062.

[6] JP Patent (1993) 58919.

[7] JP Patent (1994) 330055.

[8] JP Patent (1996) 126844.

[9] JP Patent (1999) 127546.

[10] R.M. Lago, W.O. Haag, R.J. Mikovski, D.H. Olson, S.D. Hellring, K.D. Schmidt, G.T. Kerr, New Development in Zeolite Science and Technology, Elsevier (1986) 677.

[11] W.O. Haag, R.M. Lago, Eur Patent (1981) 34444.

[12] A.K. Neyestanaki, N. Kumar, L.E. Lindfors, Appl. Catal. B: Environmental. 7 (1995) 95.

[13] K. Chakarova, E. Ivanova, K. Hadjiivanov, D. Klissurski, H. Knozinger, Phs. Chem. Chem. Phys. 6 (2004) 3702.

[14] W. Aylor, L. J. Lobree, J. A. Reimer and A. T. Bell, J. Catal. 172 (1997) 453.

[15] E.C. Horning, M.G. Horning, J. Am. Chem. Soc. 69 (1947) 1359.

[16] H, Krannila, W. O. Haag, B. C. Gates, J.Catal. 135 (1992) 115.

[17] S. Kotrel, M. P. Rosynek, J. H. Lunsford, J. Catal. 191 (2000) 55.

[18] K. Kubo, H. Iida, S. Namba, A. Igarashi, Micropor. Mesopor. Mater. 149 (2012) 126.

[19] N. Katada, K. Suzuki, T. Noda, W. Miyatani, F. Taniguchi, M. Niwa, Appl. Catal. A Gen. 373 (2010) 208.

[20] D.J. Trevor, R.L. Whetten, D.M. Cox, A. Kaldor, J. Am. Chem. Soc. 107 (1985) 518.

[21] G.C. Bond, Metal-Catalysed Reactions of Hydrocarbons (2006)

Table 1 The BET surface area estimated by N_2 adsorption and the acid amounts estimated by NH_3-TPD analyses of H-ZSM5 catalysts.

Catalyst	**Pd amount / wt%**	**S_{BET} / $m^2 \cdot g^{-1}$**	**Acid amount / $mmol \cdot g^{-1}$**
H-ZSM5 (500)	0	340	0.091
Pd/ZSM5 (500)	0.35	333	0.077
H-ZSM5 (260)	0	407	0.096
Pd/ZSM5 (260)	0.35	410	0.089
H-ZSM5 (150)	0	384	0.234
Pd/ZSM5 (150)	0.35	388	0.181
H-ZSM5 (80)	0	434	0.259
Pd/ZSM5 (80)	0.35	446	0.238
H-ZSM5 (50)	0	438	0.44
Pd/ZSM5 (50)	0.35	423	0.311
H-ZSM5 (30)	0	417	0.519
Pd/ZSM5 (30)	0.35	425	0.390

Table 2. The rate constant (k_c) at various temperatue and activation energy (Ea) for the conversin of *n*-hexane.

	k_c (833 K) mol/g·h	k_c (863 K) mol/g·h	k_c (893 K) mol/g·h	k_c (923 K) mol/g·h	Ea kJ/mol
Pd/ZSM5 (500)	0.161	0.244	0.413	0.646	100
H-ZSM5 (500)	0.159	0.313	0.537	0.938	125
Pd/ZSM5 (150)	0.687	1.146	2.012	3.195	110
H-ZSM5 (150)	0.904	1.573	2.788	4.447	114

Table 3. The rate constant (k_p) at various temperatue and activation energy (Ea) for the formation of propene.

	k_p (833 K) mol/g·h	k_p (863 K) mol/g·h	k_p (893 K) mol/g·h	k_p (923 K) mol/g·h	Ea kJ/mol
Pd/ZSM5 (500)	0.108	0.154	0.275	0.462	105
H-ZSM5 (500)	0.091	0.192	0.331	0.556	128
Pd/ZSM5 (150)	0.513	0.866	1.597	2.637	118
H-ZSM5 (150)	0.704	1.284	2.387	3.962	129

Table 4. The rate constant (k_h) at various temperatue and activation energy (Ea) for the formation of hydrogene.

	k_h (833 K) mol/g·h	k_h (863 K) mol/g·h	k_h (893 K) mol/g·h	k_h (923 K) mol/g·h	Ea kJ/mol
Pd/ZSM5 (500)	0.043	0.067	0.119	0.200	110
H-ZSM5 (500)	0.031	0.088	0.181	0.317	164
Pd/ZSM5 (150)	0.164	0.303	0.636	1.116	138
H-ZSM5 (150)	0.184	0.444	0.945	1.468	149

Table 5. Hydrocarbon composition of light naphtha analysed by PONA.

wt%	N-Paraffins	I-Paraffins	Olefins	Naphthenes	Aromatics	Total
C_3	0					0
C_4	4	0	0			4
C_5	13	9	0	1		23
C_6	12	11	0	6	1	30
C_7	8	7		5	2	23
C_8	4	5	0	3	2	15
C_9	1	2	0	0	0	4
C_{10}	0	0	0	0	0	1
C_{11}	0	0		0		0
C_{12}	0					
Total	43	35	1	16	6	100

Table 6. Analysis of light naphtha

Density at 288 K (g/cm3)	0.6848
Average molecular weight	87.06
Vapor pressure at 310.78 K (kPa)	73.0
Inpurity composition	
Cl (ppm)	< 1
N (ppm)	2
S (ppm)	265
As (ppb)	< 5
Hg (ppb)	1
Pb (ppb)	< 5

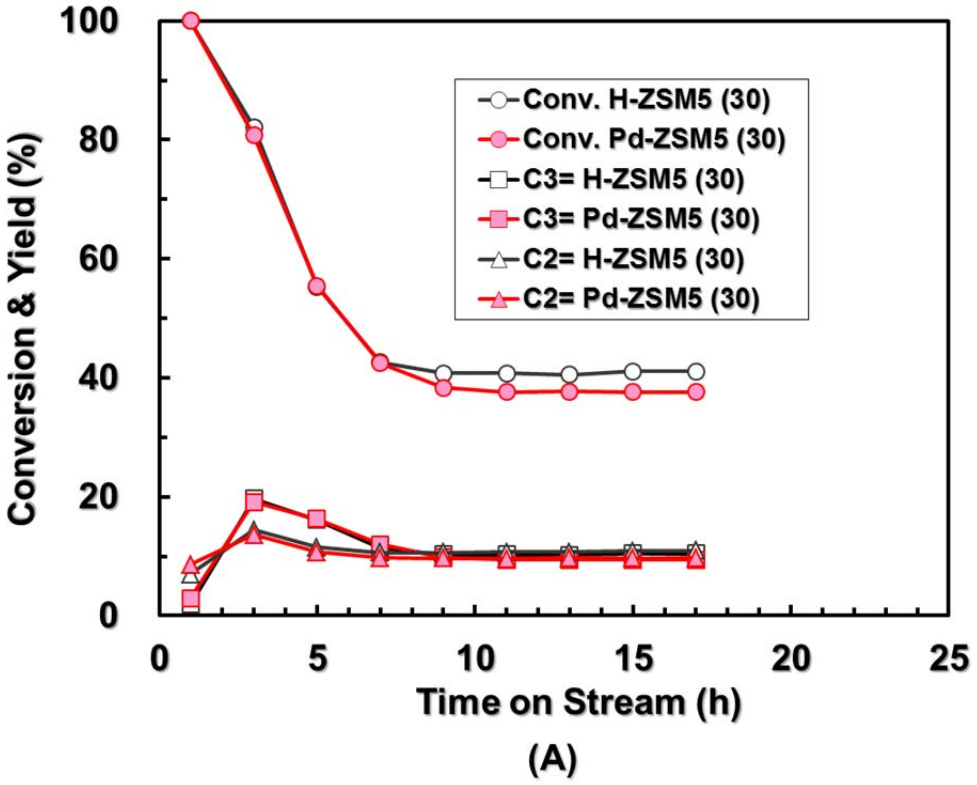
Conv. H-ZSM5 (30)
Conv. Pd-ZSM5 (30)
C3= H-ZSM5 (30)
C3= Pd-ZSM5 (30)
C2= H-ZSM5 (30)
C2= Pd-ZSM5 (30)
Conversion & Yield (%)
Time on Stream (h)
0
20
40
60
80
100
0
5
10
15
20
25

(A)

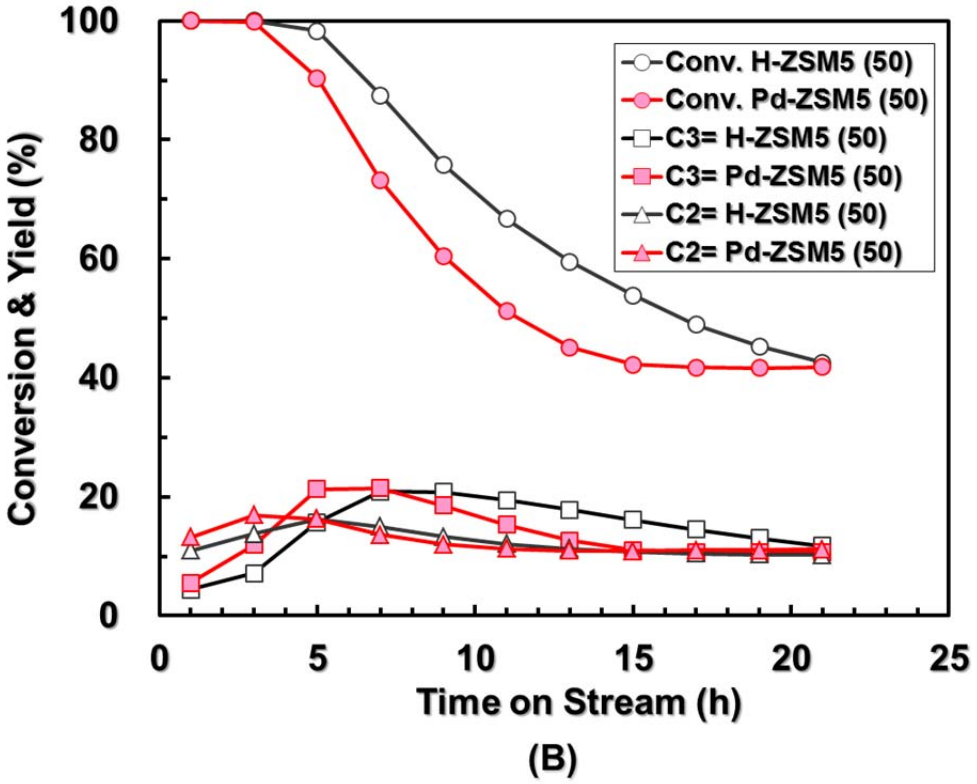
Conv. H-ZSM5 (50)
Conv. Pd-ZSM5 (50)
C3= H-ZSM5 (50)
C3= Pd-ZSM5 (50)
C2= H-ZSM5 (50)
C2= Pd-ZSM5 (50)
Conversion & Yield (%)
Time on Stream (h)
0
20
40
60
80
100
0
5
10
15
20
25

(B)

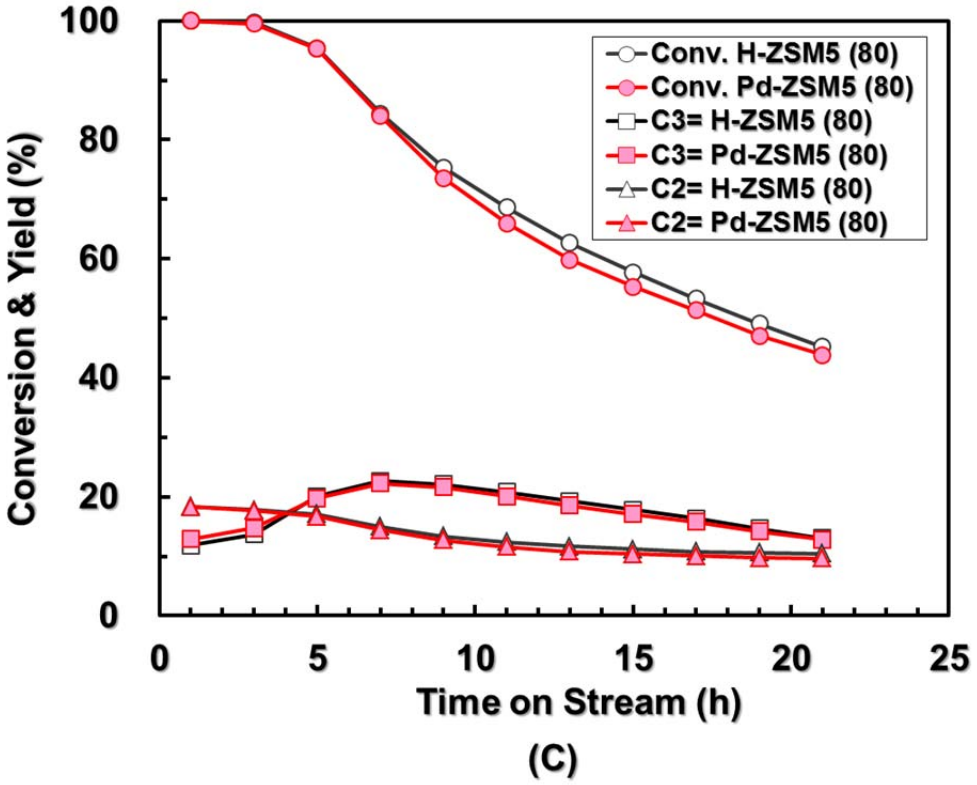
Conv. H-ZSM5 (80)
Conv. Pd-ZSM5 (80)
C3= H-ZSM5 (80)
C3= Pd-ZSM5 (80)
C2= H-ZSM5 (80)
C2= Pd-ZSM5 (80)
Conversion & Yield (%)
Time on Stream (h)
0
20
40
60
80
100
0
5
10
15
20
25

(C)

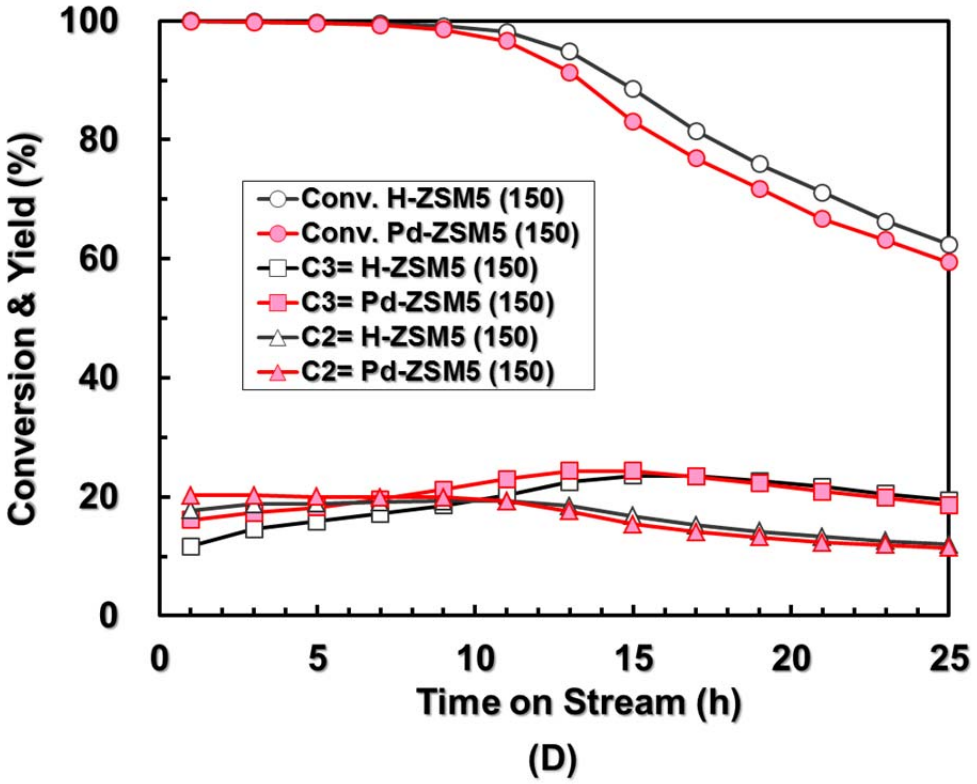
Conv. H-ZSM5 (150)
Conv. Pd-ZSM5 (150)
C3= H-ZSM5 (150)
C3= Pd-ZSM5 (150)
C2= H-ZSM5 (150)
C2= Pd-ZSM5 (150)
Conversion & Yield (%)
Time on Stream (h)
0
20
40
60
80
100
0
5
10
15
20
25

(D)

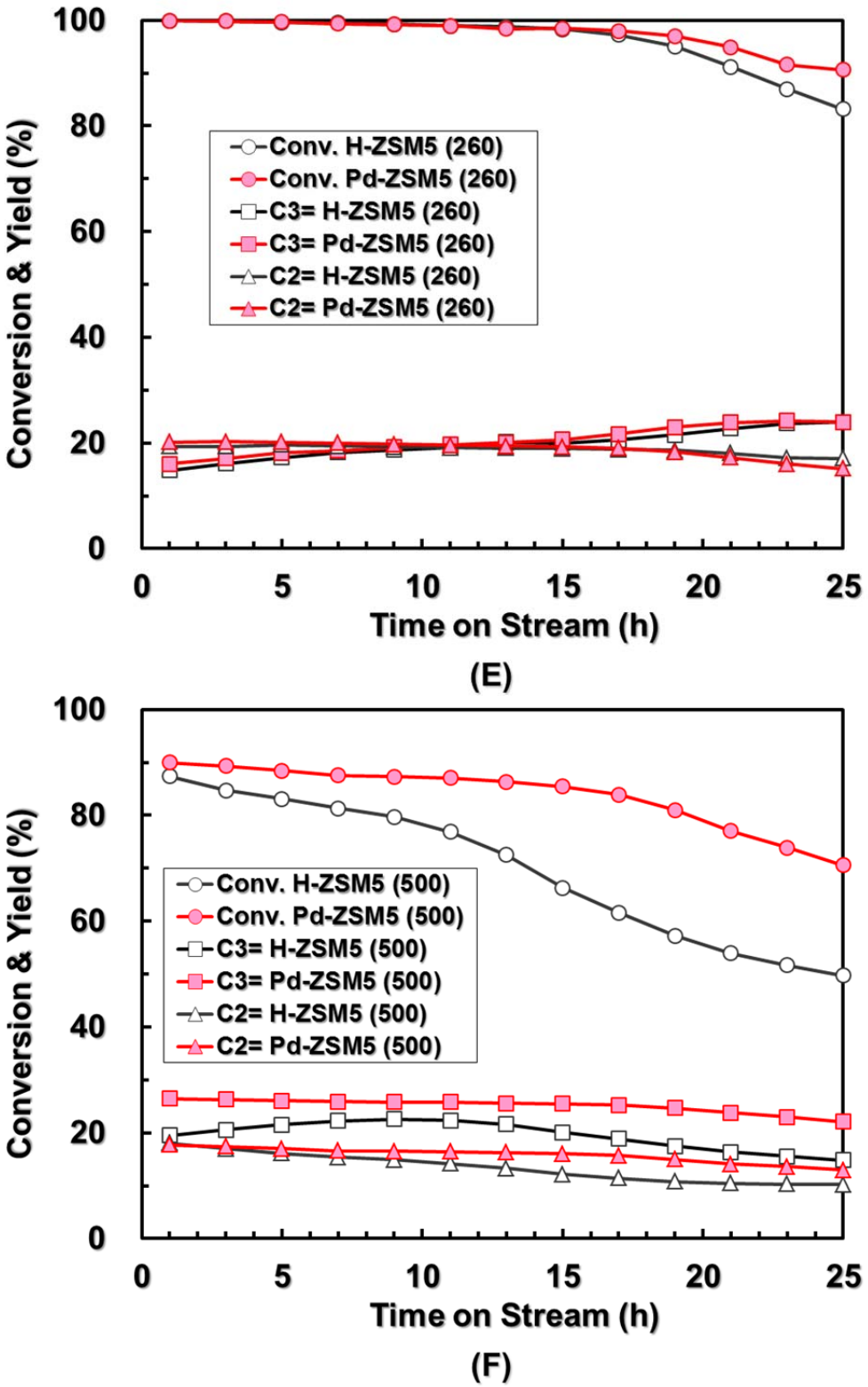

Fig. 1 The time course of the conversion (●) and the yield of propen (■) and ethene (▲) from *n*-hexane cracking over Pd/ZSM5 (fill) and H-ZSM5 (blank). Si/Al_2 ratio; (A) : 30, (B) : 50, (C) : 80, (D) : 150, (E) : 260, (F) : 500

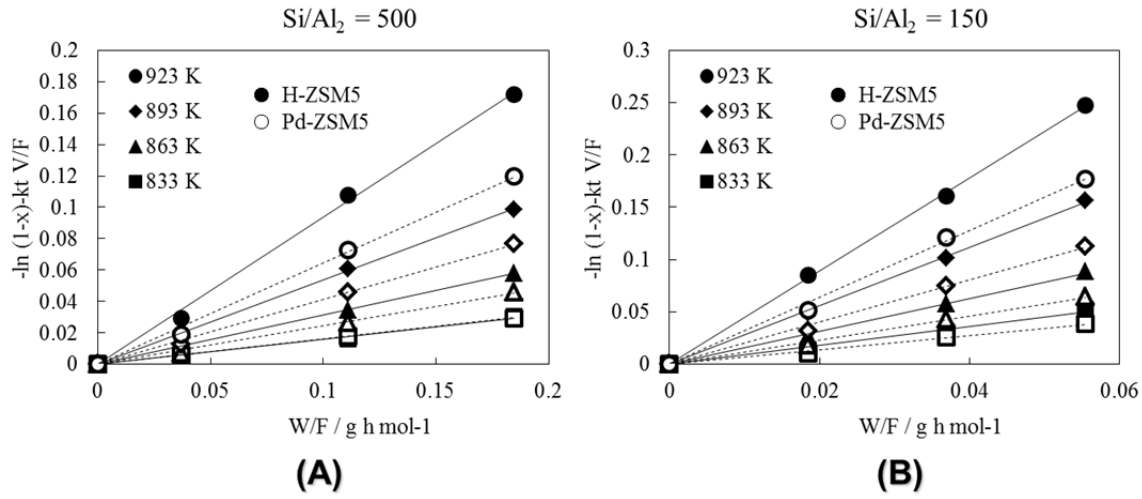

Fig. 2 Effect of W/F on cracking rate of *n*-hexane over various catalyst: H-ZSM5 (500) (A)-fill, Pd/ZSM5 (500) (A)-blank, H-ZSM5 (150) (B-fill), Pd/ZSM5 (150) (B-blank) at various temperature: 923 K (●), 893 K (◆), 863 K (▲), 833 K (■).

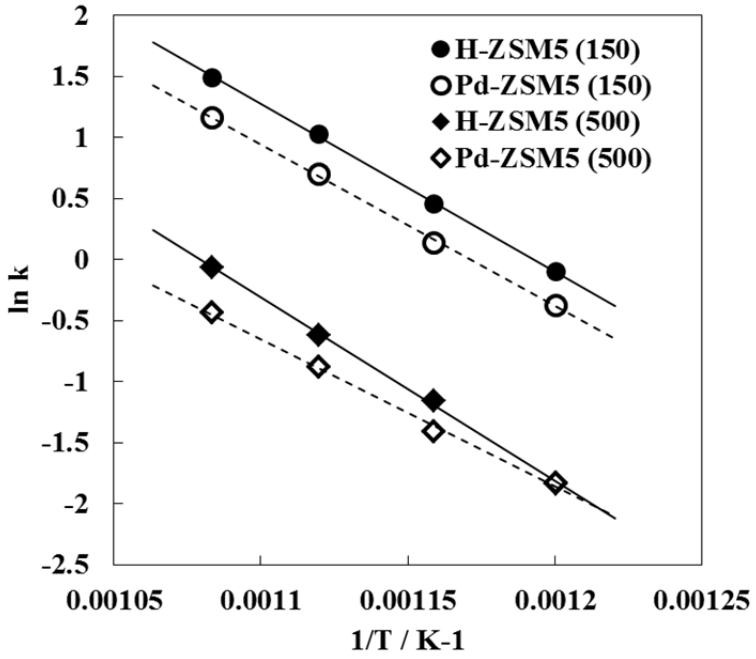

Fig. 3 Arrhenius plots for *n*-hexane cracking over various catalysts: H-ZSM5 (150) (●), Pd/ZSM5 (150) (○), H-ZSM5 (500) (◆), Pd/ZSM5 (500) (◇).

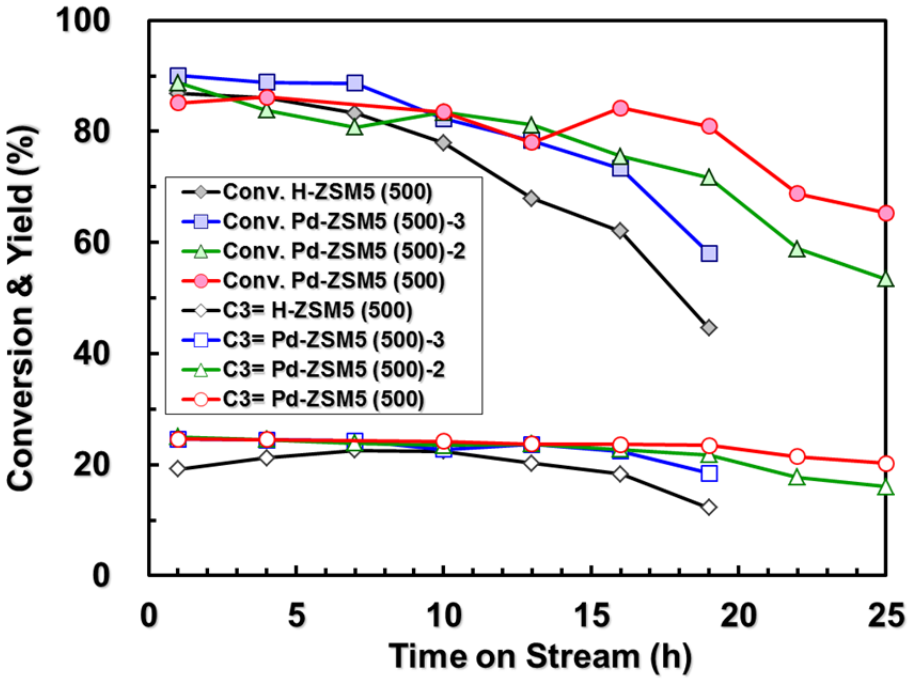

Fig. 4 The time course of the conversion (fill) and the yield of propene (blank) from *n*-hexane cracking over various amount of Pd loading to H-ZSM5 (500).

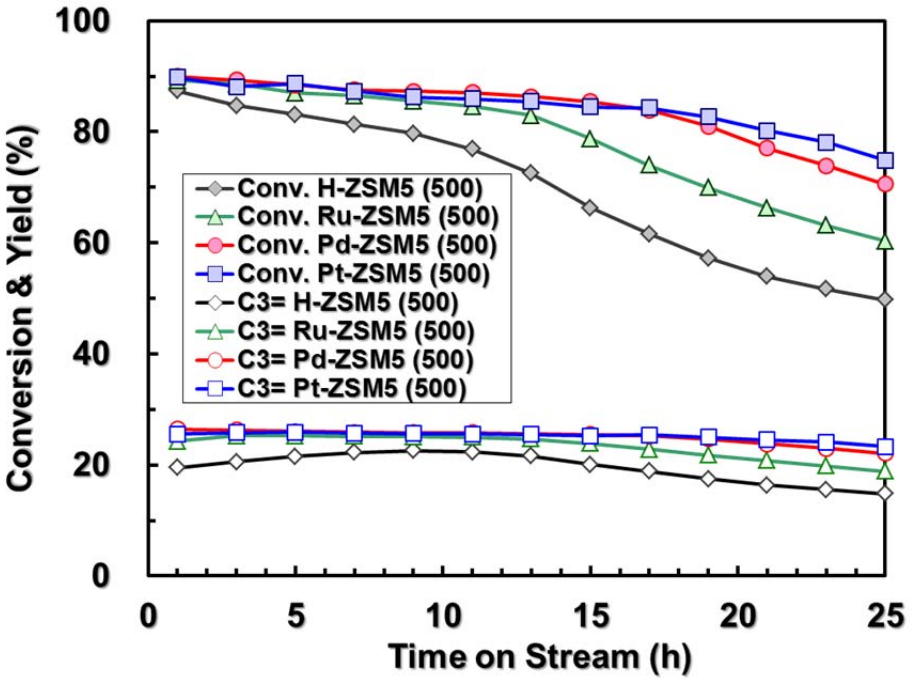

Fig. 5 The time course of the conversion (fill) and the yield of propene (blank) from *n*-hexane cracking over various metal loading H-ZSM5 (500).

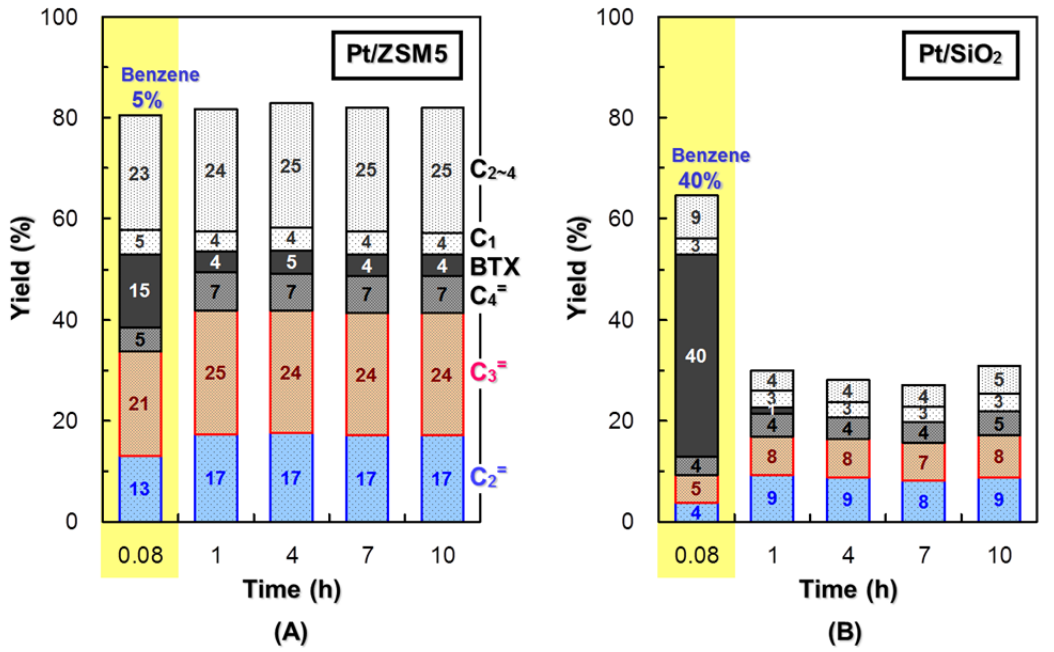

Fig. 6 The time course of the product distribution of *n*-hexane cracking over Pt/ZSM5 (500) (A) and Pt/SiO_2 (B).

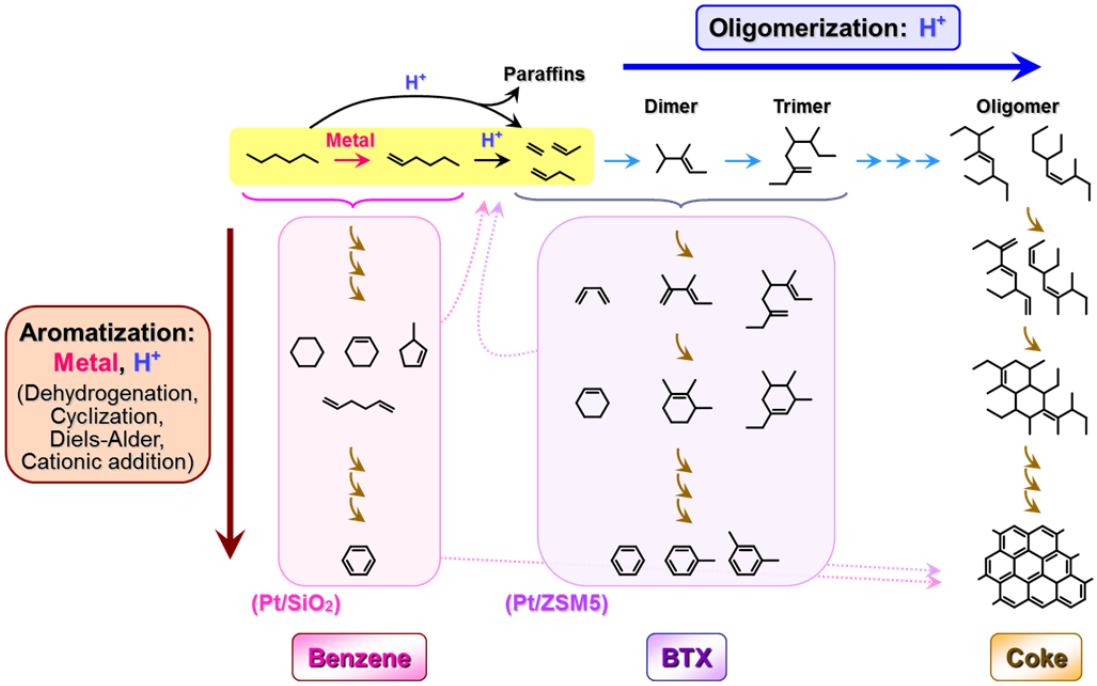

Fig. 7 Study of reaction mechanism for n-hexane cracking over metal loaded catalyst.

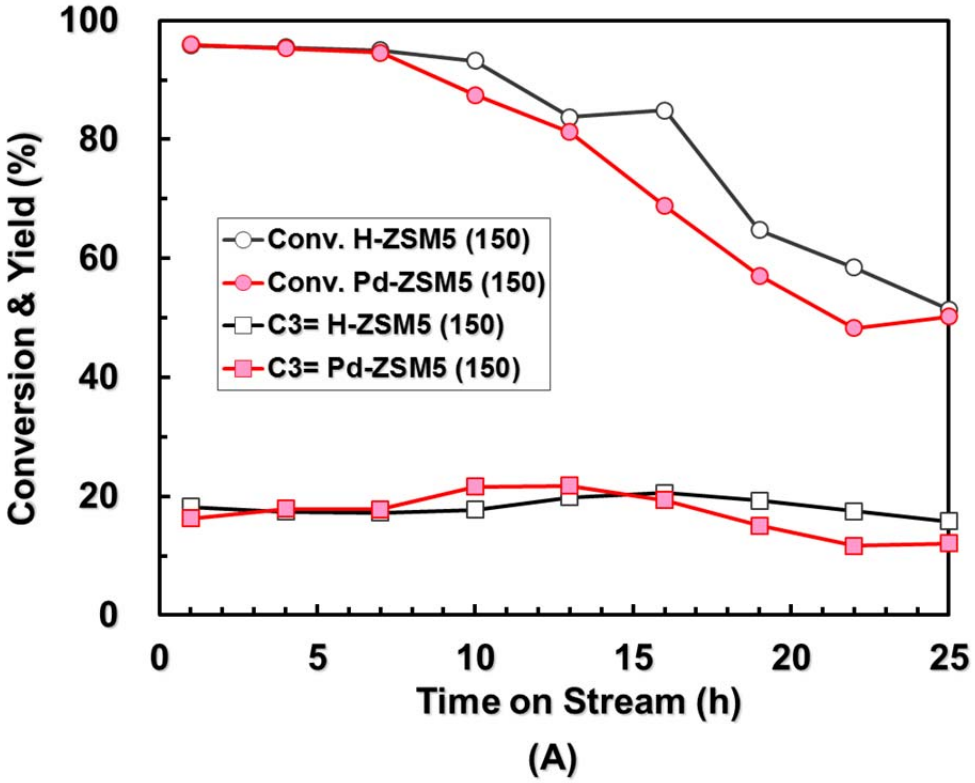
Conversion & Yield (%)
Time on Stream (h)
Conv. H-ZSM5 (150)
Conv. Pd-ZSM5 (150)
C3= H-ZSM5 (150)
C3= Pd-ZSM5 (150)
0
20
40
60
80
100
0
5
10
15
20
25

(A)

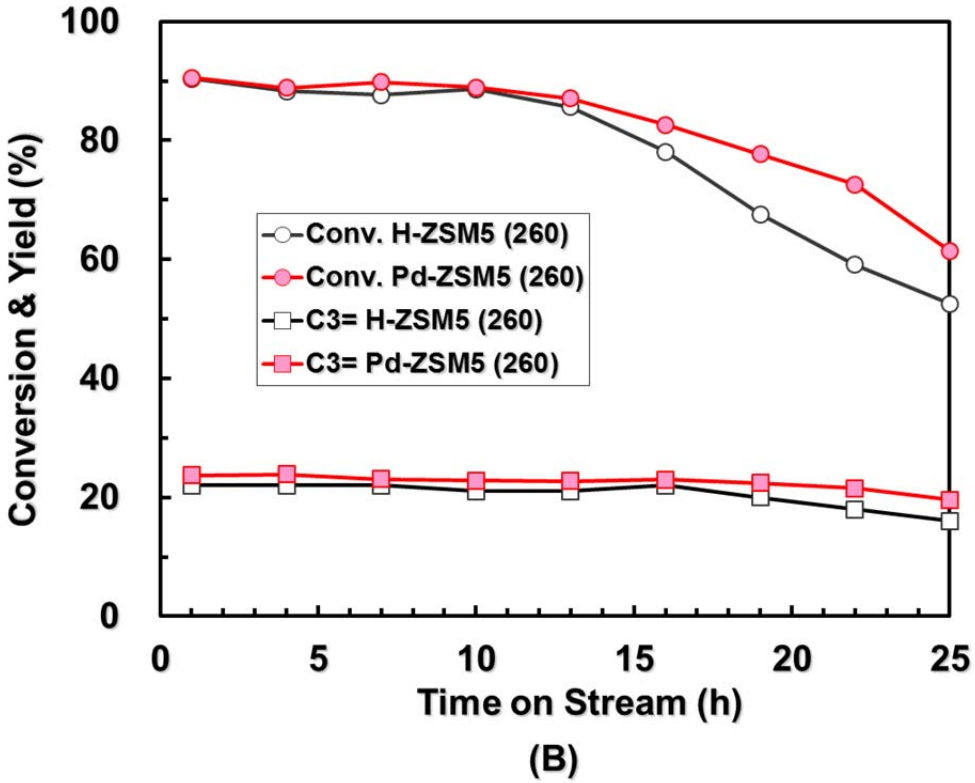
Conversion & Yield (%)
Time on Stream (h)
Conv. H-ZSM5 (260)
Conv. Pd-ZSM5 (260)
C3= H-ZSM5 (260)
C3= Pd-ZSM5 (260)
0
20
40
60
80
100
0
5
10
15
20
25

(B)

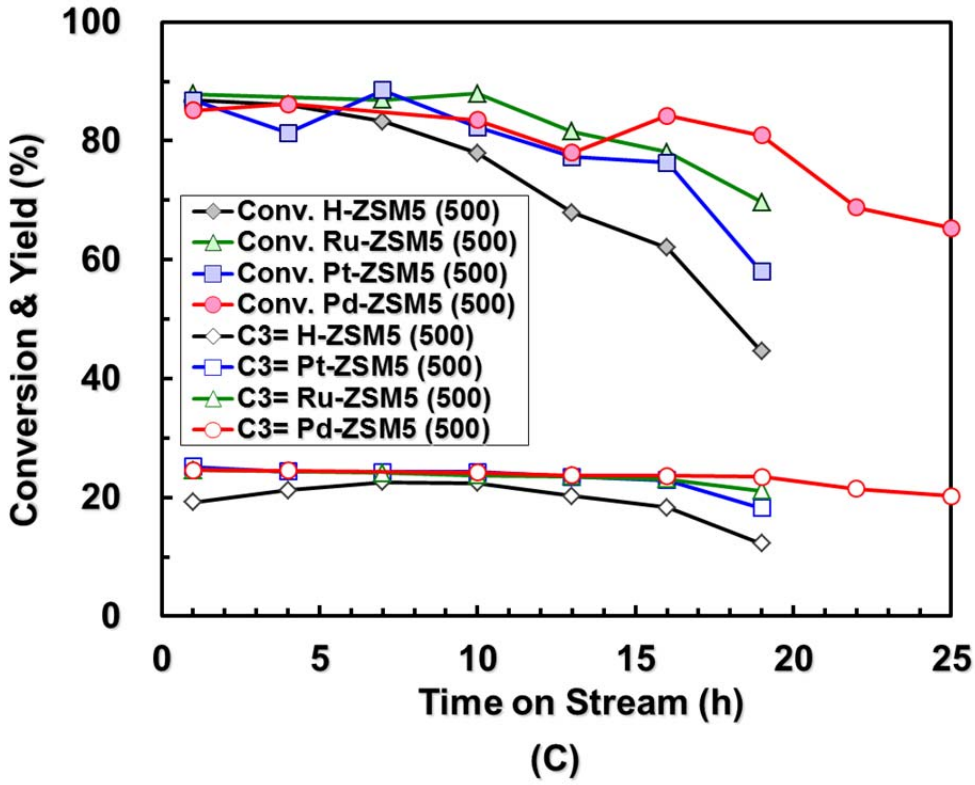

Fig. 8 The time course of the conversion (●) and the yield of propen (■) from naphtha cracking over Pd/ZSM5 (fill) and H-ZSM5 (blank).
Si/Al_2 ratio; (A) : 150, (B) : 260, (C) : 500.

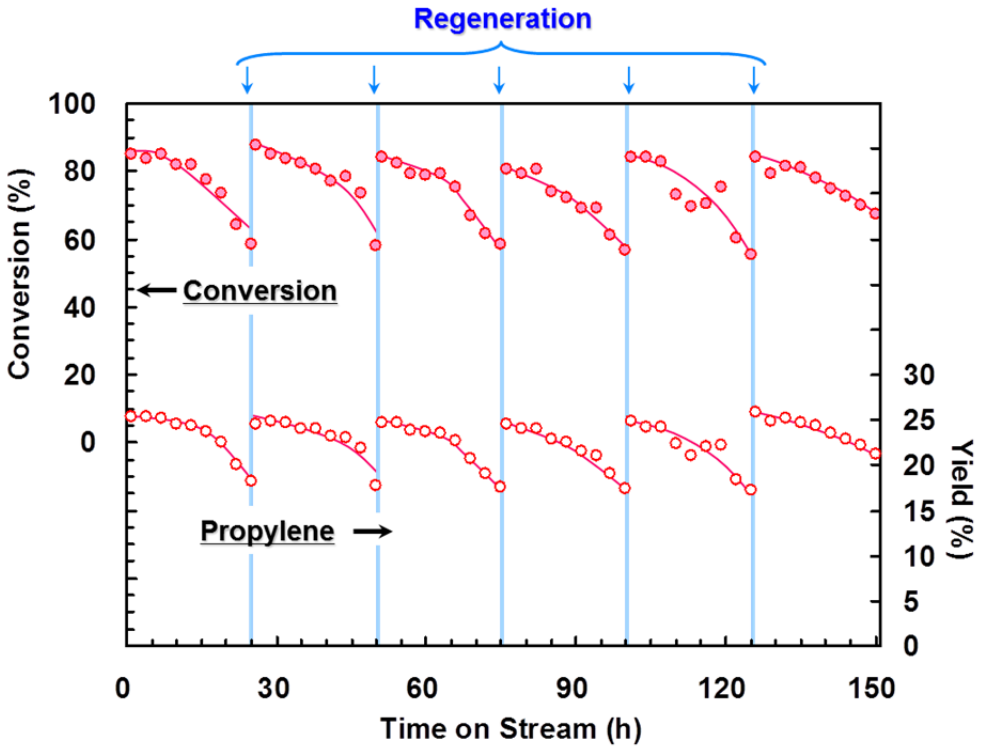

Fig. 9 The time course of the conversion (fill) and the yield of propene (blank) from naphtha cracking reaction and regeneration repeated test over Pd/ZSM5 (500).

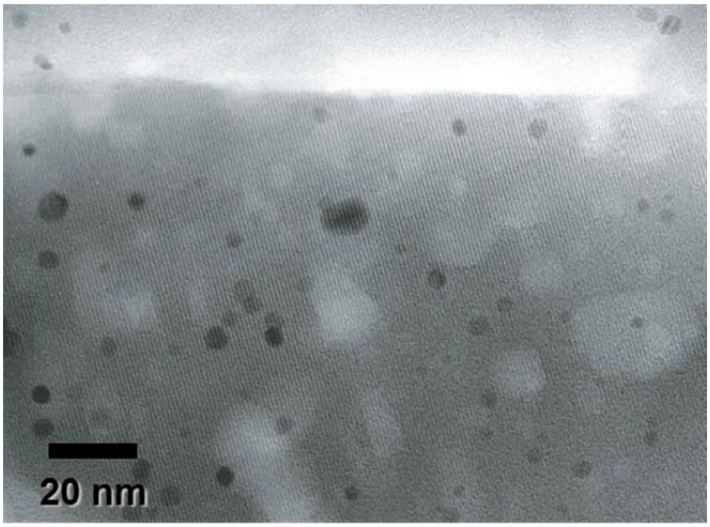

(A)

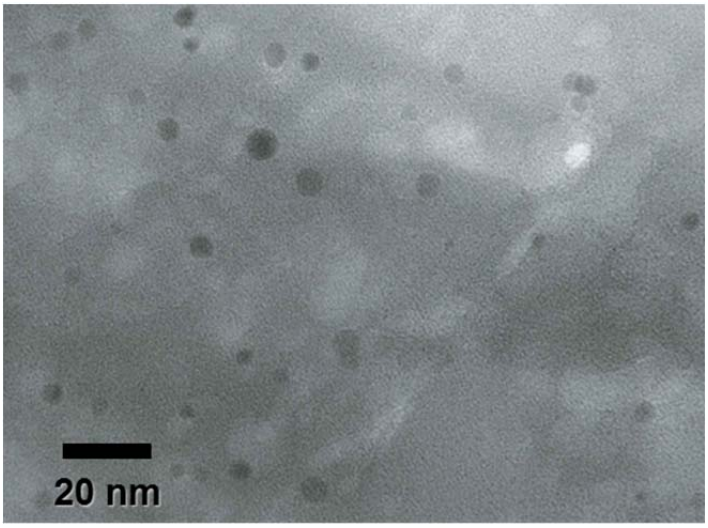

(B)

Fig. 10 The TEM images of Pd/ZSM5 (500) before (A) and after (B) repeating reaction and regeneration 6 times.

Chapter 5

Improvement in Durability of Catalytic Cracking of Naphtha over Metal Mixed ZSM5 Zeolite Catalyst with Oxidizing Gas

Abstract

When catalytic cracking of naphtha over zeolite catalyst is carried out, coke deposition on catalyst and dealumination from the zeolite skeleton caused by contact with high temperature steam are the main causes of the catalyst decay. By using CO_2 as oxidizing gas instead of H_2O, zeolite catalyst life was dramatically increased without dealumination. Coke or coke precursor reacted with CO_2 catalyzed by Palladium loaded to ZSM5 zeolite or Pd/CeO_2 which had gasification and reforming activity. On the other hand, using H_2O as oxidizing gas is also industrially important for cost or availability. Nextly, the study on the hydrothermal stability of zeolite was investigated. Zeolite catalyst was immediately inactivated without Phosphorus loading. Phosphorus is known to improve the hydrothermal stability of zeolite. Although phosphorus loading H-ZSM5 mixed with Pd/CeO_2 developed high performance of catalytic cracking of *n*-hexane, decrease in conversion of feedstock was observed at the early stage because of dealumination. In order to reinsert Aluminum into the zeolite framework, Al was added to zeolite in addition to P. As a result, it was confirmed that Al-P/ZSM5 showed high stability for high temperature steam. Al-P/ZSM5 mixed with Pd/CeO_2 produced highly yield of ethene and propene.

5.1 Introduction

Lower olefins such as ethylene, propene, butenes and butadiene, or aromatics such as benzene, toluene, ethylbenzene, and xylenes are important basic chemical raw materials constituting the petrochemical industry backbone. These basic chemical raw materials are mainly produced naphtha, which is light petroleum fraction of crude oil. Among these basic chemical raw materials, the lower olefins are produced by steam cracking in naphtha cracker in the presence of steam at least over 1073 K from the light naphtha which has relatively low boiling point components as raw materials. In addition, by the thermal decomposition of light naphtha, not only lower olefins but also aromatic compounds are also co-produced. However, cracking of the heavy naphtha containing many high-boiling components is known more commonly as production method of these aromatics than that of light naphtha. And this is more efficient production process as compared to production from light naphtha. From this point of view, it would be desirable to increase as much as possible the proportion of lower olefins and to reduce the aromatic components from light naphtha. With focus on the recent demand trend of lower olefins, the demand for propylene derivatives, such as polypropylene, cumene and propylene oxide is expanding. At present, growth in propylene demand has exceeded the growth of ethylene demand. And the difference in growth of them is believed to further accelerate in the future. On the other hand, since lower saturated hydrocarbons, main components of the naphtha, is less reactive, high temperature at least 1073 K is required for naphtha cracking and temperature range is limited for obtaining economical yield. Generally, ethene yield is higher as compared to propene at higher temperature. Propene / ethene ratio in the product is about 0.6 – 0.7 in the high temperature region above 1073 K. Since the propene / ethene ratio can not be changed greatly at this temperature range, the selective production of propene in the current naphtha cracker can be said that extremely difficult. Thus, since the product distribution in the thermal cracking is dependent on the cracking temperature, it is difficult to balance the product distribution flexibly matching supply and demand at the current naphtha cracker. In

addition to this, rapidly raw material switching is progressing around the natural gas producing countries, such as the Middle East. The cheaper ethene derived from ethane as raw feedstock having highly cost competitiveness as compared to naphtha as a raw material is flowing into the market. From these circumstances, the Asian naphtha crackers have been forced to measures production adjustment. Under such tight situations, Naphtha cracking process which is capable of controlling product distributions in accordance with the demand is desired, and catalytic cracking technology using acidic zeolite catalyst as a promising technology are disclosed [1]. This technology as compared to the current naphtha cracker will lead reducing energy consumption, and also reduction of carbon dioxide emitted in large quantities due to the naphtha cracking [2].

In the disclosed catalytic cracking technology of naphtha, medium pore zeolite, MFI-zeolite typified by ZSM5, have superior performance upon generation of lower olefins and aromatic compounds. It is possible to send down the reaction temperature to 973 K. It is possible to greatly improve propylene selectivity and propene / ethene ratio. By lowering the reaction temperature, the amount of methane as low-value chemical raw material is also suppressed. However, these disclosed technologies have not reached the level enough to replace the existing thermal decomposition cracker. To make catalytic cracking technology of naphtha over zeolite a practically usable level, it is necessary to extend the catalyst life significantly. The catalyst life is a major challenge commonly in reaction process using zeolite catalyst. Especially in extent harsh reaction conditions, a significant decrease in catalyst performance occurs. Deterioration of catalyst performance causes degradation of yield of the desired product and increase of load on the purification process due to a change in the product distribution. Main factor of performance degradation of the zeolite catalyst is the pore blockage by deposition of carbonaceous called coke and loss of acidity due to aluminum disassociation from the zeolite skeleton caused by contact with hot steam. Coke formation is caused by sequentially proceeding of side reaction such as multimerization, cyclization, and aromatization of lower olefins under severe reaction conditions. On the

other hand, zeolites have well defined pores derived from the crystal structure, and shape selective reactions proceed by contacting acid sites in the pores. Therefore, by using zeolite catalyst which does not have 12-membered ring or larger pores, sequential side reactions leading to coke formation is also limited because of the spatial limitation. However, since acid sites having no shape selectivity exist at the outer surface of the pores of zeolite at a constant rate, coke formation occurs due to progress of non-selective reactions [3]. Because the catalytic cracking of naphtha is a reaction at a high temperature, the performance degradation of the zeolite catalyst by such coking is a serious problem, and method for suppressing coking is the key in practical use.

It is known that coke materials lower catalyst activity in catalytic conversion reaction process of saturated hydrocarbons at high temperature, but the inactivation is suppressed by the addition of an oxidizing gas to raw materials. Steam, carbon dioxide, and so on is used as oxidizing gas. For example water vapor is added to the raw material to propene production by propane dehydrogenation reaction by using Pt catalyst [4], or styrene production by ethylbenzene dehydrogenation reaction using Fe catalyst [5]. Steam acts as an oxidizing gas under high temperature conditions and promotes removal of coke and coke precursor by a steam reforming reaction separately from the main reaction in the catalyst layer and suppresses cokingis. On the other hand, zeolite catalysts are generally known to be permanently deactivated by contacting steam under high temperature conditions. This permanent activity deterioration is caused by hydrolysis of the Al-O-Si bonds in the zeolite framework under high temperature conditions, elimination of the Al component, and disappearance of the acid properties. Therefore in order to use steam as an oxidizing gas for a high temperature reaction process using a zeolite catalyst, it is necessary to use a zeolite catalyst treated to improve steam tolerance. The catalytic cracking technologies of lower saturated hydrocarbons such as naphtha disclosed so far requires high temperature of 823 K or more. That is severe condition for a process using zeolite catalyst. However, in this condition, remarkable coking, which is difficult to suppress, occurs, so that coking is relaxed by adding water vapor to the raw material. On the other hand, in the catalytic

cracking reaction process of lower saturated hydrocarbons, the catalyst needs to be repeatedly used for reaction and regeneration, and it is necessary to use it for a long time. By adding water vapor, the catalyst is exposed to high temperature water vapor over a long time period, as a result, activity deterioration tends to occur easily. Also, energy consumption for the production of high-temperature steam is a factor that deteriorates unit energy consumption of the whole process. From the viewpoint of practicality and economy, it is necessary to suppress the amount of steam to be added as low as possible.

Some examples of catalytic cracking of naphtha to which water vapor were added as a using zeolite catalysts improved in steam tolerance have been reported. H-ZSM5 catalyst supporting phosphorus [6] and H-ZSM5 catalyst containing phosphorus, calcium and lanthanum [7] were used to carry out hexane cracking reaction for 48 hours or longer. However, in any case, the reaction conditions are such that the volume ratio of the raw material to the steam calculated from the described reaction conditions is large so the amount of water vapor added is large, and further nitrogen is circulated in order to dilute the reaction. From the viewpoint of practicality and economic efficiency, it can not be said that continuous operation is realistic. Besides that, some examples in which catalytic cracking reaction of lower saturated hydrocarbon was performed by adding steam to raw materials have been disclosed. However, practical continuous operation has not been practiced in any of the examples from a practical point of view [8-10].

Catalytic cracking reaction of naphtha under steam addition condition over zeolite catalysts added with metals active in steam reforming reaction has been reported. R. Le. Van Mao et. al. reported that H-ZSM5 containing Ni and Ru active in steam reforming reaction as a catalyst performed naphtha catalytic cracking reaction under steam addition conditions, and conducted continuous operation for 10 hours [11]. However, the catalyst layer temperature was as high as 998 K, and the amount of steam added was large. They also reported Naphtha catalytic cracking under steam addition conditions was carried out using H-ZSM5 contained Pd as metal having steam reforming

performance [12]. In order to improve the reactivity, methanol was added to raw material naphtha in addition to steam, and the reaction was carried out at a catalyst layer temperature of 905 K. However, the conversion rate remained at the maximum at 52.2%, and it was not able to sufficiently to be proceeded the cracking reaction.

Similarly to steam, carbon dioxide gas is also known for its effect of suppressing coking. With the same mechanism as water vapor, removal of coke and coke precursor by dry reforming reaction is promoted, and as a result, coking is suppressed. In addition to the dry reforming reaction, carbon dioxide gas is known to promote oxidative dehydrogenation reaction. Examples of process for adding carbon dioxide gas as an oxidizing gas to saturated hydrocarbon raw materials include utilizing oxidative dehydrogenation reaction for example (1) benzene production by aromatization reaction from lower saturated hydrocarbons such as methane, ethane and propane, (2) lower unsaturated hydrocarbons by dehydrogenation reaction of saturated hydrocarbons such as ethane, propane, butane, and (3) styrene production by dehydrogenation reaction of ethylbenzene [13]. Particularly, regarding the aromatic production process, metal-containing zeolite catalysts are suitably used under the condition of adding carbon dioxide [14-15]. On the other hand, in the process of producing lower unsaturated hydrocarbons by the catalytic cracking reaction of lower saturated hydrocarbon, it is necessary to suppress the progress of excessive dehydrogenation reaction, no study example in which carbon dioxide gas was added has been reported.

In oxidation reactions such as reforming reaction, VOC decomposition reaction in exhaust gas, or automobile exhaust gas purification reaction, the activity can be improved by using oxygen ion conductor having high lattice oxygen supplying ability such as perovskite type oxide and cerium oxide as a support [16-22]. However, in the catalytic cracking reaction of lower saturated hydrocarbon, no report about utilizing the lattice oxygen supply ability of the catalyst support for improving the catalyst life has been disclosed in view of these series of prior arts.

Thus, considering the catalytic cracking reaction of naphtha, techniques for suppressing coking, which causes reduction in catalyst durability by adding oxidizing

gas to raw materials, have not necessarily been studied in detail and have not reached practical use level.

In view of these circumstances, in this paper, we disclosed metal-containing zeolite catalysts capable of suppressing coke formation by an oxidizing gas and capable of efficiently producing lower olefins efficiently for a long period in a catalytic cracking reaction of naphtha.

5.2 Experiment

5.2.1.1 H-ZSM5

Ammonium type ZSM5 sample, NH_4-ZSM5 zeolite (Si/Al_2 = 500), was supplied from Sud-Chemie. The proton type ZSM5, H-ZSM5, was obtained by calcination of the NH_4-ZSM5 (Si/Al2 = 500) at 823 K for 10 h.

5.2.1.2 Impregnation of Palladium to H-ZSM5

Palladium loaded H-ZSM5 (Si/Al_2 ratio: 500) was prepared by impregnation of Tetraammine palladium dichloride monohydrate salt ($Pd(NH_3)_4Cl_2 \cdot H_2O$). 0.044 g of $Pd(NH_3)_4Cl_2 \cdot H_2O$ was dissolved in 100 ml of ion-exchanged water. 5.0 g of H-ZSM5 (500) was introduced to the Palladium solution and stirred at 353 K for 3 h, and the solution was evaporated to obtain powder sample. Finally, the powder sample was calcined at 823 K for 10 h to obtain Pd/ZSM5 to which 0.35 wt% of Palladium (0.033 mmol of Palladium to 1.0 g of zeolite, [Pd]/[Al] = 0.5 in H-ZSM5) was loaded.

5.2.1.3 Impregnation of Palladium to CeO_2

Impregnation of Pd to CeO_2 was carried out by Incipient Wetness method. $Pd(NH_3)_4Cl_2 \cdot H_2O$ solution prepared so as to have supported amount of 330 mmol with respect to 1 g of cerium oxide was dropped and dried, and then calcined at 973 K for 10 hours to obtain Pd/CeO_2. When Pd/CeO_2 was used as catalyst for n-hexane cracking,

mixture of Pd/CeO_2 and zeolite was thoroughly physically mixing in a mortar so that the cerium oxide component is one tenth of the zeolite component.

5.2.1.4 Catalytic cracking of n-hexane

The catalytic performance were tested by the catalytic cracking of *n*-hexane (Wako, 96%). *n*-hexane was selected as a model alkane compound because of the similar molecular weight as the mean one of light naphtha. The cracking of *n*-hexane was carried out in a 7 mm hastelloy C276 tubular flow reactor loaded with 0.36 g of 250–500 μm zeolite pellets without a binder, which was the catalyst was centered at the reactor in a furnace. The reactor was heated to the reaction temperature (873 K) with N_2 flow into the temperature of catalyst bed at 923K, N_2 flow was stopped and *n*-hexane was introduced without carrier gas. The weight hourly space velocity of *n*-hexane (WHSV) was set to 10 h^{-1}. The reaction products were analyzed with on-line gas chromatographs (Shimadzu GC-2014) with two FID detectors and a TCD detector. The selectivity to the products and the *n*-hexane conversion were calculated based on the carbon numbers.

5.2.1.5 Catalytic cracking of n-hexane with CO_2

The catalytic performance under existence of CO_2 were tested by the catalytic cracking of *n*-hexane (Wako, 96%). Except for adding CO_2, tests were carried out by the method described in 2.1.3. The reactor was heated to the reaction temperature (873 K) with N_2 flow into the temperature of catalyst bed at 923K, N_2 flow was stopped and *n*-hexane and CO_2 was introduced without other carrier gas. The weight hourly space velocity of *n*-hexane (WHSV) was set to 10 h^{-1}. The partial pressure of hexane was set to 0.11 MPa and the partial pressure of CO_2 was set to 0.055 Mpa.

5.2.1.6 Measurement of coke amount deposited on catalyst

The amount of coke deposited on the catalyst was analyzed by raising the temperature to 1173 K at 10 K per a minute under air flow using a thermogravimetric

analyzer (Thermoplus EVO Ⅱ TG-8120 manufactured by Rigaku). The weight of the burned coke with respect to the catalyst weight excluding coke was taken as the coke amount (wt%).

5.2.1.7 Detect of CO under reaction condition

CO was analyzed with on-line gas chromatographs (Shimadzu GC-2014) with TCD detector.

5.2.2.1 Catalytic cracking of n-hexane with H_2O

The catalytic performances under existence of H_2O were tested by the catalytic cracking of *n*-hexane (Wako, 96%). Except for adding H_2O instead of CO_2, tests were carried out by the method described above in 2.1.5. The reactor was heated to the reaction temperature (873 K) with N_2 flow into the temperature of catalyst bed at 923K, N_2 flow was stopped and *n*-hexane and H_2O was introduced without other carrier gas. The ratio of volume of steam to volume of n-hexane (Vs/Vo) was 0.5. The ratio of weight of steam to weight of n-hexane (S/O) was about 0.1. The weight (of zeolite) hourly space velocity of *n*-hexane (WHSV) was set to 10 h^{-1}. The partial pressure of hexane was set to 0.11 MPa and the partial pressure of H_2O was set to 0.055 Mpa.

5.2.2.2 Loading of phosphorus to zeolite

Ammonium type ZSM5 sample, NH_4-ZSM5 zeolite (Si/Al_2 = 30), was supplied from Zeolyst International. Impregnation of phosphorus was carried out by Incipient Wetness method. Diammonium hydrogen phosphate $(NH_4)_2HPO_4$ solution prepared so as to have supported amount of 700 μmol with respect to 1 g of NH_4-ZSM5 ([P]/[Al] = 0.63, molar ratio, 2 wt% as P atom to zeolite) was dropped and dried, and then calcined at 823 K for 10 hours to obtain P/ZSM5.

5.2.3.1 Loading of phosphorus and aluminum to zeolite

0.67 g of boehmite (Wako Pure Chemical Industries, Ltd.) and 1.7 g of diammonium hydrogen phosphate (Wako Pure Chemical Industries, Ltd.) were added to 100 ml of distilled water, and 10 g of NH_4-ZSM5 (Si/Al_2 = 30) was added to the mixture, and the mixture was further stirred at room temperature. The resulting mixture was evaporated to dryness under reduced pressure using an evaporator. After drying the residue after evaporation to dryness, it was calcined in air at 823 K for 5 hours, and a mixed gas of nitrogen and water vapor was brought into contact with the sample so as to have a flow rate of nitrogen of 160 Ncc / min and water vapor of 40 Ncc / min at 973 K for 24 hours to prepare Al-P/ZSM5.

5.2.3.2 Severe hydrothermal treatment of P/ZSM5 and Al-P/ZSM5 and cracking test

A mixed gas of nitrogen and water vapor was brought into contact with P/ZSM5 and Al-P/ZSM5 catalyst so as to have a flow rate of nitrogen of 160 Ncc / min and water vapor of 40 Ncc / min at 973 K for 161 hours to prepare P/ZSM5-s and Al-P/ZSM5-s respectively. After the treatment, catalytic cracking reaction of n-hexane was carried out in the same way of section 2.1.4 above except for the reaction condition: WHSV = 15 h^{-1}, S/O = 0.1, N2 flow = 9 Ncc / min, total pressure = 0.10 MPa.

5.2.3.3 NH_3 TPD & N_2 adsorption

Temperature-programmed desorption of ammonia (NH_3-TPD) spectra were recorded on Belcat-A (Microtrac-Bel). Typically, 25 mg catalyst was pretreated at 773 K in He for 1 h and then was cooled to adsorption temperature at 373 K. Prior to the adsorption of NH_3, the sample was evacuated. Approximately 5 vol% of NH_3 was allowed to contact with the sample for 30 min. Subsequently, the sample was evacuated to remove weakly adsorbed NH_3 for 15 min. Finally, the sample was heated from 373 to 973 K at a ramping rate of 10 K min^{-1} with the He flow passed through the reactor. A mass spectrometer (mass number 17) was used to monitor desorbed NH_3. The amount of acid sites was determined by using the area of the so-called *h*-peak in the profiles.

Nitrogen adsorption-desorption isotherms were measured to obtain information on

the micro- and meso-porosities at 77 K on a Belsorp-max (Microtrac-Bel). The BET specific surface area (S_{BET}) was calculated from the adsorption data in the relative pressure ranging from 0.04 to 0.2. External surface area (S_{EXT}) was estimated by the *t*-plot method.

5.2.3.4 ^{27}Al MAS-NMR

Solid state ^{27}Al magic-angle spinning (MAS) NMR spectra were obtained with π/2 pulse width of 6 μs and pulse delay of 5 s on a JEOL ECA-400 spectrometer. Al resonance frequency employed was at 104 MHz and the sample spinning rate speed was 5.3 KHz. ^{27}Al chemicals shifts were referenced to a saturated $Al(NO_3)_3$ solution.

5.2.3.5 n-Hexane cracking test with H_2O over Pd/CeO2 + Al-P/ZSM5 and Al-P/ZSM5

The catalytic performances under existence of H_2O were tested by the catalytic cracking of *n*-hexane (Wako, 96%) in the same way described in section 2.1.4 except for adding H2O, WHSV and S/O, the reaction condition: WHSV = 3 h^{-1}, S/O = 0.5, total pressure = 0.10 MPa.

5.3 Results and Discussion

5.3.1 Improvement of durability in catalytic cracking of naphtha by CO_2

We reported that the ZSM5 zeolite with controlled amount of acid and amount of loading metal which has dehydrogenation property had the improved durability and increased yield of lower olefins in catalytic cracking of naphtha at Chapter 3. However, from the viewpoint of practical application, it is necessary to achieve further long catalyst life. Since naphtha cracking is carried out at significantly high temperature, coke formation is inevitable. If coke materials or coke precursors can be decomposed during the reaction, the catalyst life can be extended. Oxidizing gas [14-15] plays this role.

The addition of CO_2 to reaction system has the effect of lowering the naphtha partial pressure during naphtha catalytic cracking and suppressing the progress of the sequential reaction. And as well as H_2O, CO_2 itself reacts with the coke precursors and gasifies them to decompose. Reforming also occurs to cause generation of CO.

Gasification:

$$C + CO_2 \rightarrow 2\ CO \quad (1)$$

$$(C + H_2O \rightarrow CO + H_2) \quad (2)$$

Reforming:

$$C_nH_m + n\ CO_2 \rightarrow 2n\ CO + m/2\ H_2 \quad (3)$$

$$(C_nH_m + n\ H_2O \rightarrow n\ CO + (n + m/2)\ H_2) \quad (4)$$

In order to confirm this effect for catalytic cracking on *n*-hexane over Pd/ZSM5, performance tests were carried out by adding CO_2 into the reaction system. In order to avoid dilution of hexane by addition of CO_2, the partial pressure of hexane was set to 0.11 MPa similarly to the case where the reaction was carried out without adding CO_2, and the reaction was carried out. The reaction results is shown in Fig. 1. Compared with H-ZSM5, Pd/ZSM5 showed less decline in conversion even without addition of CO_2, and improved ethene and propene yield. The addition of CO_2 led to a dramatic improvement in durability and suppression of a decrease in the ethene and propene yield.

As a result of measuring the amount of coke produced in these reactions, an increase in the amount of coke produced was observed in Pd/ZSM5 as compared with H-ZSM5 (Fig.2). It is considered that the dehydrogenation reaction progressed by adding Pd and the coke production amount increased. However, since the reaction promoting effect by the dehydrogenation reaction was high, the influence on the catalyst life was considered to be small. When CO_2 was added and the reaction was carried out, the coke production amount decreases. This is thought to be due to the progress of the decomposition of the coke precursor by the gasification reaction. According to the equation (1) and (3), CO is generated as a result of the progress of the gasification reaction and the reforming reaction due to the addition of CO_2. Analysis of the reaction

gas as a corroboration confirmed the production of CO indeed (Fig.3). In addition, it is considered that the oxidation reaction of CO_2 can be efficiently progressed by using oxygen ion conductor having high lattice oxygen supply ability as a support [16-22]. Therefore, using cerium oxide as a support, Pd/CeO_2 supporting Pd as an active metal was mixed with H-ZSM5 and subjected to hexane decomposition reaction. Cerium oxide and zeolite were mixed at a weight ratio of 1 : 10. As a result, the same effect as Pd/ZSM5 was shown (Fig. 4). That is, even if the active metal is not supported directly on the zeolite, it can be said that the effect of prolonging the life span by utilizing the oxidizing gas was manifested by physically mixing the zeolite with the supports loaded active metal species.

From the above results, it was found that the effect of improving the durability was observed by the addition of CO_2, and that the addition of CO_2 was an effective means in the naphtha catalytic cracking reaction.

5.3.2 Improvement of durability in catalytic cracking of naphtha by H_2O

Similarly to CO_2, reaction evaluation was carried out while circulating H_2O as an oxidizing gas having gasification and reforming effect of coke and coke precursor. In order to avoid dilution of hexane by addition of H_2O, the partial pressure of hexane was set to 0.11 MPa similarly to the case where the reaction was carried out without adding H_2O and the reaction was carried out. As a result, the activity of Pd/ZSM5 remarkably decreased as compared with the case where H_2O was not added (Fig. 5). It is considered that the zeolite deteriorated due to contact with high temperature steam. It is known that when the steam is brought into contact with the zeolite at high temperature, Al is released from the skeleton of the zeolite and the acid property is lost, “dealumination” [23]. This elimination of Al is a permanent deterioration of the catalyst, it is said that once Al is eliminated, it will not return back into the skeleton and will no longer function as an acid. Therefore, the gasification and reforming function was handled by another secondary component to be physically mixed, and the zeolite was designed to support a substance imparting hydrothermal stability. Phosphorus, which is known to

have the effect of increasing hydrothermal resistance of zeolite, was loaded on the zeolite. Phosphorus was loaded to be [Phosphorus]/[Aluminum] molar ratio of 0.6. It was reported that loading of P by this ratio develops highly hydrothermal resistance [24-25]. Pd/CeO_2 developed in Section 3.1 was used as a material of the secondary component. As a result of conducting the reaction by mixing P/ZSM5 and Pd/CeO_2 at a weight ratio of 10 : 1 and introducing H_2O, it was found that the lifetime was extended (Fig. 6).

5.3.3 Improvement of hydrothermal stability and catalyst life

Hydrothermal stabilization is essential for the industrial application of zeolites. As described in Section 3.2, it is known that dealumination can be suppressed when Phosphorus is loaded. However, from the reaction result of Pd/CeO_2 + P/ZSM5 in the presence of water (Fig. 6), the conversion rate at 25 hours is lower than the CO_2 flowing reaction (Fig. 4). Hexane conversion rate of Pd/CeO_2 + H-ZSM5 at the time of CO_2 circulation: 87 %, hexane conversion rate of Pd/CeO_2 + P/ZSM5 at the time of H_2O circulation: 67 %. This suggests that although the hydrothermal resistance was improved by loading P, the deterioration was not completely prevented and the dealumination was progressed and deactivated during the reaction. In other words, it can be considered that there is a limit to the hydrothermal effect for a long time only by supporting Phosphorus.

In order to verify the hydrothermal stability of P/ZSM5, steam treatment was carried out for P/ZSM5 at 973 K, higher than the reaction temperature, for 161 hours to obtain P/ZSM5-s. It was confirmed that cracking activity of P/ZSM5-s decreased, as a result of *n*-hexane cracking test over the catalyst after severe hydrothermal treatment (Fig. 7). Certainly, even if P was loaded, it can be said that it couldn’t completely stop the deactivation due to dealumination [23].

In order to improve practicality, it is necessary to further improve the hydrothermal stability. In the presence of high temperature steam, dealumination from the zeolite

skeleton causes deactivation, but in some reports, treatment of zeolite in Al vapor or water reinserts Al into the zeolite skeleton and the again improves [26-30].

Therefore, the following catalyst design was devised.

(1) As mentioned above, dealumination is suppressed by loading phosphorus, and hydrothermal resistance is maintained.

(2) By loading Al on the zeolite beforehand, Al is reinserted from the outside of the skeleton to the zeolite skeleton again even if dealumination proceeds.

In this way, it was thought that a catalyst showing high steam resistance could be obtained by retaining Al in the framework even in the presence of steam. We investigated the hydrothermal stability of the catalyst supporting Al in addition to P. To NH_4-ZSM5 (Si/Al_2 molar ratio: 30), boehmite was loaded as Al source so that the Al atom was 4 wt% with respect to the zeolite and P was loaded on the zeolite so that the [P] / [Al] molar ratio of the whole catalyst was 0.6. After that, the severe hydrothermal treatment at 973 K was carried out similarly to P/ZSM5 to obtain Al-P/ZSM5-s. As a result of *n*-hexane cracking over this steamed catalyst Al-P/ZSM5-s, no degradation in activity was observed before and after hydrothermal treatment (Fig. 8).

Figures 9 (A) and (B) show the results of ^{27}Al MAS-NMR measurement before and after steaming of P/ZSM5 and Al-P/ZSM5, respectively. In all catalysts, it was confirmed that the tetracoordinated aluminum indicating the acid property decreased after the steam treatment and the signal derived from the tetracoordinated aluminum phosphate species in about 54 - 20 ppm region increased. The peak near 14 ppm observed in the spectrum of Al-P/ZSM5 was a signal derived from boehmite.

The results of NH_3-TPD measurement and nitrogen adsorption measurement before and after steam treatment are shown in Table 1. The specific surface area of Al-P/ZSM5 was lower than that of P/ZSM5. The low specific surface area of Al-P/ZSM5 was considered to be due to the large amount of P loading. Besides, the specific surface area of each sample increased by steam treatment. The phosphorus compounds that had blocked the pores before the hydrothermal treatment react with Al by hydrothermal treatment and turns into aluminum phosphate. In the course of this reaction, it was

considered that migration of P restored the blocked pores and increased the specific surface area. In addition, it can be seen that the acid amount was greatly decreased by the steam treatment. As a result of ^{27}Al MAS-NMR, NH_3-TPD and nitrogen adsorption, the behavior of Al-P/ZSM5 by steam treatment showed the same tendency as P/ZSM5. However, contrary to this, Al-P/ZSM5 showed higher activity than P/ZSM5 even after severe steam treatment. The reason for showing this high activity of Al-P/ZSM5 has not been clarified yet and we want to consider it in the future. Finally, Pd/CeO_2 with gasification and reforming effect of coke and coke precursor was mixed with Al-P/ZSM5 and subjected to *n*-hexane cracking. The life of Pd/CeO_2 + Al-P/ZSM5 was longer than that of Al-P/ZSM5 in the coexistence of steam and the yield of propylene was improved (Fig.10).

In this way, we found that Al-P/ZSM5 with high hydrothermal resistance was developed and further long life could be achieved for catalytic cracking of *n*-hexane by mixing Pd/CeO_2.

5.4 Conclusion

Addition of CO_2 to the feedstock of cracking reaction of *n*-hexane led to a dramatic improvement in durability of Pd/ZSM5 catalyst and suppression of a decrease in the ethene and propene yield. It is thought that the gasification or reforming reaction occurs with coke or coke precursor by CO_2 flow. This effect developed when H-ZSM5 was mixed with Pd loaded CeO_2 which was oxygen ion conductor having high lattice oxygen supply ability as a support. Similarly to CO_2, addition of H_2O led improvement in catalyst life. However, the permanent inactivation was observed by using H_2O because of release of aluminum from zeolite skeleton due to contact with high temperature steam. In order to improvement in hydrothermal durability, not only P well known to the effect but also Al was loaded to H-ZSM5. Al-P/ZSM5 had higher steam stability than P/ZSM5even after severe hydrothermal treatment. Al-P/ZSM5 mixed with

Pd/CeO_2 produced ethene and propene at high efficiency for 48 h under steam coexistence.

Reference

[1] S. Takahashi, F. Kanashima, JP Patent (1994) 192135.
[2] T. Ren, M. Patel, K. Blok, Energy, 31 (2006) 425.
[3] T. Tago, M. Sakamoto, K. Iwakai, H. Nishihara, S. R. Mukai, T. Tanaka, T. MasudaJ. Chem. Eng. Jpn, 42 (2009) 162.
[4] M.M Bhasin, J.H McCain, B.V Vora, T Imai, P.R Pujadó, Appl. Cat. A: Gen., 221 (2001) 397.
[5] E.H. Lee, Catal. Rev. 8 (1974) 285.
[6] A. Yamaguchi, J. DingPheng, T. Ikeda, N. Hiyoshi, K. Sato, T. Inoue, F. Mizukami, M. Shirai, T. Hanaoka, JP Patent (2012) 193127.
[7] T. Inoue, K. Otaki, H. Sugiyama, Y. Kiyosumi, S. Hamakawa, F. Mizukami, T. Furukawa, M. Kawahara, G. Sawada, H. Shoji, JP Patent (2010) 104878.
[8] Y. Yoshimura, K. Murata, T. Hayakawa, K. Suzuki, M. Takehira, K. Wakui, K. Shiozawa, K. Sato, G. Sawada, JP Patent (1999) 180902.
[9] JP Patent (2011) 523584.
[10] N. Al-Yassir, R. Le Van Mao, Catal. Lett. 100 (2005) 1.
[11] R. Le Van Mao, N. T. Vu, N. Al-Yassir, H. T. YanInd, Eng. Chem. Res. 47 (2008) 2963.
[12] H.T. Yan, R. Le. Van Mao, Catal. Lett. 142 (2012) 60.
[13] S. Wang, Z.H. Zhu, Energy & Fuels, 18 (2004) 1126.
[14] R. Ohnishi, S. Liu, Q. Dong, L. Wang, M. Ichikawa, J. Catal. 182 (1999) 92.
[15] S.K. Ihm, Y.K. Park, S.W. Lee, Appl. Organometal. Chem. 14 (2000) 778.
[16] N. Laosiripojana, W. Sutthisripok, S. Assabumrungrat, Chem. Eng. J. 112 (2005) 13.
[17] S. Natesakhawat, R.B. Watson, X. Wang, U.S. Ozkan, J. Catal. 234 (2005) 496.
[18] T.J. Huang, H.J. Lin, T.C. Yu, Catal. Lett. 105 (2005) 239.
[19] K. Urasaki, Y. Sekine, S. Kawabe, E. Kikuchi, M. Matsukata, Appl. Catal. A: Gen. 286 (2005) 23.
[20] J.W. Nam, H. Chae, S.H. Lee, H.Jung, K.Y. Lee, Stud. Sur. Sci. Catal. 119 (1998) 843.
[21] L. Yue, C. He, X. Zhang, P. Li, Z. Wang, H. Wang, Z. Hao, J. Hazard. Mater 244-245 (2013) 613.
[22] H. Tanaka, Catal. Surv. Asia 9 (2005) 63.
[23] H.E. Bij, B.M. Weckhuysen, Chem. Soc, Rev. 44 (2015) 7406.
[24] T. Blasco, A. Corma, J. Martinez-Triguero, J. Catal. 237 (2006) 267.

[25] H.E. Bij, F. Meirer, S. Kalirai, J. Wang, B.M. Weckhuysen, Chem. Eur. J. 20 (2014) 16922.
[26] C. Inaki, H. Ito, K. Honda, K. Oyama, A. Okita, WO patent (2008) 026638
[27] JP Patent (1991) 63430
[28] D.D. Shihabi, J. Catal. 93 (1985) 471.
[29] C.D. Chang, J. Chem.Soc., Faraday Trans. 81 (1985) 2215.
[30] T. Sano, Catalyst and Catalysis, 41 (1999) 543.
[31] J.C. Summers, K. Baron, J. Catal. 57 (1979) 380.
[32] J.S. Hepburn, H.G. Stenger, Energy & Fuels 2 (1988) 289.
[33] H.S. Gandhi, M. Shelef, Appl. Catal. 77 (1991) 175.
[34] C.P. Hubbard, K. Otto, H.S. Gandhi, K.Y.S. Ng, Catal. Lett. 30 (1995) 41.

Table 1. The BET surface area estimated by N_2 adsorption and the acid amounts estimated by NH_3-TPD analyses of H-ZSM5 catalysts.

Catalyst	**S_{BET} / $m^2 \cdot g^{-1}$**	**Acid amount / $mmol \cdot g^{-1}$**
P/ZSM5	346	0.153
P/ZSM5-s	397	0.003
Al-P/ZSM5	286	0.151
Al-P/ZSM5-s	328	0.06

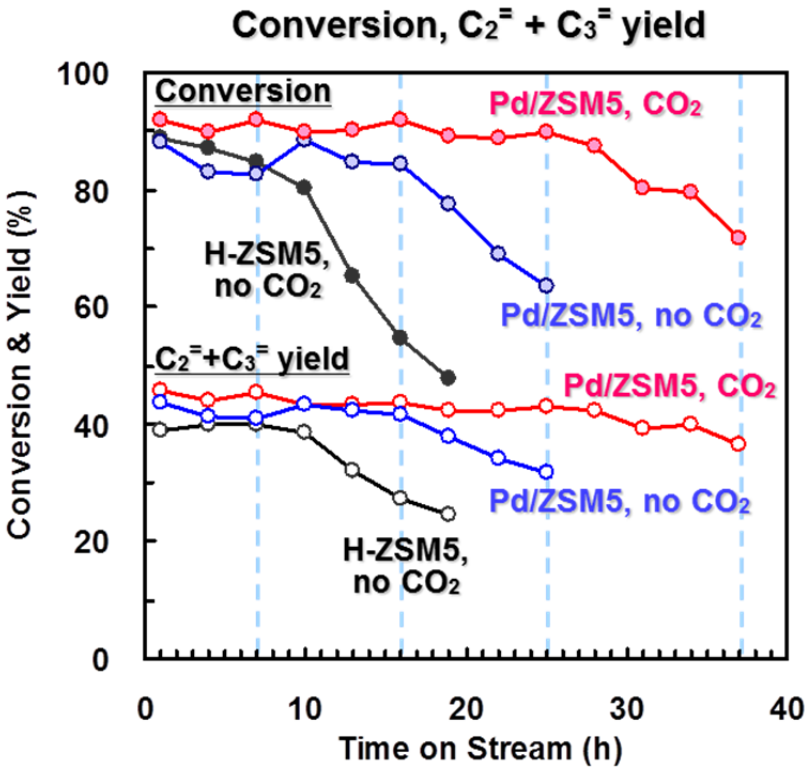

Fig. 1 The effect of CO_2 addition for the time course of the conversion (fill) and the total yield of ethene & propene (blank) from *n*-hexane cracking over Pd/ZSM5 and H-ZSM5.
Reaction condition: 923 K, WHSV = 10 h-1, pressure of *n*-hexane : 0.11 MPa, pressure of CO_2 : 0.055 MPa.

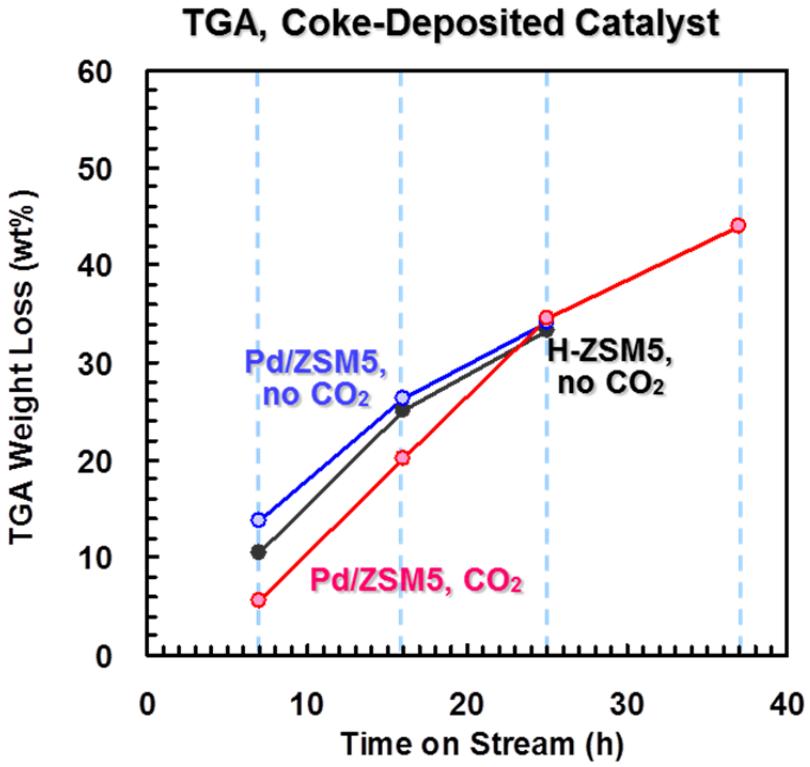

Fig. 2 The effect of CO_2 addition for TGA weight loss of coke deposited catalyst withdrawn during the cracking reaction.
TG/DTA condition: r.t. – 1273 K, heated at 10 K/min under 50 cc/min air flow.

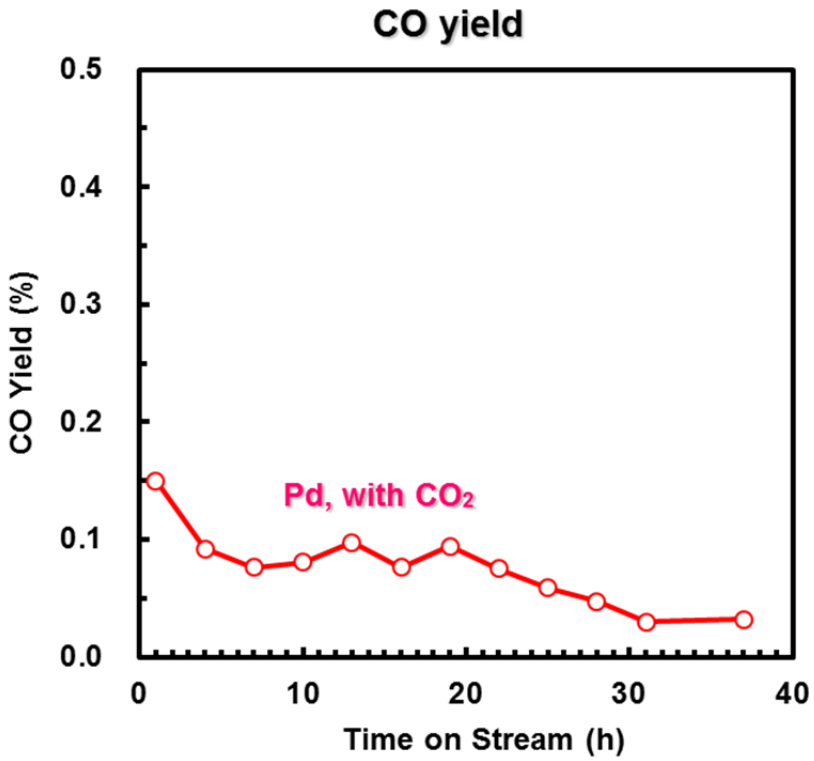

Fig. 3 The time course of the yield of CO of *n*-hexane cracking with CO_2 over Pd/ZSM5.

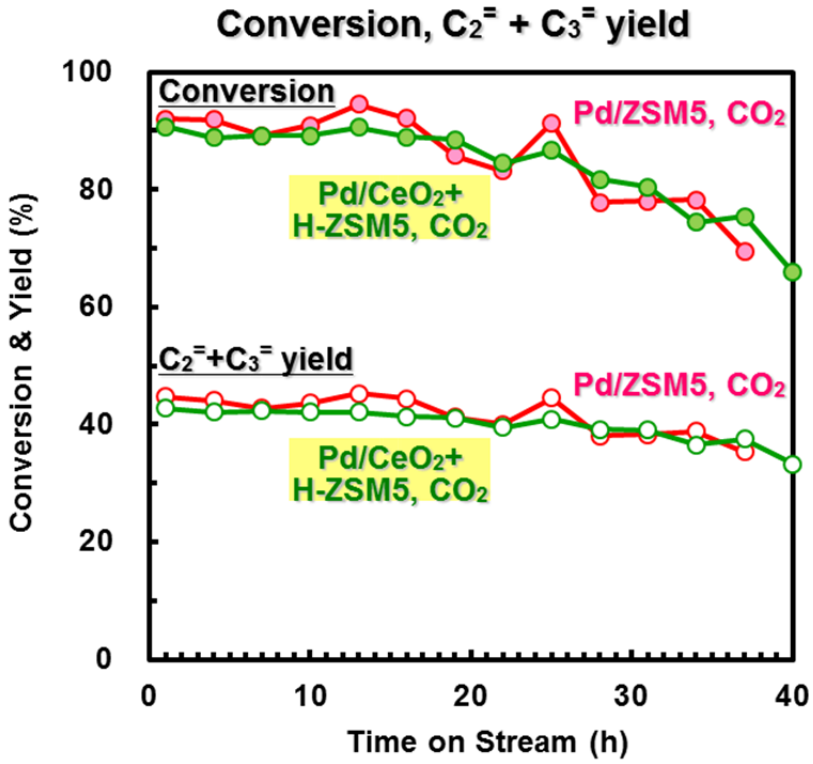

Fig. 4 The effect of CO_2 addition for the time course of the conversion (fill) and the total yield of ethene & propene (blank) from n-hexane cracking over Pd/CeO_2 + H-ZSM5.
Reaction condition: 923 K, WHSV = 10 h-1, pressure of *n*-hexane : 0.11 MPa, pressure of CO_2 : 0.055 MPa.

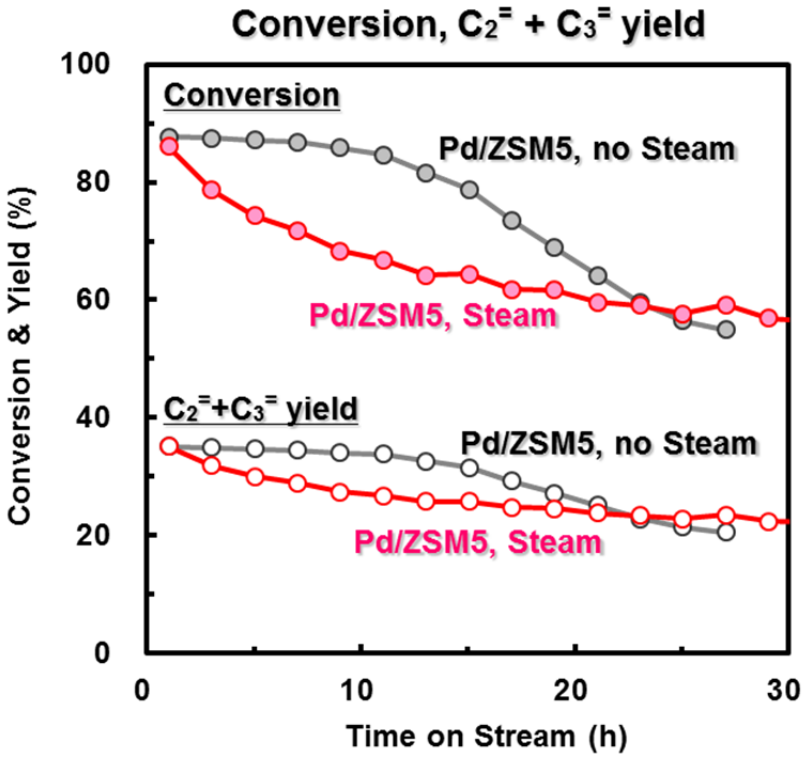

Fig. 5 The effect of steam addition for the time course of the conversion (fill) and the total yield of ethene & propene from *n*-hexane cracking over Pd/ZSM5. Reaction condition: 923 K, WHSV = 10 h-1, pressure of *n*-hexane : 0.11 MPa, pressure of H_2O: 0.055 MPa.

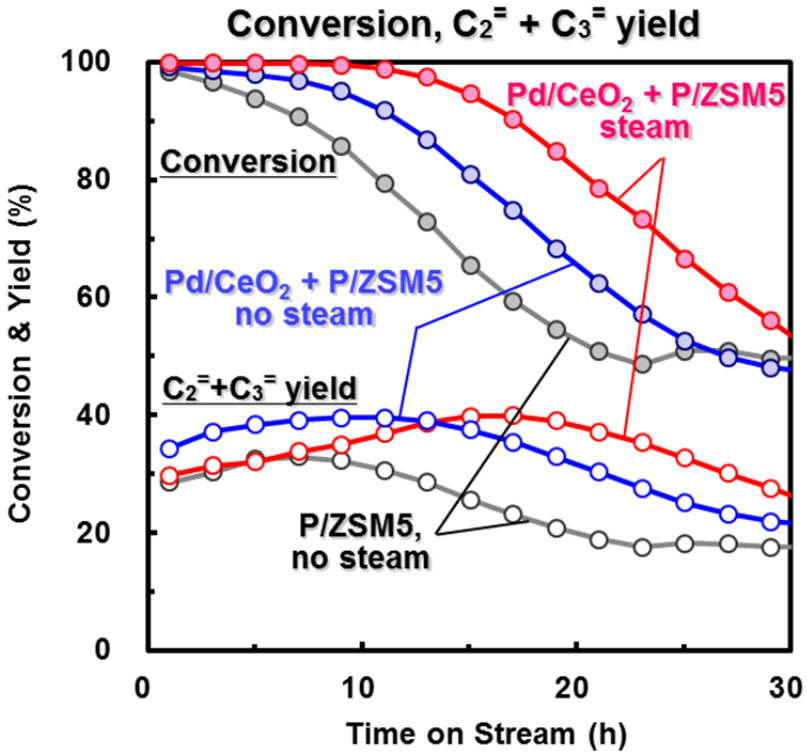

Fig. 6 The effect of steam addition for the time course of the conversion (fill) and total yield of ethene & propene from *n*-hexane cracking over Pd/CeO_2 + P/ZSM5

Reaction condition: 923 K, WHSV = 10 h-1, pressure of *n*-hexane : 0.11 MPa, pressure of H_2O: 0.055 MPa.

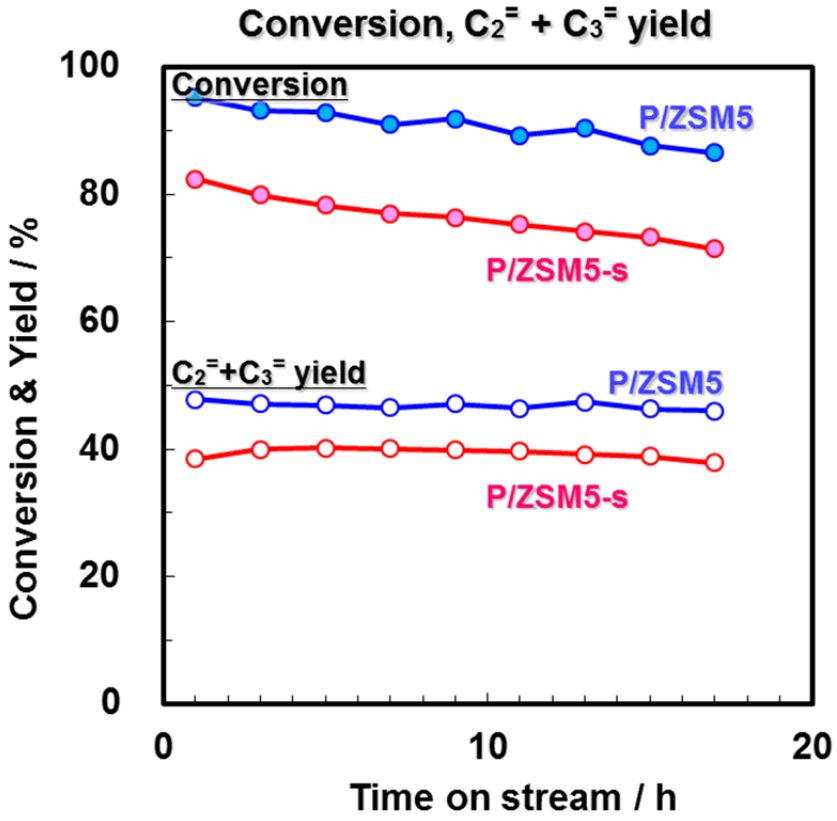

Fig. 7 The effect of the severe steam treatment for the time course of the conversion (fill) and the total yield of ethene & propene (blank) from n-hexane cracking over P/ZSM5 before and after sever steam treatment.
Reaction condition: 923 K, WHSV = 15 h^{-1}, total pressure : 0.10 MPa, Steam / Oil = 0.1 (wt ratio), *n*-hexane / H_2O / N_2 = 0.54 : 0.26 : 0.20 (molar ratio).

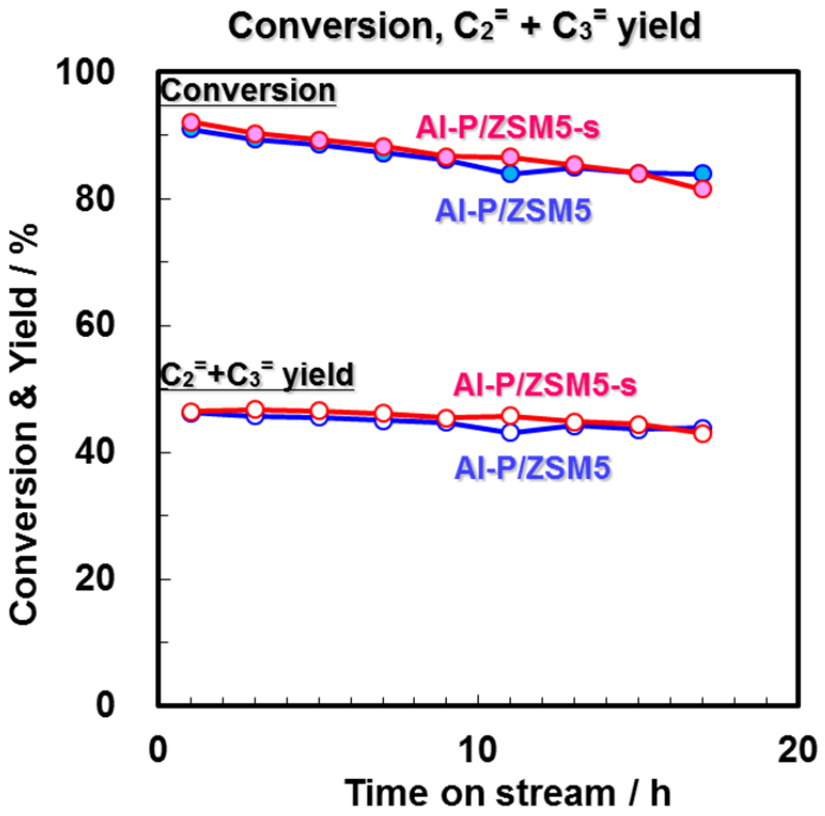

Fig. 8 The effect of the severe steam treatment for the time course of the conversion (fill) and the total yield of ethene & propene (blank) from *n*-hexane cracking over Al-P/ZSM5 before and after sever steam treatment.
Reaction condition: 923 K, WHSV = 15 h^{-1}, total pressure : 0.10 MPa, Steam / Oil = 0.1 (wt ratio), *n*-hexane / H_2O / N_2 = 0.54 : 0.26 : 0.20 (molar ratio).

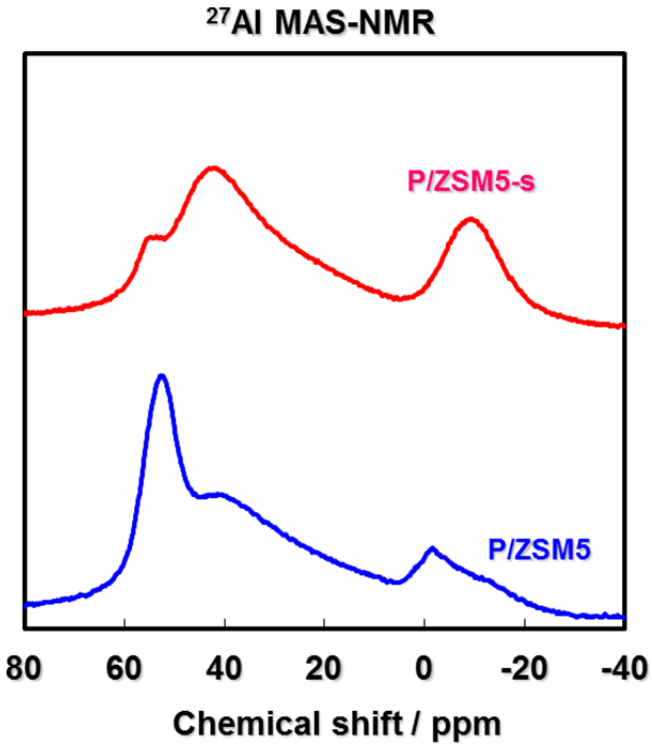

(A)

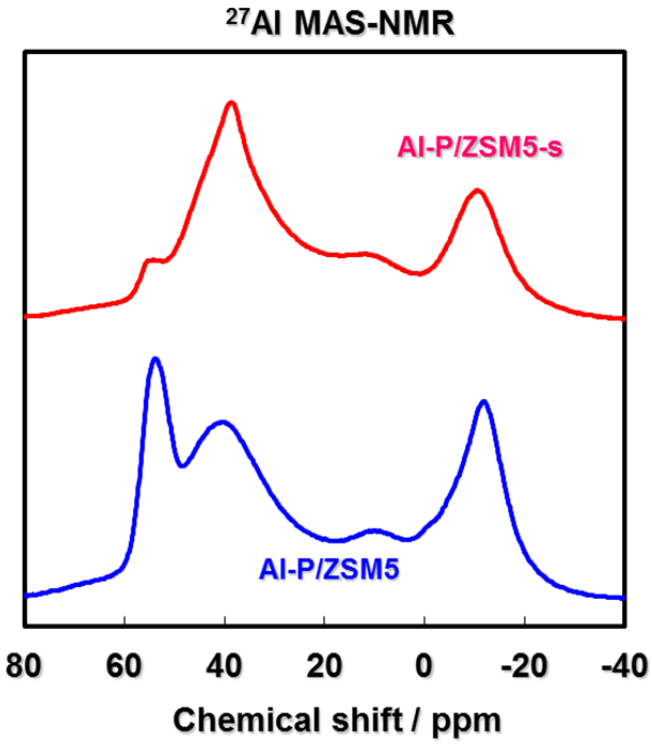

(B)

Fig. 9 27Al MAS-NMR spectra of P/ZSM5 (A), and Al-P/ZSM5 (B) before and after the severe steam treatment

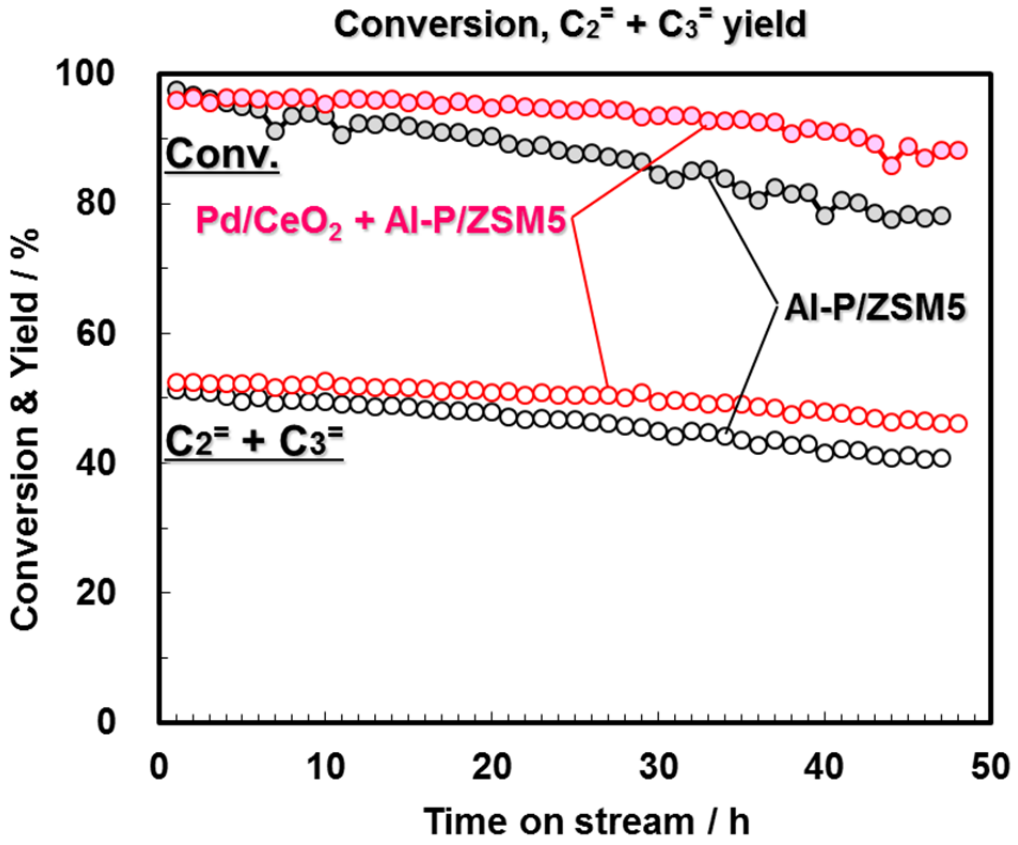

Fig. 10 The time course of the conversion (fill) and the total yield of ethene & propene from *n*-hexane cracking over Pd/CeO_2 + Al-P/ZSM5.
Reaction condition: 923 K, WHSV = 3 h^{-1}, S / O = 0.5 (molar ratio), total pressure : 0.10 MPa.

Chapter 6

Summary

Lower olefins such as ethene and propene are produced mainly in naphtha thermal cracking process in Japan, Asian countries and Europe. Meanwhile, in the Middle East, the United States, and China, many lower-olefin producing processes using resources that are very inexpensive compared with naphtha such as natural gas and coal as raw materials have been built in recent years. Low-priced lower olefins produced by these processes are extremely price competitive and it is only a matter of time for them to sweep the markets such as Japan. Therefore, realization of a naphtha catalytic cracking process which can flexibly control the product composition according to demand is greatly expected. Against this background, I studied on developing catalysts for naphtha catalytic cracking.

Chapter 2

For production of lower olefins by catalytic cracking from saturated hydrocarbons such as naphtha as raw materials, materials having a stable crystal structure even at high temperature, pores with shape selectivity of product, high surface area and acidic property are selected as a good catalyst. Zeolite can be mentioned as materials satisfying such conditions. Depending on the type of zeolite, the arrangement of the skeleton forming pores is different. There are 232 kinds of topology, the difference of this skeleton, presently. Screening was carried out with the aim of investigating which topology zeolite was effective for this reaction. Since it was practically impossible to test all topologies, a few of 20 zeolites that seemed promising and had a topology that could be obtained and synthesized were evaluated. As a result, ZSM5 (MFI) zeolite

showed the highest activity and the conversion rate was slightly reduced. In addition, MCM22 (MWW), Beta (BEA), MCM68 (MSE) also showed relatively high activity, but the activity decreased comparatively faster. Therefore, in this research, the performance improvements of ZSM5 zeolite were examined.

Chapter 3

On the external surface of the zeolite, there are acid sites which do not have shape selectivity. Since these acid sites are not subjected to steric constraints, oligomerization of cracking products proceeds and the growth of coke materials are promoted. Since the catalyst is deactivated by coke formation, investigation was made to cover the acid sites on the external surface of the zeolite with a silylating reagent for the purpose of prolonging the lifetime of the ZSM5 zeolite catalyst in the hexane cracking reaction. It was found that when cyclic siloxane such as TMCTS or PMCPS was used as a silylating compound, it could efficiently coat the acid sites on the external surface of zeolite and was effective for prolonging the lifetime of catalytic cracking reaction. The covering of acid sites on external surface of zeolite was evaluated by reaction evaluation and FT-IR analysis using various probe molecules. In the reaction evaluation, catalytic decomposition reaction was carried out using 1,3,5-triisopropylbenzene which does not enter the zeolite pores and reacts at the acid sites on the external surface of the zeolite as a raw material. In the FT-IR analysis, adsorption was evaluated using hexamethyleneimine adsorbed on the outer surface acid sites as a probe molecule without entering the zeolite pores as well. In addition, the process of hexane entering the pores from the external surface of the zeolite using hexane, a model compound of naphtha, was traced for silylated and untreated catalyst. In both analyzes, it was shown that the cyclic siloxane-treated ZSM5 zeolite showed that the acid sites on the external surface were inactivated.

Chapter 4

ZSM5 zeolite with various Si/Al_2 ratios was prepared and the effect of supporting metal having dehydrogenating ability such as palladium, platinum, ruthenium was verified. It was found that when a metal is supported on zeolite having a large amount of acid, deactivation of the catalyst is accelerated, whereas when a metal is supported on zeolite having a small amount of acid, the lifetime is prolonged. Next, the reaction rate analysis was carried out using a metal supported and unsupported catalyst. As a result, it was found that activation energy in hexane conversion was lower than that in other catalysts when metal is supported on zeolite with a small acid content. We concluded that cracking reaction and dehydrogenation reaction proceeded cooperatively by loading the metal on the zeolite with a small acid content, and it was inferred that the reaction proceeded efficiently. In addition, Catalytic decomposition reaction was carried out using a catalyst supporting a metal on a support not having acid sites as a confirmation of dehydrogenation ability. As a result, it was confirmed that benzene was the only aromatic among the products, because cracking and oligomerization by acid catalyst did not occur. On the other hand, it was also confirmed that the aromatic component in the product of the catalytic cracking reaction using the metal-supported zeolite contained not only benzene but also toluene and xylene due to its function by acid. Incidentally, the catalyst obtained in this study was evaluated by using not only hexane as the model compound of naphtha but also real naphtha containing a sulfur compound as a raw material, and actual naphtha showed the same result as that of hexane. In addition, it was also confirmed that a large decrease in activity was not observed by repeated evaluation of reaction regeneration.

Chapter 5

Addition of CO_2 to the feedstock of cracking reaction of *n*-hexane led to a dramatic improvement in durability of Pd/ZSM5 catalyst and suppression of a decrease in the ethene and propene yield. It is thought that the gasification or reforming reaction occurs with coke or coke precursor by CO_2 flow. This effect developed when H-ZSM5 was mixed with Pd loaded CeO_2 which was oxygen ion conductor having high lattice oxygen supply ability as a support. Similarly to CO_2, addition of H_2O led improvement in catalyst life. However, the permanent inactivation was observed by using H_2O because of release of aluminum from zeolite skeleton due to contact with high temperature steam. In order to improvement in hydrothermal durability, not only P well known to the effect but also Al was loaded to H-ZSM5. Al-P/ZSM5 had higher steam stability than P/ZSM5even after severe hydrothermal treatment. Al-P/ZSM5 catalyst mixed with Pd/CeO_2 produced ethene and propene at high efficiency for 48 h under steam coexistence.

Significance of this research

The result of this research has a potential to be applied to upgrading of existing naphtha cracker as the technology so that it can reduce environmental load, improve the yield of the product from naphtha cracker, and control the product distribution to match the demand flexibly. In the case of the existing thermal cracking process, the ratio of propylene to ethylene (P / E) can be increased by lowering the temperature of the decomposition reaction, but this ratio is limited to about 0.7. In terms of the global environment, pyrolysis requires a high temperature of 1073 k or more, consumes a lot of energy and releases a lot of CO_2. The accident of Fukushima Daiichi Nuclear Power Plant occurred in March 2011, and the domestic energy policy was reviewed and innovative producing methods that contribute to further reduction of GHG (green house gas) are desired more and more. The technology developed in this research is used for

the purpose of strengthening the competitiveness of the naphtha cracker of the petrochemical industry and at the same time it can achieve energy saving of the core process of the petrochemical industry and also contributes greatly to greening, which is social need.

In Japan's existing industrial petroleum complex, the product / utility balance centering on naphtha crackers has already been fully assembled and it is not realistic to completely replace existing facilities, but the technology developed in this research is likely to be incorporated as an improved facility for existing naphtha crackers. In the catalytic cracking process, in addition to high total yield of useful components such as ethene, propene, butenes, BTX, P / E can be increased to 0.9 or more. Furthermore, the yield of methane to be fuel is low, instead the yield of ethane and propane which can be used as cracking raw materials is high, and by recycling and decomposing it, it is possible to further increase the yield of useful components. Therefore, the amount of naphtha required to obtain the same amount of useful ingredients will be reduced, which also leads to improvement of raw material consumption unit and energy consumption rate. Therefore, we conclude that the result of this technology development can reach the next step toward practical application.

List of Publications

[1] S. Akiyama, H. Mochizuki, H. Yamazaki, T. Yokoi, T. Tatsumi, J. N. Kondo
"The effective silylation of external surface on H-ZSM5 with cyclic siloxane for the catalytic cracking of naphtha"
Journal of Molecular Catalysis A: Chemical, accepted. (Chapter 3)

[2] S. Akiyama, A. Okabe, M. Umeno, H. Mochizuki, T. Yokoi, T. Tatsumi, J. N. Kondo
"Catalytic cracking of naphtha over H-ZSM5 catalyst controlled in acid amount and metal loading amount" in preparation. (Chapter 4)

[3] S. Akiyama, A. Okabe, M. Umeno, T. Yokoi, T. Tatsumi, J. N. Kondo
"Improvement in durability of catalytic cracking of naphtha over metal mixed ZSM5 zeolite catalyst with oxidizing gas" in preparation. (Chapter 5)

Patent Application

[1] JP Patent (2012) 特願 017152.

[2] JP Patent (2012) 特願 050894.

[3] JP Patent (2012) 特願 050895.

[4] JP Patent (2012) 特願 094037.

[5] JP Patent (2012) 特願 192264.

[6] JP Patent (2013) 特願 120724.

List of Conference presentations

Oral presentation at domestic conference

[1] S. Akiyama, A. Okabe, M. Umeno, A. Miyaji, M. Murakami, H. Mochizuki, H. Yamazaki, T. Yokoi, S. Namba, J. N. Kondo, T. Tasumi
1H01 触媒討論会秋田大学, 秋田, 2013.

[2] A. Okabe, S. Akiyama, M. Umeno
1H02 触媒討論会秋田大学, 秋田, 2013.

[3] M. Umeno, S. Akiyama, A. Okabe
1H03 触媒討論会秋田大学, 秋田, 2013.

謝辞

本論文は筆者が三井化学株式会社（2008 年 4 月～）、独立行政法人新エネルギー・産業技術総合開発機構（NEDO）「触媒を用いる革新的ナフサ分解プロセス基盤技術開発プロジェクト」東工大集中研究室（2009 年 11 月～2014 年 2 月）、東京工業大学大学院総合理工学研究科物質電子化学専攻博士後期課程（2012 年 10 月～）にて従事した研究の成果をまとめたものです。研究を開始した 2008 年当初、自身が博士号を取得できるとは露ほどにも思っていませんでしたが、周囲の皆様の多大なるご指導、サポートのもと、博士論文をまとめることができました。ここに、謹んで感謝の意を表したいと思います。

博士課程の指導教官ならびに主査である東京工業大学科学技術創生研究院化学生命科学研究所准教授 野村淳子先生には、触媒反応のなぜ・どうしてを解明すべく先生の研究室の門を叩いた私を快く招き入れていただき、研究方針、論文の書き方からまとめ方、実験操作に至るまで手取り足取りご指導賜りました。怠け癖のある私に対し、幾度となく発破をかけて尻を叩いてくださったおかげで何とかあきらめずに論文を最後まで仕上げることができました。心より深謝の意を表します。

本論文の審査を快く引き受けてくださいました東京工業大学大学院総合理工学研究科化学環境学専攻教授 馬場俊秀先生、同研究科物質科学創造専攻准教授 鎌田慶吾先生、同研究科物質電子化学専攻准教授 北村房男先生、同研究科物質電子化学専攻准教授 松下伸広先生には、鋭いご指摘含めて様々な観点から多くのアドバイスをいただきました。心より御礼申し上げます。

東京工業大学名誉教授 辰巳敬先生には、ゼオライトのいろはや工業化に向けたアドバイスを、同大学産学官連携研究員 難波征太郎先生には、結果に対する真摯な考察や反応機構などの原理原則を追究することの重要性を、同大学助教 横井俊之先生には、最新のゼオライトの研究動向やゼオライト研究のアプローチを丁寧にお教えいただきました。今思い返しても、ゼオライトの世界的権威である先生方に囲まれ、非常に恵まれた環境で研究を遂行できたのだなと実感しています。深く感謝申し上げます。

辰巳・野村研究室の先輩である望月大司博士、山崎弘史博士には速度解析やゼオライト合成、赤外分光について多大なる協力をいただきました。お二人のサポートなしに本論文は成りえませんでした。心より感謝申し上げます。また、研究室の皆様の支えによって卒業の日を迎えられますことに深く感謝申し上げます。

北海道大学教授 増田隆夫先生、東京工業大学教授 多湖輝興先生、北海道大学助教 中坂佑太先生、産業総合技術研究所 水上富士夫先生、同 花岡隆昌先生、岩手大学 白井誠之

先生、産業総合技術研究所 井上朋也先生、同 山口有朋先生、同 佐藤剛一先生、同 日吉範人先生、同池田拓史先生、東京工業大学教授 小松隆之先生、北海道大学准教授 古川森也先生、北九州市立大学准教授 今井裕之先生、横浜国立大学教授 窪田好浩先生、同大学准教授 稲垣怜史先生には、国家プロジェクトを通してゼオライト合成や速度論解析、コーク性状解析など本研究を進めるに当たり幅広くかつ深くご指導いただきましたことに心より感謝の意を表します。

触媒技術研究組合部長 松本正人氏には、好き勝手放題の出向研究員をまとめプロジェクト完遂をマネジメントいただきました。心より御礼申し上げます。

住友化学株式会社 池口真之博士、住友化学株式会社 村上昌義氏、日本無機化学工業株式会社 宮路淳幸博士には、集中研への出向研究員として毎日顔を合わせ侃々諤々と議論し、お互い不思議な環境下にいることで妙に結束し和気藹々と研究活動を共にさせていただきましたこと、心より感謝申し上げます。私にとっては戦友のような存在と勝手に思わせていただいております。

共同研究者かつ会社上司・先輩である三井化学株式会社 藤原謙二博士、西村徹博士、水津宏氏、梅野道明氏、岡部晃博博士には、社会人博士課程の入学を許可し、公私に亘りいつも優しい言葉で励ましていただきました。出向中は何度、勇気づけられたことか。博士課程の研究を行いやすい環境づくりにもご支援いただきました。先輩方の研究に対する打ち込み方を目にし、私も博士課程に進もうと決めました。偉大な背中を追いかけてやってきましたが、いまだ足元にも及ばないように思います。心より御礼申し上げますとともに今後とも叱咤激励のほどよろしくお願い申し上げます。

本研究で出会ったすべての人との出会いが私にとっての財産であり、学びだったと思っています。これからも学びの歩みを止めず、より一層精進し、全身全霊をささげて科学の発展に貢献していきたいと思います。

最後に、私を生み育てこれまでずっと暖かく応援してくれた父 秋山佳明、母 保子、博士課程中は私が家事をせず博士論文を執筆し続けても嫌な顔せず仕事と出産・育児でてんてこ舞いの中、全力で激励してくれた最愛の妻 紘子、笑顔と笑い声で疲れを吹き飛ばしてくれた長男 智輝、長女 英恵に心から感謝します。どうもありがとうございました。

2017 年 2 月　秋山 聰